CO-CHAPERONE REGULATION OF THE RIBONUCLOETIDE REDUCTASE COMPLEX

by

Laura Knighton

A dissertation submitted to the faculty of
The University of North Carolina at Charlotte
in partial fulfillment of the requirements
for the degree of Doctor of Philosophy in
Biology

Charlotte

2020

Approved by:

_____
Dr. Andrew Truman

_____
Dr. Christine Richardson

_____
Dr. Shan Yan

_____
Dr. Junya Tomida

_____
Dr. Daniel Rabinovich

ABSTRACT

LAURA E. KNIGHTON. Co-Chaperone Regulation of the Ribonucleotide Reductase Complex. (Under the direction of DR. ANDREW W. TRUMAN)

The molecular chaperone Hsp70 folds a significant proportion of the proteome and is responsible for the activity and stability of many disease-related proteins, including those in cancer. Substantial effort has been devoted to developing a range of chaperone inhibitors for clinical use. Recent studies have identified the oncogenic ribonucleotide reductase (RNR) complex as an substrate of chaperones. While several generations of RNR inhibitor have been developed for use in cancer patients, many of these produce severe side effects such as nausea, vomiting and hair loss. Development of more potent, less patient-toxic anti-RNR strategies is highly desirable. Here we identify the yeast Hsp70 co-chaperone Ydj1 as an interactor of the RNR complex. Ablation of Ydj1 function destabilizes Rnr2 and Rnr4. We demonstrate conservation of this mechanism in mammalian cells, where HDJ2 interacts with and stabilizes R2 and R2B. Inhibition of HDJ2 with a novel small molecule inhibitor (116-9e) sensitizes cancer cells to existing RNR therapies. Going forward, this may form part of a novel strategy to target cancer cells that are resistant to standard RNR inhibitors.

Following on from these discoveries, we examined the respective roles of yeast Hsp70 isoforms (Ssa1, 2, 3 and 4) in activating RNR. Interestingly, while Ssa1 and 2 can support RNR function, Ssa3 and 4 cannot. Biochemical analysis reveals that Ssa3 and 4 have a substantially weaker binding to RNR subunits than Ssa1 and 2 and indeed Ydj1 itself displays a lower binding for RNR in cells expressing on Ssa3 and Ssa4. Taken

together, this adds to the growing body of evidence that Hsp70 isoforms have both overlapping and unique functions in cells.

BiP, the Hsp70 isoform located in the Endoplasmic Reticulum has been shown to be important in cellular homeostasis and also important in cancer cell progression. Although several BiP inhibitors have been developed, they have not succeeded in clinical trials due to toxicity. We examine the individual roles of BiP co-chaperones ERdj1-8 in mediating anticancer drug resistance using a combination of ERdj1-8 CRISPR KO cells and chemogenomic screening. Interestingly, we find that each ERdj KO displays a unique signature of synergy with currently used anti-cancer drugs. Overall these data may suggest a personalized medicine approach whereby ERdj mutation status is assessed to design an effective anticancer treatment plan.

DEDICATION

To my family

Even though most of the time you had no idea what I was talking about, you were always there encouraging, supporting and loving me. Without you all, I wouldn't have made it here and I wouldn't be the person I am today.

ACKNOWLEDGEMENTS

Firstly, to my mentor Dr. Andrew Truman, I want to thank you for everything you have done for me and my graduate career the last several years. Every day you think about how you can help your students in our studies, research and life in general. You were always available to lend a patient ear and hand. I will forever be grateful for you taking a chance on me as a clueless undergrad (who never even heard of Hsp70!) and helping me to become a confident, critically thinking scientist.

To my committee members Dr. Christine Richardson, Dr. Shan Yan, Dr. Junya Tomida and Dr. Dan Rabinovich thank you all for your direction and feedback throughout my graduate research. Additionally, to Dr. Richardson, you go above and beyond for all us graduate students. You are always who we go to for help and I thank you for always being there, specifically for helping me with the chaos of classes, degree requirements and scientific advice. Dr. Shan Yan, thank you for your wonderful teachings in Cell Biology class and insightful advice on DNA damage. Dr. Junya Tomida, thank you for your positive feedback and perceptive questions.

I would like to thank the many undergraduates, past and current, who have researched in our lab over the years and have helped me with my projects. To the graduate students Jill Waller, Jade Takakuwa and Siddhi Paranjape for your support and assistance with my research. I would like to extend my sincere gratitude to my lab mate from the beginning, Nitika, thank you for all your support and help throughout our time. I know our friendship will be life-long and I am so glad we had each other.

Thank you to the friends I have made throughout the department for your constant support of all my endeavors and your companionship through both the good and bad times especially Austin Jeffries, Dr. Brittany Johnson, Dr. Donna Goodenow, and Dr. Priyanka Grover.

I want to sincerely thank Tonya Bates whom I met in my undergraduate studies and since then has been a mentor and role model for me. Even to this day, I can go to you for advice on anything and receive nothing but support. Without you, I wouldn't have learned about research opportunities and probably wouldn't be completing my PhD today.

Thank you to Dr. Ken Pillar for being so kind, helpful and incredibly knowledgeable about biotech. Even though you would never admit to it, I wouldn't have gotten my dream job without you and I will never stop thanking you!

Thank you to Brad Fach for giving me a chance to explore opportunities outside the lab in my internship with the Office of Research and Development. I thank you for your willingness to assist the students at UNCC develop transferable skills and gain work experience.

Thank you to David Gray for assisting me with the green initiatives throughout the department. I wouldn't have been able to be successful with these projects that meant so much to me without you.

Thank you to all the faculty and staff here in the Department of Biological Sciences and the Graduate school.

I owe my family a huge amount of gratitude for helping me throughout life and especially during graduate school.

To Jason, for loving me on the good and bad days, always making me laugh, and being my biggest supporter. Your patience and optimism have gotten me through these years and kept me semi sane. Thank you for joining me on this adventure and the many ahead, including moving to Boston even though you hate the cold. I love you.

To my Mom, Julie, thank you for always encouraging me to dream big and strive for more in my life while supporting me along the way! Our camping and weekend trips have been a great escape during the more chaotic times. Thank you for loving me.

To my Dad, John, and Step-Mom Sue, thank you for always being the calm within the storm. Thank you, Dad for always putting things in perspective and making me lighten up and laugh. Thank you, Sue for always listening to me no matter when I call and letting me vent after really hard days. Thank you both for loving me.

Thank you to my siblings Corey, Greg and Nikki for making me look for to non-stop laughing and good times during holidays and family trips. We have grown so much together, and I love you all.

Thank you to my first and best friend in Charlotte Alyssa Chapuis for being a ray of sunshine in my life. You have been such a great friend over these years and our time laughing, exploring, eating, shopping and just talking have been invaluable. Thank you to my soul sister Sara Seegers for being a constant support in my life since we met. One of the best things to come from grad school is meeting you. We are cut from the same cloth and I am so grateful to have you in my life.

Finally, thank you to Daisy, KP and Wolfie for greeting me every day when I come home and turning bad days into good ones.

TABLE OF CONTENTS

LIST OF FIGURES

CHAPTER 4

CHAPTER 5

LIST OF ABBREVIATIONS

DDR-DNA damage response

HS-Heat Shock

HSF-Heat Shock Factor

Hsp-Heat Shock Protein

HU-Hydroxyurea

UV-Ultra-Violet Radiation

MMS-methyl methanesulphonate

NBD-Nucleotide-binding domain

SBD-Substrate-binding domain

RNR- Ribonucleotide Reductase

ER- Endoplasmic Reticulum

CHAPTER 1: INTRODUCTION

Sections of this chapter have been published:

Knighton, L. E., Delgado, L. E., & Truman, A. W. (2019). Novel insights into molecular chaperone regulation of ribonucleotide reductase. *Current genetics*, *65*(2), 477-482.

Lotz, S. K.*, Knighton, L. E*., Jones, G. W., & Truman, A. W. (2019). Not quite the SSAme: unique roles for the yeast cytosolic Hsp70s. *Current genetics*, *65*(5), 1127-1134.

1.1 Heat Shock Proteins (Hsps)

Heat shock proteins (Hsps) are a set of well-conserved, highly expressed molecular chaperones that are vital for cellular function (1, 2). Originally identified as proteins induced by thermal stress, it is now understood that Hsps are play important roles in protecting cells against a range of cell stresses that include DNA damage, oxidative stress, metabolic challenges and aging (1-4). Heat shock protein 70 (Hsp70) and Heat shock protein 90 (Hsp90) are both are imperative for the folding and stabilization of the majority of the proteome (2, 5). Hsp70 is responsible for many housekeeping tasks such as de novo folding, transportation across cellular compartments, folding of denatured proteins and, if needed, protein degradation of "client" proteins. Hsp90 is required for the stability, function and degradation of many proteins from a variety of cellular pathways (6-9). While Hsp70 and Hsp90 both contribute to protein folding in the cell, their roles differ. Hsp70 can bind unfolded polypeptides and direct them to a partially or near-native structure. After transfer of partially folded clients from Hsp70 to Hsp90, Hsp90 potentiates final structural re-arrangements that allow full client activity (10).

1.2 Cytosolic Hsp70s in yeast

Yeast contains seven cytosolic Hsp70 family proteins, Ssa1-4 (the expression of at least one isoform is essential for viability) as well as the ribosomal Ssb1-2 and Ssz1 chaperones (34, 35). Although highly conserved, the Ssa1-4 proteins differ in expression level. Ssa1/2 are expressed constitutively at high levels whereas Ssa3/4 are only expressed during cell stress (36). Like other Hsp70s, these chaperones bind a substantial range of client proteins, performing housekeeping tasks related to the entire life cycle of a protein from initial folding, transport across cellular compartments and, ultimately, protein degradation (19, 25).

1.3 Co-chaperones of yeast Hsp70

The Hsp70 family of proteins require the presence of co-chaperone proteins consisting of a mixture of Hsp40 homologs ("J-proteins") and nucleotide exchange factors (NEFs). These factors dramatically alter the ATPase cycle of Hsp70, with J proteins stimulating ATPase activity and client binding (5). Humans have 17 different Hsp70 isoforms but 41 J-proteins and 13 NEFs (5). Other conserved co-chaperones also associate with Hsp70, and some of these interactions are altered in cancer (37). In yeast, there are 23 J-proteins, the most well studied being Ydj1 and Sis1 (38). Ydj1 and Sis1 are both localized to the cytosol, and the Ssa proteins bind them to generate specific Hsp70-dependent roles (39). Although Ydj1 and Sis1 have some overlapping function, deletion of Ydj1 can be complemented by over expression of Sis1 whereas the reverse is not true, suggesting that Sis1 plays unique roles in the cell (40).

1.4 Hsp70 and Hsp90 in cancer

Because of their cytoprotective qualities, overexpression of Hsp70 and Hsp90 are implicated in multiple diseases including cancer (11-15). High levels of Hsps are associated with poor prognosis and a resistance to standard cancer therapeutics. Many of the mutations that are present in oncoproteins render them intrinsically unstable and consequently these proteins require extra chaperone function to maintain stability and activity. Oncoproteins that Hsp90 and Hsp70 stabilize include CDK4, p53, p21, Cyclin D, ERK5, SRC and the Androgen receptor (16-21).

1.5 Proteomic analyses of chaperone networks are useful for identifying novel anticancer strategies

Chaperone inhibitors trigger loss of client activity and client degradation. This knowledge can be combined with powerful proteomic technologies to identify new clients and potentially new anticancer strategies. A recent study analyzed global proteome changes in bladder cancer cells upon treatment with five established Hsp90 inhibitors AUY922, ganetespib, SNX2112, AT13387, and CUDC305 (5). Substantial decreases in protein abundance were observed for proteins involved in oxidative phosphorylation, DNA synthesis and replication, cell cycle and glutathione metabolism (5). While many of these proteins have been previously established as chaperone clients, several were novel interactors (5). It will be interesting to see if future studies confirm these as *bona fide* clients.

While many interactions of chaperones have been identified on a single client basis, several studies have utilized large-scale genetic or proteomic screens to understand the

Hsp70 and Hsp90 “interactome (1, 9, 19, 20, 22-25). Chaperone-client interactions are dynamic, altering upon cell condition. Recent proteomic chaperone studies have attempted to probe this, by analyzing global changes in chaperone interaction upon chaperone phosphorylation or upon expression of various oncoproteins (20, 26-28) .

In an effort to understand the global roles of Hsp70 and Hsp90 in genome integrity, Truman et al., purified Hsp70 and Hsp90 complexes from yeast in untreated and MMS-treated (DNA damaging agent) cells were analyzed by mass spectrometry. 256 chaperone interacting proteins were identified, with 142 new interactions seen. 1.5% of Hsp70-client interactions and 2% of Hsp90-client interactions were increased upon DNA damage. Only one protein (Rnr4) was observed to increase interaction with both Hsp70 and Hsp90 upon DNA damage stress, suggesting a previously undiscovered role for chaperones in regulation of ribonucleotide reductase (25, 29).

1.6 RNR, an important player in DNA replication

Ribonucleotide reductase (RNR) is an important enzyme that is involved in the production of deoxyribonucleotides (dNTPs) which are subsequently used in DNA synthesis and repair (30-34). RNR is comprised of two diverse subunits, the large subunit R1 (R1 in vertebrates, Rnr1/Rnr3 in yeast) which contains the allosteric regulatory sites, and the small subunit R2 (R2/R2B in vertebrates, Rnr2/Rnr4 in yeast), which consists of a cell cycle regulated binuclear iron center and a tyrosyl free radical (30-34). Throughout the cell cycle, the expression levels of the subunits will increase or decrease depending on the cellular need for dNTPs. In S phase, the total pool of dNTPs peaks in order to permit DNA replication. Conversely, the number of dNTPs dramatically drops 10-fold in G_0/G_1 phase

when DNA repair and mitochondrial DNA synthesis demands the bulk of dNTPs (25, 31, 32, 35). Tight regulation of RNR is key to ensure correct levels of all four dNTPs at all times. Historically, researchers focused on the allosteric regulation of this enzyme, however, recently it has been discovered that RNR control is extremely complex and may require other forms of regulation as well. This includes regulation of expression of RNR genes, proteolysis of RNR subunits, control of the cellular localization of the small RNR subunit, and regulation of RNR activity by small protein inhibitors. RNR is critical for both original DNA synthesis as well as DNA repair, making it a classical target for cancer therapeutics. Further understand of the regulatory mechanisms of RNR is vital to developing novel treatments for cancer and other diseases (33, 36).

1.7 RNR inhibitors as anticancer agents

Because RNR is an attractive target in cancer, many RNR inhibitors have been developed as cancer therapeutics (30, 33, 36). One of the first RNR inhibitors developed was Hydroxyurea (HU). The anticancer properties of HU were first observed in the 1960s and since then it has been widely used to treat both cancer and sickle-cell anemia (37, 38). HU works by reducing the diferric-tyrosyl radical center in the small R2 subunit via one-electron transfer from the drug complex. HU was developed for human use but works similarly in yeast for studying mechanisms (37, 38). Another potent RNR inhibitor used as an anti-cancer drug is Gemcitabine (dFdC) (39, 40). It has been approved for medical use since 1995 and has since been approved for additional uses clinically. Gemcitabine is an analog of deoxycytidine and once it enters cells is phosphorylated by deoxycytidine kinase to its active form (39, 40). Gemcitabine is incorporated into DNA through DNA

synthesis and blocks further DNA polymerase processing. This results in “masked termination” and eventually cell death (39, 40).

1.8 RNR activity is dependent on Hsp70 and Hsp90

Interestingly, the R2 subunits in both yeast and mammalian cells are clients of both Hsp70 and Hsp90. Rnr2 and Rnr4 interact with Ssa1 and Hsp82 and inhibition of chaperone activity with VER-155008 or 17-AAG promotes Rnr2/4 degradation. Likewise, Hsp70 and Hsp90 bind human R2 and treatment of MCF-7 cells with VER-155008 or 17-AAG triggers R2 degradation (25, 29).

Given that RNR is reliant on chaperone activity, it stands to reason that chaperone inhibition would sensitize cells to RNR inhibitors. Several studies have confirmed this, with 17-AAG being utilized to sensitize both breast and lung cancer cells to gemcitabine (25, 41-43).

1.9 Inhibition of co-chaperones as an anti-RNR strategy

Hsp70 and Hsp90 require the assistance of helper “co-chaperone molecules in order to properly function. Co-chaperones are non-client proteins bind chaperones and assist in protein folding/stabilization activity. Co-chaperones have multiple functions-some bind and partially fold client proteins while others act as regulatory units to their chaperone counterpart (19, 44-48). Regulatory functions of co-chaperones include accelerating Hsp70/Hsp90 nucleotide binding and hydrolysis or acting as a linker between two chaperone molecules. It is assumed that co-chaperones are highly specialized in the manner

in which they choose a client to present to Hsp70 or Hsp90 and facilitate binding and releasing (44). The most well-characterized class of Hsp70 co-chaperones are the J-domain proteins after their highly conserved chaperone binding region. These J-domain proteins are typically associated with Hsp70 and protein folding functions (19, 44-50).

Recently there has been interest in co-chaperones as anticancer targets, especially as co-chaperone expression in altered in a variety of cancers (51-56). In some cases, co-chaperones themselves have been shown to play an important role in cell death related pathways such as apoptosis. While inhibitors of Hsp70 and Hsp90 are effective in killing cells, the essential nature of chaperone function makes many of these compounds highly toxic to patients (51, 52, 57). Targeting co-chaperones, which specifically fine-tune chaperone function may form part of a novel anticancer strategy. Identification of a novel small molecule inhibitor of mammalian HDJ2 (C86) that destabilizes the androgen receptor and inhibits the growth of castration-resistant prostate cancer furthers the idea that targeting HDJ2 and related co-chaperones may offer an alternative therapeutic avenue (58).

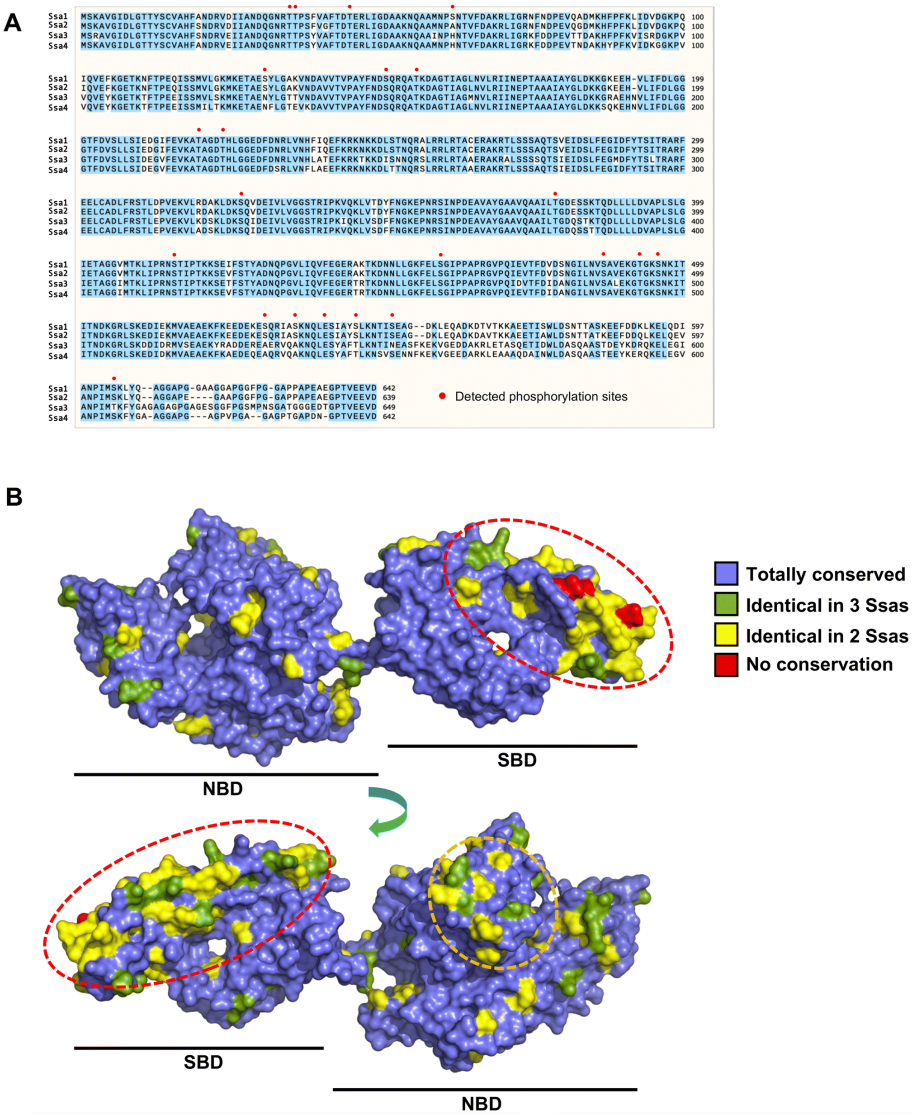

Figure 1. The Ssa proteins are highly conserved. **(A)** Alignment of amino acid sequences of *Saccharomyces cerevisiae* Hsp70 isoforms Ssa1, Ssa2, Ssa3 and Ssa4. Amino acids previously identified as being phosphorylated via mass spectrometry are annotated with a red dot. (**B)** Position of sequence variance between Ssa1–4 mapped onto the structure of Hsp70 (based on PDB entry 2KHO). Areas of clustered variance are enclosed in dashed red and orange circles.

1.10 Yeast cytosolic Hsp70 isoforms; Ssa1, Ssa2, Ssa3 and Ssa4

The Ssa1-4 proteins arose from genome duplication and are highly conserved, with Ssa1 sharing 99%, 84% and 85% amino acid identity with Ssa2, 3 and 4, respectively (Fig. 1a). The highest sequence variation occurs within the SBD, specifically the outer-facing region of the "lid" (Fig. 1b, red highlighted region). While the lack of conservation of sequence in this area might suggest a low functional importance, a more likely scenario is that it dictates the nature of client proteins that bind to each Ssa isoform. Interestingly, a second area that also displays variation is in the NBD (Fig. 1b, orange highlighted region). This surface has been defined as a region for interaction with J-protein co- chaperones and may imply variation in the complement of co-chaperones that interact with each Ssa isoform (47, 59, 60)

Despite sequence similarity, the Ssa1-4 proteins differ substantially in expression level in the cell. Ssa1/2 are expressed constitutively at high levels whereas Ssa3/4 are only expressed during cell stress (61-64). Studies of protein stability have identified significant differences in Ssa isoform half-lives; 20.2 h for Ssa1, 14.9 h for Ssa2, 11.0 h for Ssa3 and greater than 100 h for Ssa4 (65). Cells lacking Ssa1/2 show dramatic upregulation of Ssa3/4 levels as a compensatory mechanism and cells overexpressing Ssa1 but lacking Ssa2-4 are fully viable and have no significant phenotypes (61-64). While historically these proteins have been considered identical in function, recent findings suggest they may regulate unique facets of cell function.

1.11 Methodologies to understand redundant and non-redundant functions of Ssa proteins

Initial studies on Ssa function used cells lacking individual Ssas, possible due to the relative ease of PCR- based gene knockout (66). These studies were complicated by the partial redundancy of Ssa1-4 and compensatory expression of Ssa3 and 4 in cells lacking Ssa1 and 2. Follow-up studies creatively utilized strains lacking Ssa1–3 while expressing a temperature-sensitive version of Ssa1, ssa1–45 ((67). The ssa1–45 mutant protein possesses a single-point mutation at P417L which alters SBD structure and loses function at elevated temperatures allowing study of client response to Hsp70 inhibition. More recently, researchers have been aided by the creation of ssa1–4Δ yeast strains in which all 4 genomic Ssa genes have been removed; these are kept viable by expression of Ssa1 from a URA3-based plasmid (68, 69). These strains can be transformed with plasmids expressing Ssa isoforms, Ssa1 point mutations or Hsp70s from other organisms (68, 69). Curing of these strains on 5-fluoroorotic acid containing media promotes loss of the original Ssa1 plasmid, leaving cells expressing the desired Hsp70 variant as the sole cytosolic Hsp70 (68, 69). This newer system offers several advantages over ssa1–45. In the newer ssa1-4Δ the exogenous Hsp70 expressed is the sole cytosolic Hsp70 in the cell, as opposed to the present (but inactive Ssa1) in ssa1–45 cells. In addition, ssa1-45 cells must be incubated at elevated temperature to suppress native Ssa1 function, non-ideal when studying regulation of the heat shock response.

1.12 Early indications of functional differences in Ssa isoforms

Initial indications of a functional difference in Ssas came from in vitro studies attempting to understand the role of Hsp70 in uncoating bovine brain-coated vesicles (70). Despite the ability of Ssa1,2 and 4 to bind coated vesicles (Ssa3 was not examined), Ssa1 displayed considerably less uncoating activity than the other two isoforms (70). Nearly a decade later, researchers identified a requirement for Ssa2 in the import of yeast Fructose 1,6-biphosphatase, FBP1 into similar vesicles (71). Lysate prepared from ssa2Δ cells do not support the import FBP1 into vid (vacuole import and degradation) vesicles and FBP1 becomes stabilized in ssa2Δ cells (71). Follow-up studies con- firmed that Ssa2 was indeed critical in Vid pathway function, and that the specificity of this function came from a single amino acid difference between Ssa1 and Ssa2; A83 in Ssa1, G83 in Ssa2 (72).

1.13 Genetic and physical interactions of the Ssa proteins

Proteins have unique physical and genetic interactions; comprehensive analysis of this interaction "fingerprint" can provide useful insight into their specific function and even where a protein resides in the cell (73-76). Analysis of currently known physical interactors of each Ssa isoform reveals substantial differences in interactomes sizes (Fig. 2a). The constitutively expressed Ssa1 and 2 have much larger interactomes compared to inducible Ssa3 and 4 (717 and 375 proteins, respectively, vs 69 and 57). This result is unsurprising given the relative expression of these isoforms under the conditions these studies were carried out (30 °C in mid-log phase). It is possible that Ssa3 and Ssa4 have the ability to bind some of the Ssa1 and Ssa 2 interactors, but never have the chance due to low stoichiometry. Yeast respond to high-temperature stress by inducing a large number of

genes (mostly directed by Hsf1, see below). It is feasible that Ssa3 and Ssa4 have unique heat- induced interactors only seen at high temperature. While there are some shared physical interactors between Ssa1–4, they only make up 1.5% of the total interactions which is curious given their amino acid similarity. Proteins tend to be identified as client proteins of the Hsp70 isoforms on an individual basis as researchers discover their protein of interest has Hsp70-binding properties. To date, few attempts have been made to isolate the full complement of Hsp70 interactors, essential for a greater understanding of global Hsp70 function. Several groups, including ours have recently utilized affinity purification followed by mass spectrometry (AP-MS) to uncover the global interactomes of Hsp70 and Hsp90 chaperones under a variety of conditions and genetic backgrounds (25, 26, 29, 77-79). At this time, no attempt has been made to characterize all the individual Ssa isoform interactomes, with only Ssa1 being examined in this fashion (20, 25, 29). Proteomic analysis of Ssa1 interactomes under a range of physiological conditions will provide a greater insight into possible client interactions.

Genetic interactions between pairs of genes have long been used in yeast to understand unique and redundant gene function. However, large-scale screens in yeast utilizing the yeast knockout gene collections, pioneered by the Andrews and Contanzo groups have provided unparalleled mapping of yeast pathway control (73-75). Analysis of the genetic interactors of Ssa1–4 reveal a very different picture than portrayed by the physical interaction data. The Ssas have almost no overlap in genetic interactors, even between pairs of constitutive Ssas (Ssa1 and 2) or inducible forms (Ssa 3 and 4) (Fig. 2b). In addition, Ssa3 has almost the same number of unique genetic inter- actors as Ssa1 and 2, surprising given the low expression of Ssa3 at 30 °C and the very mild phenotype

exhibited by ssa3Δ cells. Future analyses combining gene pairs and cell stresses may provide greater insight into the unique functions of Ssa3 and Ssa4.

The potential for both overlapping and unique functionality amongst the Ssa family was further highlighted through global gene-expression analysis of yeast cells harboring Ssa1, 2, 3 or 4 as the sole Ssa in the cell (80). While a wide variety of genes encoding for proteins in different cellular metabolic pathways were found to share similar expression profiles across the Ssa family, there was a large number of apparently Ssa-specific genes that showed altered regulation (80). To fully appreciate the global cellular significance of each individual Ssa, a comprehensive meta-analysis of all phenotypic, genetic and molecular system-level data needs to be carried out.

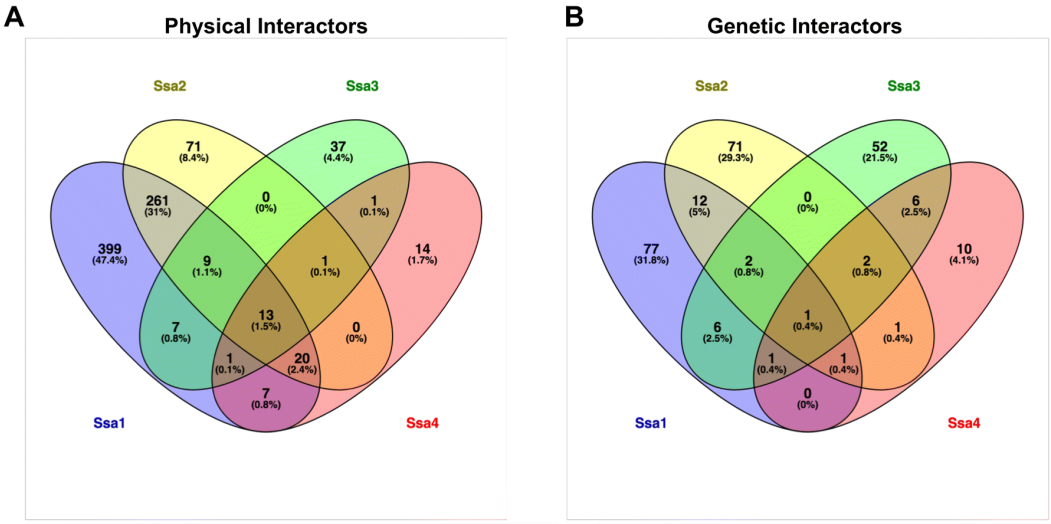

Figure 2. Physical and genetic interactions of Ssa1–4. **(A)** Physical interactors of Ssa1–4 were obtained from the Saccharomyces genome database (https://www.yeastgenome.org/) and analyzed by Venn diagram using Venny 2.1 (https://bioinfogp.cnb.csic.es/tools/venny/). **(B)** Genetic interactors of Ssa1–4 were obtained from the Saccharomyces genome database (https://www.yeastgenome.org/) and analyzed by Venn diagram using Venny 2.1 (https://bioinfogp.cnb.csic.es/tools/venny/)

1.14 Endoplasmic Reticulum Hsp70, BiP and associated co-chaperone isoforms.

BiP is an ER-resident Hsp70 isoform that depends on the binding and hydrolysis of ATP to fold client proteins (81-83). BiP associates with a suite of ERdj co-chaperones isoforms (Erdj1-8) that regulate ATPase activity and interaction with clients (81). ERdj1 and ERdj2 interact with the Sec61 translocon allowing protein transport in the ER. In contrast, ERdjs3-6 bind to clients once they arrive in the ER. Although a study using a peptide expression assay attempted to dissect ERdj client specificity (84), detailed analysis of functional differences between the ERdjs remain to be determined.

CHAPTER 2: THE HSP70 CO-CHAPERONE YDJ1/HDJ2 REGULATES RIBONUCLEOTIDE REDUCTASE ACTIVITY

This chapter has been published:

Sluder, I. T., Nitika., Knighton, L. E., & Truman, A. W. (2018). The Hsp70 co-chaperone Ydj1/HDJ2 regulates ribonucleotide reductase activity. PLoS genetics, 14(11), e1007462.

2.1 Introduction

Heat Shock Protein 70 (Hsp70) is a well-conserved, highly expressed molecular chaperone protein. While Hsp70 assists both in the folding of newly synthesized proteins and denatured proteins ("clients"), it also targets damaged proteins for degradation by the proteasomal system (2, 47, 59). Many housekeeping proteins require Hsp70 for stability, making Hsp70 essential for cell viability. Cancer cells require Hsp70 to maintain the function of unstable oncoproteins and as such are "addicted" to chaperone function and Hsp70 is often found to be overexpressed in breast and prostate cancers (14, 85, 86). Small molecule inhibitors of chaperones have been developed and assessed for their ability to inhibit cancer cell proliferation *in vivo* and *in vitro.* Despite promising data *in vitro,* chaperone inhibitors have met with limited success in clinical trials due to inherent toxicity of a drug that targets an essential cellular protein (57).

The activity of Hsp70 is regulated by a suite of co-chaperone proteins comprising mainly of Hsp40s and nucleotide exchange factors (NEFs) that assist in the stimulation of ATPase activity and the transfer of clients to Hsp70 for folding (47, 48, 60). They are a heterogeneous group that can be characterized by the presence of a remarkably conserved

70 amino acid J-Domain (47, 48, 60). In yeast the major Hsp70 isoform Ssa1 is activated by two related Hsp40s, Ydj1 and Sis1 (87, 88). Although these two proteins are somewhat functionally redundant, Sis1 is essential for cell viability whereas Ydj1 is not (87, 88). The study of the behavior of chimeric Ydj1-Sis1 constructs has revealed that the C-terminus of these proteins is the determining factor in client binding and functional distinctiveness (89). Interestingly, the C-terminus of Ydj1 contains a CAAX farnesylation motif that targets a small population of Ydj1 to the outer surface of the Endoplasmic Reticulum (88, 90). While both the regulation and function of this targeting remains ill defined, it appears that it is required for interaction with Hsp90 and select client proteins (91).

There are 47 Hsp40s expressed in humans, distributed across the cytoplasm, nucleus, ER and mitochondria (47, 48, 60). Many of these are well conserved with yeast isoforms. The human homologue of Ydj1 is HDJ2 (also known as DNAJA1), a protein implicated in regulating HIV replication as well as cancer cell growth (92). Each Hsp40 binds to a specific set of client proteins, thus offering the potential for selective inhibition of tumorigenic vs WT cells. There are no specific Hsp40 inhibitors in clinical trials and it is only recently that Hsp40s have been considered as possible drug targets, possibly due to the lack of characterization of many Hsp40 isoforms. Several dihhydropyrimidines are able to inhibit Hsp40-stimulation of Hsp70 including MAL3-39, MAL3-101 and 116-9e (93).

Upon DNA damage stress, there is a large remodeling of Hsp70 and Hsp90 complexes and tight association with the ribonucleotide reductase (RNR) complex (25, 29). The RNR complex catalyzes the production of deoxyribonucleotides (dNTPs) required for DNA repair and S-phase progression. RNR is well conserved between yeast and humans and are comprised of a large (R1) subunit and a small subunit (R2) (35, 94-96). R1 (R1 in

vertebrates, Rnr1/Rnr3 in yeast) forms the catalytic domain while R2 (R2B/R2 in vertebrates, Rnr2/Rnr4 in yeast) acts as regulatory subunits. Although Rnr2 and Rnr4 share sequence homology, only Rnr2 contains the key ligands for tyrosyl radical cofactor (35). As a result, Rnr2 is essential for cell viability whereas Rnr4 is not. *In vitro* studies have demonstrated a role for Rnr4 in assisting with Rnr2 folding (32). The subunit stoichiometry of RNR changes depending RNR subunit expression and localization regulated tightly in response to cell cycle stage and in response to DNA damage (94).

RNR is a well-validated anticancer target. Since RNR is required for DNA repair and DNA replication, inhibition of RNR slows cell proliferation and eventually results in S-phase arrest. Hydroxyurea (hydroxycarbamide, HU) was the first small-molecule RNR inhibitor characterized and was approved for clinical use in 1967 (30, 31). RNR inhibitors are particularly effective when used in conjunction with radiation or other DNA damaging agents (97-99). Recent studies have demonstrated that pretreatment of cancer cells with either Hsp70 or Hsp90 inhibitors causes destabilization of the RNR complex, sensitizing cells to RNR inhibitors such as HU or gemcitabine (25, 42). Little is known about the composition of RNR-Chaperone complex, particularly the co-chaperones involved in this process. In this study, we identify Ydj1 and Hdj2 as regulators of RNR activity in yeast and humans, respectively. Moreover, we demonstrate the feasibility of sensitizing cancer cells to RNR inhibitors such as HU by suppressing HDJ2 function.

2.2 Materials and Methods

Yeast Strains and growth conditions

Yeast cultures were grown in either YPD (1% yeast extract, 2% glucose, 2% peptone) or grown in SD (0.67% yeast nitrogen base without amino acids and carbohydrates, 2% glucose) supplemented with the appropriate nutrients to select for plasmids and tagged genes. *Escherichia coli* DH5α was used to propagate all plasmids. E. coli cells were cultured in Luria broth medium (1% Bacto tryptone, 0.5% Bacto yeast extract, 1% NaCl) and transformed to ampicillin resistance by standard methods. A full table of yeast strains and plasmids that were used can be found in Supplemental Table S1.

For serial dilutions, cells were grown to mid-log phase, 10-fold serially diluted and then plated onto appropriate media using a 48-pin replica-plating tool. Images of plates were taken after 3 days at 30°C. For *RNR3-lacZ* fusion expression experiments, cells were grown overnight in SD-ura media at 30˚C and then re-inoculated at A_{600nm}=0.2-0.4 and then grown for a further 4 hours. Cells were treated with 150 mM or 200 mM for 2 hours and then *RNR3-lacZ* fusion assays were carried out as described previously (100).

For tagging the genomic copy of *RNR1*, *RNR2* and *RNR4* with a GFP epitope at the carboxy-terminus, the pFA6a-GFP(S65T)-His3MX6 plasmid was used.

For cycloheximide experiments, WT and *ydj1*Δ cells were grown to exponential phase and then treated with 200 µg/ml cycloheximide for 6 hours. Cell lysates were obtained and Rnr2 levels were probed via Western Blotting as above.

Western Blotting

Protein extracts were made as described (Kamada et al., 1995). 20 µg of protein was separated by 4%–12% NuPAGE SDS-PAGE (Thermo). Proteins were detected using

the following antibodies; anti-HIS tag (QIAGEN #34670), anti-GFP (Roche #1814460), Anti-FLAG tag (Sigma, #F1365), anti-GAPDH (Thermo #MA5-15738), anti-Ydj1 (StressMarq #SMC-166D), anti-R2B (SCBT, #sc-376963), anti-HDJ2 (Thermo #MA512748).

Blots were imaged on a ChemiDoc MP imaging system (Bio-Rad). After treatment with SuperSignal West Pico Chemiluminescent Substrate (GE). Blots were stripped and re-probed with the relevant antibodies using Restore Western Blot Stripping Buffer (Thermo).

Purification of FLAG-tagged Rnr2 from yeast

Cells transformed with control pRS313 plasmid or the pRS313 plasmid containing HIS-tagged Rnr2 were grown overnight in SD-HIS media, and then reinoculated into a larger culture of selectable media and grown to an OD_{600} of 0.800. The cells were then either unstressed or stressed with 200 mM HU for four hours. Cells were harvested and FLAG-tagged proteins were isolated as follows: Protein was extracted via bead beating in 500 µl binding buffer (50 mM Na-phosphate pH 8.0, 300 mM NaCl, 0.01% Tween-20). 200 µg of protein extract was incubated with 30 µl anti-Flag M2 magnetic beads (Sigma) at 4° C overnight. Anti-Flag M2 beads were collected by magnet then washed 5 times with 500 µl binding buffer. After the final wash, the buffer was aspirated and beads were incubated with 65 µl Elution buffer (binding buffer supplemented with 100 µg/ml 3X FLAG peptide (Apex Bio)) for 1 hour at 4° C, then beads were collected via magnet. The supernatant containing purified FLAG-Rnr2 was transferred to a fresh tube, 25 µl of 5x

SDS-PAGE sample buffer was added and the sample was denatured for 5 min at 95° C. 20 µl of sample was analyzed by SDS-PAGE.

Mammalian cell culture and drug treatment

HEK293T cells were cultured in Dulbecco's modified Eagle's minimal essential medium (DMEM; Invitrogen, Carlsbad, CA, USA) supplemented with 10% fetal bovine serum (FBS; Invitrogen), 100 U/ml penicillin (Invitrogen) and 100 µg/ml streptomycin (Invitrogen). All cell lines were incubated at 37 C in a 5% CO2 containing atmosphere. For 116-9e treatment, HEK293 cells were treated with 116-9e (#E1036, Sigma) at 0.4 µM concentration and kept in incubator at 37°C and 5% CO_2 for 72 hours. After 72h cells were washed with 1X PBS and total cell extracts were prepared using Mammalian Protein Extract Reagent (Thermo).

HAP1 cells and HDJ2 Knockout cells were obtained from Horizon Biosciences and were cultured in Iscove's Modified Dulbecco's Medium (IMDM) supplemented with 10% fetal bovine serum (FBS; Invitrogen), 100 U/ml penicillin (Invitrogen) and 100 µg/ml streptomycin (Invitrogen). For IC_{50} calculations, HAP1 cells and HDJ2 Knockout were seeded in triplicate in 96-well white bottom Nunc plates in growth media at 20% confluency 1 day prior to initiation of drug treatment. On Day 1 of treatment, cells were treated with a ten-fold serial dilution of Hydroxyurea (400µM to 1.56 µM). After 72 h, cell viability was measured using Promega CellTiter-Glo cell viability assay on a Synergy H1 plate reader. Similarly, cells were treated with either DMSO (control) or 0.4 µM of 116-9E in combination with a ten-fold serial dilution of triapine (250µM to 0.0005 µM). After

72 h, cell viability was measured using Promega CellTiter-Glo cell viability assay on a Synergy H1 plate reader.

Immunoprecipitation of HIS-tagged R2B from mammalian cells

HEK293T cells were either un-transfected or transfected with HIS-R2B Lipofectamine 3000 (Thermo). After 48 hours, the cells were washed with 1XPBS and total cell extract was prepared from the cells using M-PER (Thermo) containing EDTA-free protease and phosphatase inhibitor cocktail (Thermo) according to the manufacturer's recommended protocol. Protein was quantitated using the Bradford Assay. His-tagged proteins were purified as follows: 200 µg of cell lysate was incubated with 30 µl of His-Tag Dynabeads (Invitrogen) with gentle agitation for 20 minutes at 4° C. Dynabeads were collected by magnet then washed 5 times with 500 µl Binding/Wash buffer. After final wash, buffer was aspirated and beads were incubated with 65 µl Elution buffer (300 mM imidazole, 50 mM Na-phosphate pH 8.0, 300 mM NaCl, 0.01% Tween-20) for 20 min, then beads were collected via magnet. The supernatant containing the purified HIS-H2B complex was transferred to a fresh tube, 15 µl of 5x SDS-PAGE sample buffer was added and the sample was denatured for 5 min at 95° C. 20 µl of sample was analyzed by SDS-PAGE and Western Blotting.

2.3 Results

A subset of Hsp70 co-chaperones mediate cellular resistance to Hydroxyurea

Hsp90 and Hsp70 mediate the cellular response to DNA damage by regulating RNR activity. Given that co-chaperones mediate many of the client binding functions in Hsp70 and Hsp90, we sought to uncover candidate co-chaperones that may regulate RNR function. We screened 28 yeast co-chaperone knockout strains for cellular sensitivity to Hydroxyurea (HU). While the majority of knockouts showed no significant difference to WT, cells lacking Ydj1, Erj5, Scj1 and to a lesser degree Zuo1 showed increased sensitivity to HU (Fig. 3A and supplemental Fig. 3). Erj5, Scj1 and Zuo1 are highly specialized co-chaperones that function in the ER and Ribosome respectively. Given that the RNR subunits are not present in either the ER or ribosome under standard conditions, we decided to focus our efforts of understanding the role of Ydj1 on RNR activity.

Ydj1 regulates the DNA damage response

HU is a potent activator of the DNA damage response pathway, triggering transcription of DNA repair enzymes. In an effort to determine whether Ydj1 controls transcriptional output of the DDR, we compared expression of b-galactosidase driven by a DNA-damage responsive promoter *(RNR3-lacZ)* in HU-treated WT and *ydj1*Δ cells. Consistent with the increased HU sensitivity of *ydj1*Δ, cells lacking Ydj1 were severely compromised for *RNR3* transcription, suggesting a role for Ydj1 in activation of the DDR response (Fig. 3B).

The C-terminus of Ydj1 is required for HU resistance

The Ydj1 protein comprises of four functional domains. The conserved helical J-domain is responsible for binding to Hsp70 and stimulating its ATPase activity (48, 101). A disordered region rich in glycine and phenylalanine (known as the G/F region) acts as a flexible linker between J- and C-terminal regions which consist of a Zinc-finger like domain and substrate binding domain. To query the structural requirement for Ydj1-mediated HU resistance, we analyzed an array of Ydj1 C-terminal truncations their ability to suppress the HU growth defect of *ydj1*Δ cells. Interestingly, cells required a complete CTDII domain for resistance to HU (Fig. 4A). Several Ydj1 mutants have been characterized affecting specific facets of Ydj1 function. Two such mutants, G153R and G315D are able to promote GR and ER activity in the absence of hormone when expressed in yeast and are unable to properly fold client proteins such as v-SRC (102, 103). We examined G153R and G315D for their ability to HU growth defect of *ydj1*Δ cells. While cells expressing G315D were moderately sensitive to HU, G153R were unable to grow even at 150mM HU (Fig. 4A). Taken together, this suggests that both CTDI and CTDII domains play an important role in Ydj1-mediated HU resistance.

The N-terminus of Sis1 can substitute for Ydj1 in the cellular response to HU

Ydj1 has high homology to another J-protein Sis1. Both possess an N-terminal J domain that binds and regulates Ssa1 (89). Although highly related, Sis1 and Ydj1 have overlapping yet distinct functions in the cell. Cells lacking Ydj1 are viable, whereas those lacking Sis1 are not (89, 104). Several studies have attempted to dissect the distinct roles of Ydj1 and Sis1 by creating and expressing Ydj1-Sis1 chimeras (105, 106). To

complement the truncation data in Fig. 4B, we asked whether a selection of Ydj1-Sis1 fusions could provide the same function as Ydj1 in mediating the cellular response to HU. While replacement of either the Ydj1 J-domain or G/F domain with the equivalent Sis1 region alone had little impact, replacement of both resulted in HU sensitivity. This suggests that while the C-terminus of Ydj1 is critical for the response to HU, the N-terminus is also required and that Sis1 and Ydj1 are functionally distinct for this role.

Farnesylation of Ydj1 is required for the cellular response to HU

While the majority of Ydj1 is localized to the cytoplasm, a fraction exists bound to the cytoplasmic side of the endoplasmic reticulum (90, 107, 108). This localization is achieved through farnesylation of a "CAAX box" motif on the C-terminus on Ydj1 at C406 (107). Disruption of Ydj1 farnesylation prevents the interaction of Ydj1 with Hsp90 and client proteins (91). We queried whether loss of Ydj1 farnesylation impacted cellular resistance to HU. *ydj1*Δ cells expressing either WT ydj1 or *ydj1*-C406S were plated on media containing 150mM or 200mM HU. *ydj1*-C406S cells were partially compromised for HU resistance, being more sensitive than WT cells but more resistant than *ydj1*Δ cells to HU (Fig. 4C).

RNR subunit stability is compromised in cells lacking Ydj1

Given that RNR stability is supported by Hsp90 and Hsp70 in yeast and mammalian cells, we wondered whether Ydj1 may be performing a similar role. We queried the total levels of Rnr1, Rnr2 and Rnr4 in WT and *ydj1*Δ cells. While Rnr1 levels were unchanged, Rnr2 levels were significantly compromised in cells lacking Ydj1 under both unstressed

and hydroxyurea treated cells. Rnr4 levels were affected in a less dramatic manner; loss of Ydj1 decreased Rnr4 only in HU-treated cells (Fig. 5).

Protein levels in cells are balanced by both rate of transcription and protein degradation. To determine whether the decreased Rnr2 levels observed in *ydj1*Δ cells was a result of increased Rnr2 degradation, we examined rate of Rnr2 loss in WT and *ydj1*Δ cells treated with cycloheximide, an inhibitor of transcription. Rnr2 loss was accelerated in *ydj1*Δ, suggesting increased instability of Rnr2 protein (Fig. 6A). Given this result, we tested the effect of substantially overexpressing Rnr2 in *ydj1*Δ cells using a multicopy *MET25* promoter driven plasmid. Interestingly, cells remained sensitive to HU (Fig. 6B). We analyzed the levels of Rnr2 from these cells and still observed a noticeable decrease in Rnr2 levels *ydj1*Δ cells compared to WT (Fig. 6C). Taken together, these results imply that the HU sensitivity seen in *ydj1*Δ is due to destabilized RNR components, independent of transcription.

Ydj1 interacts with Rnr2 in yeast and humans

Previous studies have demonstrated that Hsp90 and Hsp70 bind RNR components (25). Given that Ydj1 binds both Hsp70 and Hsp90 and plays a role in RNR activity, we sought to determine whether Ydj1 interacted with Rnr2 in yeast. We immunoprecipitated Rnr2 from cells and probed for the presence of Ydj1. Ydj1 was detected as an interactor of Rnr2 in both unstressed and HU-treated cells (Fig. 7A). Ribonucleotide reductase is an important chemotherapeutic target in cancer. We considered the possibility that R2B, the human homologue of Rnr2, might similarly interact with HDJ2 (human Ydj1). To examine this, we transfected HEK293 cells with HIS-epitope tagged R2B, purified the R2B complex

and probed for associated HDJ2. Interaction of the RNR subunit with HDJ2 was observed, consistent with a conserved role for the co-chaperone (Fig. 7B).

Hsp70-co-chaperone interaction is important for RNR activity

Hsp40-related co-chaperones bind to Hsp70 via conserved J-domains. The J domain is a 70-amino acid sequence consisting of four helices and a loop region between helices II and III that contains a highly conserved tripeptide of histidine, proline, and aspartic acid (the HPD motif). This region while not required for client protein binding, is absolutely essential for Hsp70-Hsp40 interaction, stimulation of the Hsp70 ATPase and release of substrates post-folding (109, 110). While several co-chaperones have chaperone-independent activities, Hsp40s typically function through activation of Hsp70. We reasoned that Ydj1's role in supporting RNR function would occur through its ability to bind Ssa1. We queried whether Ydj1 unable to bind Ssa1 (HPD motif mutant, Ydj1-D36N) could suppress the HU sensitive phenotype of *ydj1*Δ cells. Cells expressing Ydj1-D36N were HU-sensitive, suggesting Ssa1-Ydj1 interaction is critical for RNR activity (Fig. 8A). We carried out a parallel experiment in mammalian cells, utilizing a novel small molecule disruptor of Hsp70-Hsp40 interactions, 116-9e (111). Treatment of HEK293 cells with 116-9e for 72 hours resulted in decreased R2B levels as detected by Western Blot (Fig. 8B). These results, taken together suggest the Ssa1-Ydj1/Hsp70-HDJ2 interaction is critical for RNR subunit stability and resistance to RNR inhibiting drugs.

Inhibition of HDJ2 sensitizes cells to RNR inhibitors

Having established that either loss of Ydj1/HDJ2 compromises RNR activity in both yeast and mammalian cells, we considered whether this regulation might be used to sensitize cancer cells to HU. We examined the difference in drug sensitivity of WT cells compared to HDJ2 knockout cells created via CRISPR disruption. HDJ2 KO cells were markedly more sensitive than WT cells, with a 60% decrease in IC_{50}, from 180μM to 80μM (Figure 9A). These results suggested that 116-9e (inhibitor of HDJ2) may be synergistic with HU. We queried the difference in drug sensitivity of cells exposed to HU and DMSO compared to cells exposed to a combination of 116-9e and HU. The combination treatment was highly synergistic, promoting a decrease in apparent $IC_{50\ of}$ HU from 140μM to 89μM (Figure 9B). While HU has been widely utilized as an anticancer drug it has a short half-life in the body, relatively low affinity for RNR and cells tend to resistance over time. Triapine is a next generation RNR inhibitor, possessing high potency in cell and enzyme-based assays. We examined the difference in drug sensitivity of cells exposed to triapine and DMSO compared to cells exposed to a combination of 116-9e and triapine. The combination treatment was highly synergistic, promoting a decrease in apparent $IC_{50\ of}$ HU from 0.8μM to 0.4μM (Figure 9C). These data clearly suggest that HDJ2 inhibition can be used to sensitize cells to RNR inhibitors.

2.4 Discussion

Hsp70 co-chaperones regulate the cellular response to hydroxyurea

Hsp70 and Hsp90 bind a wide variety of client proteins, regulating many important signaling processes. Several studies have linked chaperone function to the DNA damage response and recently RNR activity (5, 7, 41, 112, 113). Given that co-chaperones direct the activity and specificity of Hsp70 and Hsp90 it is logical that a subset of co-chaperones are responsible for supporting RNR activity. In this study, we identified 4 co-chaperones as being important for HU resistance; Ydj1, Scj1, Erj5 and Zuo1. Scj1 and Erj5 are ER-localized Hsp70 co-chaperones that bind to the ER-specific Hsp70 isoform Kar2. Kar2 and its co-chaperones are responsible for ER-folding and degradation of proteins (ERAD). Given their spatial separation from RNR components, these co-chaperones may support RNR activity indirectly or may have totally separate roles in DNA damage signaling. Zuo1 is a ribosome-associated chaperone that activates the ATPase activity of Ssb1 and Ssb2, making it likely that Zuo1 influences the transcription of RNR subunits or regulators. We hope to shed light on the role of these proteins in the DNA damage response in future studies.

Ydj1 is required for RNR stability

Ydj1 is a well-characterized Hsp40 responsible for mediating a large proportion of Hsp70 and Hsp90 effects in yeast. We show here that loss of Ydj1 results in destabilization of Rnr2 and to a lesser degree, Rnr4. The loss of Rnr4 stability seen in *ydj1*Δ cells may be an indirect consequence of Rnr2 destabilization. Rnr2 and Rnr4 hetero-dimerize *in vivo*

and *in vitro* and they each support the others folding (35). This may explain why overexpression of Rnr2 alone in *ydj1*Δ cells fails to suppress their HU-sensitive phenotype. While the majority of co-chaperone function is mediated by interaction with chaperones such as Hsp90 and Hsp70, it is not unknown for co-chaperones to have chaperone-independent activities (114). Ydj1 binds to Ssa1 via the conserved HPD region, and here we demonstrate that this interaction is required for Ydj1-mediated HU resistance. This is consistent with our previous studies identifying a role for Hsp90 and Hsp70 in stabilizing Rnr2 and Rnr4 (25). These data suggest that either Ydj1 transports and transfers RNR components to Ssa1 or more likely exists in a complex with RNR and Ssa1 to maintain RNR activity.

Structural elements of Ydj1 required for HU resistance

Ydj1 is a well-characterized Hsp40 responsible for mediating a large proportion of Hsp70 and Hsp90 effects in yeast. Ydj1 exists as a dimer in yeast and contains several functional elements such as the J-domain, G/F domain, Zinc-finger-like domains and C-terminal domain (CTDII). It is interesting to note that the same C-terminal Ydj1 truncations that result in HU-sensitivity correspond with a previously observed loss of ability of cells to sustain high-temperature growth (102). To tease apart the role of the Ydj1 N-terminus in HU resistance, we utilized chimeras of Ydj1 and its paralog Sis1. Although Sis1 and Ydj1 possess the ability to bind Ssa1, loss of Sis1 is lethal for yeast, whereas loss of Ydj1 is not (104). Although individual replacement of either the N-terminal domain or G/F domain with the equivalent Sis1 domain had minimal impact on HU resistance, replacement of both domains simultaneously (SSY chimera) increased the cells sensitivity

to HU to a level almost equivalent to *ydj1*Δ cells. In addition, while *ydj1*Δ cells are HU sensitive, they are not as sensitive as *rnr4*Δ cells and are viable (unlike *rnr2*Δ cells), suggesting that loss of Ydj1 does not result in total loss of RNR function. This is in agreement with the data that shows partial but not complete destabilization of RNR levels in *ydj1*Δ cells. One potential explanation for this is that the related Sis1 co-chaperone is partially functionally redundant with Ydj1 and can contribute to some degree in RNR activity, particularly given the data shown in Figure 2B.

It is compelling that Ydj1 farnesylation is required for HU resistance, as it is not required to bind all client proteins and only a small proportion of Ydj1 is farnesylated at any one time (91). Farnesylation anchors Ydj1 to the exterior face of the endoplasmic reticulum (ER) where it functions to prevent the passage of aggregated proteins from mother to daughter cells during cell division (108). While no previous connection between ER function and RNR activity has been identified, it is interesting to note in this study cells lacking either of two ER specific co-chaperones Erdj5 and Scj1 are also HU sensitive. Although beyond the scope of this study, the interplay between ER co-chaperones and the DNA damage will be interesting to explore further.

HDJ2 regulates RNR in cancer cells

One advantage of working with budding yeast is that many proteins and pathways are functionally well conserved with humans. Suggesting broad conservation of the yeast mechanism, we demonstrate here that human Ydj1 (HDJ2) and human RNR2 (R2B) physically interact. Consistent with the yeast model, disruption of the HDJ2-Hsp70 interaction through the novel small molecule 116-9e results in R2B degradation.

Inhibition of HDJ2 as a viable strategy to sensitize cancer cells to RNR inhibitors

Yeast lacking Ydj1 display a destabilized RNR complex and corresponding sensitivity to HU. In turn, we demonstrate that we can sensitize a cancer cells to HU and the more potent triapine by either CRISPR-mediated gene knockout of HDJ2 or by inhibiting HDJ2 with 116-9e. HU was the first small-molecule RNR approved in 1967. HU and other agents, including the nucleoside analog gemcitabine (Gemzar) and triapine, remain important agents in cancer chemotherapy. These agents are commonly combined with radiotherapy and/or genotoxic chemotherapy, which potentiate RNR inhibitors via exposing the requirement for dNTPs in DNA repair (30, 94). It would be highly desirable to identify agents that can enhance the therapeutic benefit of RNR inhibitors without incurring additional toxicity. Several studies have demonstrated the antitumor potential of small molecule inhibitors of chaperones, particularly Hsp90 (9). Despite promising *in vitro* results several potent Hsp90 inhibitors such as 17-AAG have failed clinical trials due to solubility and toxicity issues (57). Creating clinically relevant Hsp70 inhibitors is also challenging, given that Hsp70 is responsible for both the stabilization and degradation of client proteins, many of which are required for cell viability in healthy cells. The 'holy grail' of chaperone-based translational research is how to modulate chaperone function in cells such that cancer cells are selectively targeted over healthy tissue. We show here that inhibition of HDJ2 (either by CRISPR-mediated knockout or 116-9e) sensitizes cells to the RNR inhibitors HU and triapine. While we anticipate future studies to examine the dosing and timing required to optimize cancer cell inhibition, this study demonstrates the validity of destabilizing select client proteins through Hsp70 co-chaperone inhibition.

2.5 Figures

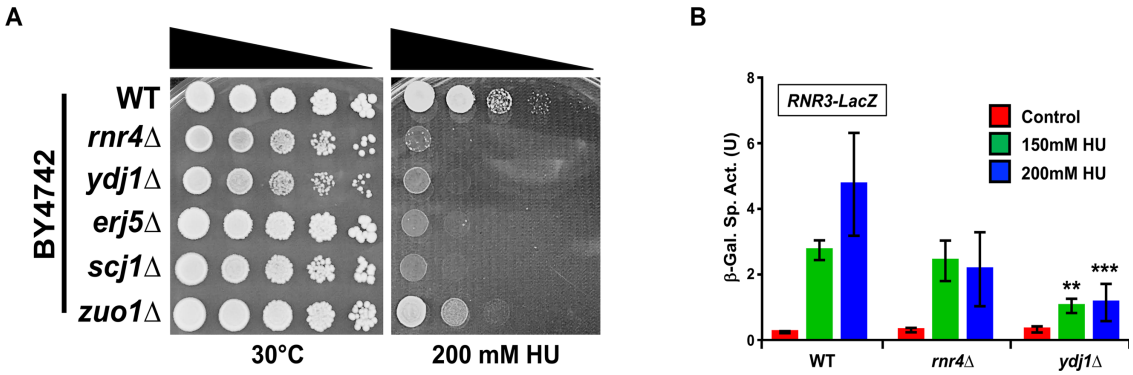

Figure 3. Loss of Ydj1 impairs the DNA damage response.
(A) Yeast lacking selected Hsp70 co-chaperones are sensitive to HU. WT BY4742 or BY4742 cells lacking Rnr4, Ydj1, Erjd5, Scj1 and Zuo1 were grown overnight to saturation and serial 10-fold dilutions were plated by pin plating from 96-well plates onto YPD alone or YPD containing 200 mM HU. Plates were imaged after 3 days. (B) Cells lacking Ydj1 are compromised for DNA damage response pathway transcription. An RNR3-LacZ reporter plasmid was transformed into the indicated yeast strains. Transformants were grown and subjected to 0, 150mM or 200mM HU for 3 hours. β-Galactosidase activity was measured in crude extracts. β-Galactosidase specific activity (in units) [-Gal Sp. Act. (U)] is shown on the y axis. Each value represents the mean and standard deviation (error bar) from three independent transformants; **, P≤0.01; ***, P≤0.001 as compared to WT cell controls.

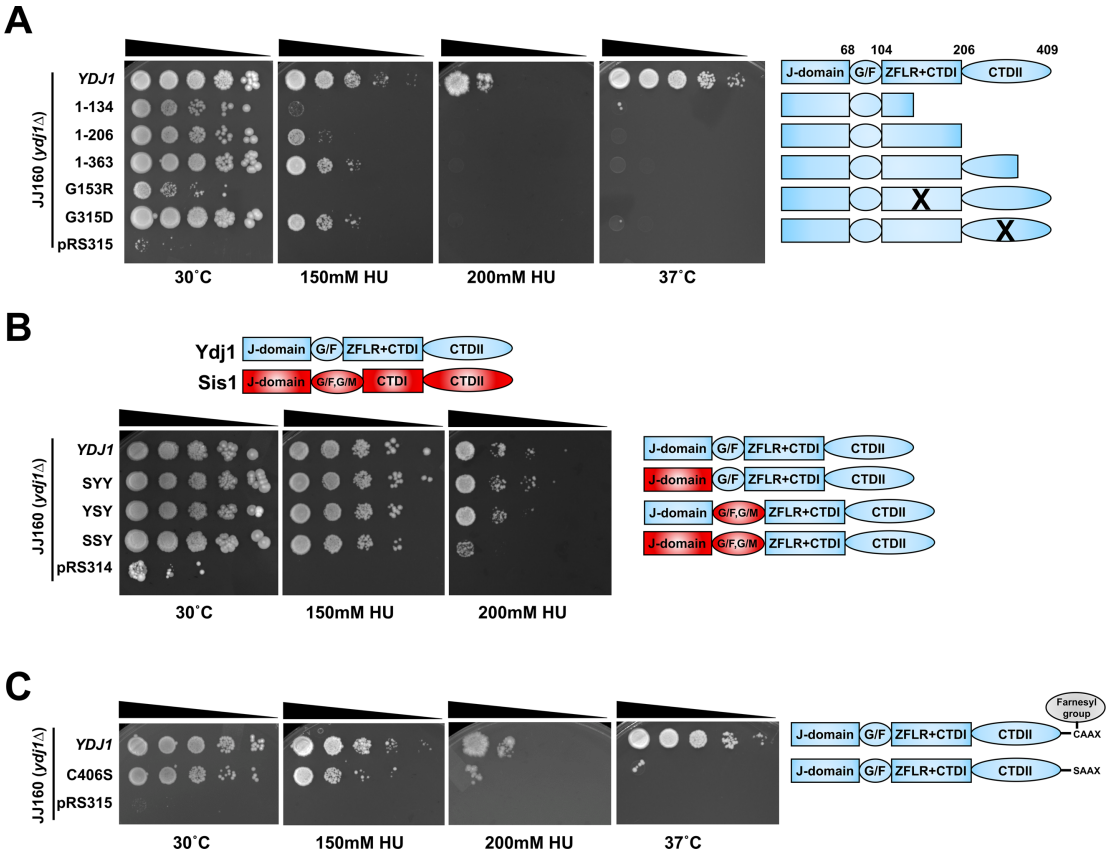

Figure 4. Ydj1 domains required for cellular resistance to HU.
(A) The Ydj1 C-terminus is required for HU resistance. JJ160 ydj1Δ cells transformed with plasmids encoding full-length Ydj1, truncations of Ydj1 or control plasmid pRS315 were grown to exponential phase, then 10-fold serially diluted onto media containing indicated stressor. Plates were imaged after 3 days. (B) Sis1 and Ydj1 domains are partially interchangeable for HU resistance. JJ160 ydj1Δ cells transformed with plasmids encoding full-length Ydj1 or indicated Ydj1-Sis1 fusions were grown to exponential phase, then 10-fold serially diluted onto media containing indicated stressor. Plates were imaged after 3 days. Domains of Ydj1 are colored blue, domains of Sis1 are colored red. (C) Farnesylation impacts Ydj1-mediated HU resistance. JJ160 ydj1Δ cells transformed with plasmids encoding WT Ydj1 or farnesylation-deficient mutant C406S were grown to exponential phase, then 10-fold serially diluted onto media containing indicated stressor. https://doi.org/10.1371/journal.pgen.1007462.g002

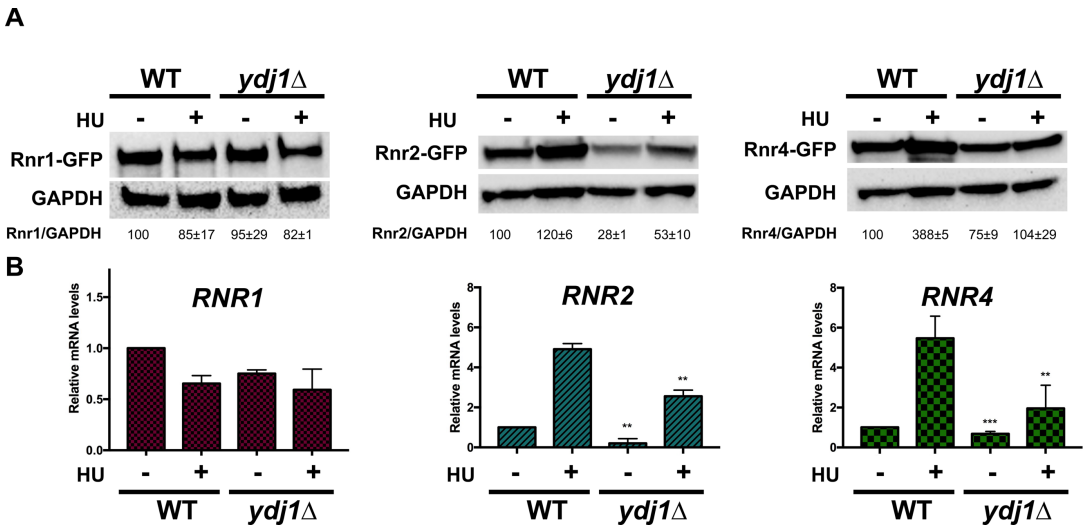

Figure 5. RNR subunit levels in cells lacking Ydj1.
(A) BY4742 WT or ydj1Δ cells expressing endogenously tagged Rnr1-GFP, Rnr2-GFP or Rnr4-GFP were grown to exponential phase and were either left untreated or were treated with 200mM HU for 3 hours. Cell extracts were obtained, resolved on SDS-PAGE gels and analyzed by immunoblotting with anti-GFP and GAPDH antibodies. (B) Quantitation of RNR1, RNR2 and RNR4 transcription in WT or ydj1Δ cells. Levels of RNR1, RNR2 and RNR4 mRNAs in BY4742 WT or ydj1Δ cells were determined by reverse transcription and RT-qPCR. Signals of RNR1, RNR2 and RNR4 were normalized against that of ACT1 in each strain, and the resulting ratios in WT cells were arbitrarily defined as onefold. Data are the average and SD from three replicates.

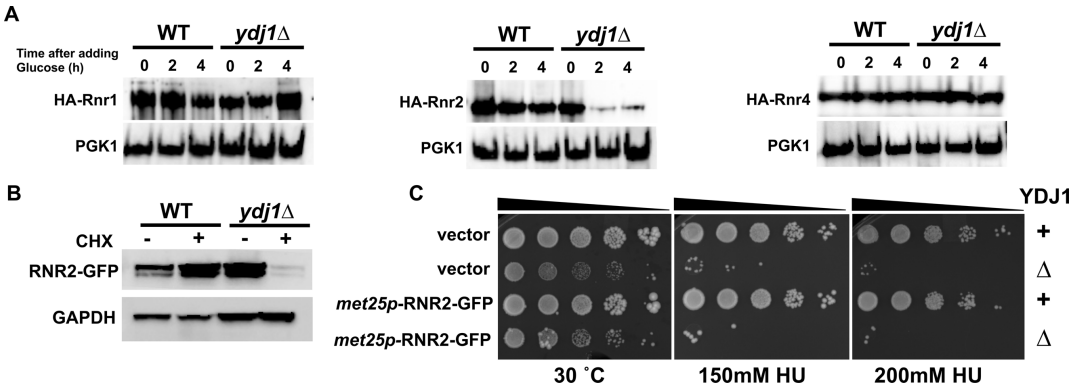

Figure 6. Rnr2 is destabilized in ydj1Δ cells.
(A) RNR subunit stability is compromised in cells lacking Ydj1. BY4742 WT or ydj1Δ cells transformed with either pGAL1-HA-Rnr1, 2 or 4 plasmids were grown to mid-log phase in YP Galactose medium. Transcription of pGAL1-HA-Rnr1, 2 or 4 was shut off by addition of 2% glucose to cultures. Cell lysates from these samples were analyzed by Western Blotting for stability of HA-RNR subunit (HA antibody) and loading control (PGK1). (B) Examination of Rnr2 stability in WT ydj1Δ cells after translational inhibition. BY4742 WT and ydj1Δ cells expressing endogenous promoter GFP-tagged Rnr2 were grown to exponential phase in YPD media and then treated with 200 μg/ml cycloheximide for 6 hours to halt protein translation. Cell lysates were obtained and analyzed via Western Blotting for GFP-Rnr2 (GFP antibody) and a GAPDH loading control (GAPDH antibody). (C) Overexpression of Rnr2 does not suppress the HU sensitive phenotype of ydj1Δ cells. WT and ydj1Δ cells were transformed with either control plasmid pUG36 or met25p-RNR2-GFP. Transformants were grown overnight to saturation and serial 10-fold dilutions were plated by pin plating from 96-well plates onto YPD alone or YPD containing 200 mM HU. Plates were imaged after 3 days.

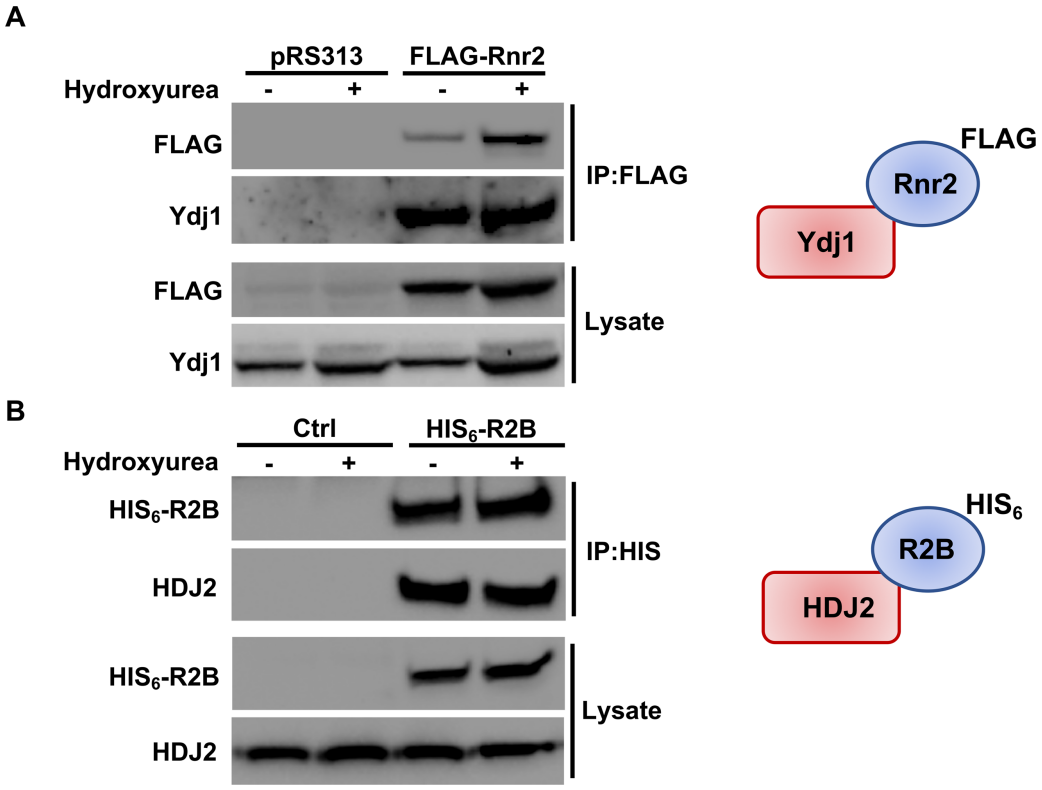

Figure 7. RNR interacts with Hsp40 in yeast and mammalian cells.
(A) Rnr2 interacts with Ydj1 in yeast. WT cells transformed with either pRS313 or plasmid expressing FLAG-tagged Rnr2 were grown to exponential phase and were either left untreated or were treated with HU as in Fig 3. Cell extracts (lysate) and immunoprecipitates (IP) with anti-FLAG M2 magnetic beads were subjected to SDS-PAGE and analyzed by immunoblotting with anti-FLAG antibodies to detect Rnr2 or anti-Ydj1 antibodies to detect Ydj1. (B) R2B interacts with HDJ2 in mammalian cells. HEK293 cells were transfected with a plasmid expressing CMV-driven HIS6-tagged R2B. Cells extracts were obtained 48 hours post-transfection. Cell extracts (lysate) and immunoprecipitates (IP) with HIS-dynabeads were subjected to SDS-PAGE and analyzed by immunoblotting with tetra-HIS antibodies to detect R2B or anti-HDJ2 antibodies to detect HDJ2.

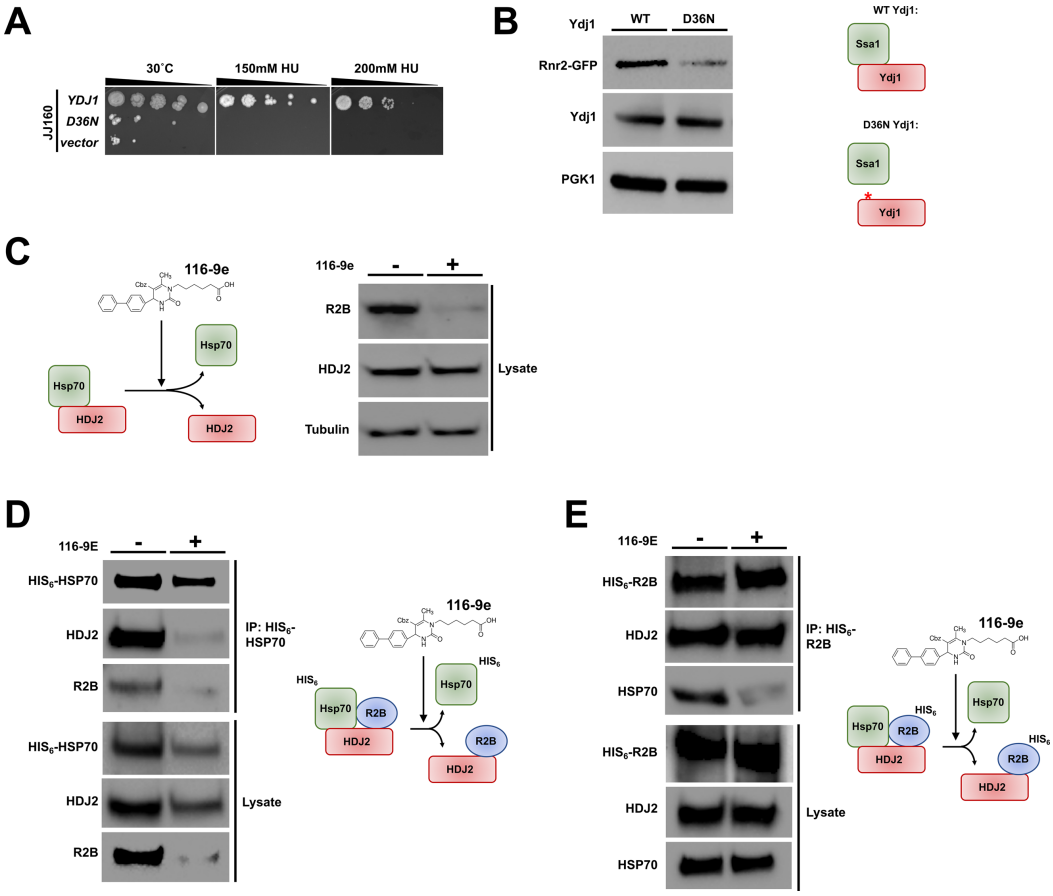

Figure 9. Disruption of the Hsp70-Hsp40 interaction impacts RNR function.
(A) Mut8tion of the HPD motif in Ydj1 sensitizes cells to HU. ydj1Δ cells transformed with either a control plasmid, WT YDJ1 plasmid or YDJ1-D36N plasmid were grown overnight to saturation and serial 10-fold dilutions were plated by pin plating from 96-well plates onto YPD alone or YPD containing 200 mM HU. Plates were imaged after 3 days. (B) Mutation of the HPD motif in Ydj1 promotes Rnr2 degradation. ydj1Δ RNR2-GFP cells transformed with either a WT YDJ1 or YDJ1-D36N plasmid were grown to mid-log phase. Cell extracts were resolved by SDS-PAGE and analyzed by immunoblotting with anti-GFP, anti- Ydj1and anti-GAPDH antibodies. (C) Inhibition of the Hsp70-HDJ2 interaction in cancer cells promotes R2B degradation. HEK293 cells were grown to mid-confluence and then treated with 40 μM 116-9e for 72 hours. Cell extracts were subjected to SDS-PAGE and analyzed by immunoblotting with anti- R2B or anti-GAPDH antibodies. (D) 116-9E disrupts both the HSP70-HDJ2 and HSP70-R2B interaction. HEK293 cells transfected with a plasmid expressing HIS6-HSP70 were treated with 116-9E as in (C). HIS-HSP70 complexes were purified from extracts made from these cells, were subjected to SDS-PAGE and were analyzed by immunoblotting with anti-HIS, anti-R2B or anti-HDJ2 antibodies. (E) 116-9E disrupts the R2B-HSP70 interaction but leaves the R2B-HDJ2 interaction intact. HEK293 cells transfected with a plasmid expressing HIS6-R2B were treated with 116-9E as in (C). HIS-R2B complexes were purified from extracts made from these cells, subjected to SDS-PAGE and were analyzed by immunoblotting with anti-HIS, anti-R2B or anti-HDJ2 antibodies.

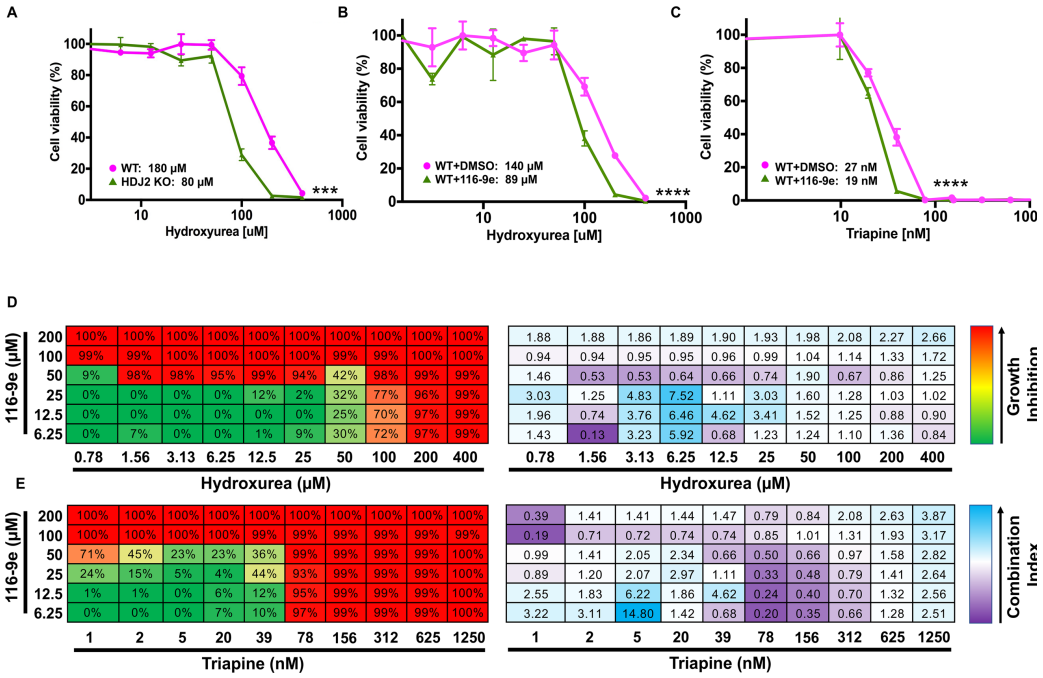

Figure 9. Inhibition of HDJ2 is synergistic with clinically utilized RNR inhibitors.
(A) HDJ2 CRISPR KO cells are more sensitive to HU than WT cells. HAP1 WT and HDJ2 CRISPR KO cells were treated with serial dilutions of HU for 3 days. Cell viability was determined using Celltiter-Glo assay and results shown are average and SD from three replicates (***P<0.001 compared to WT cells, t-test). (B) 116-9e synergizes with HU treatment. HAP1 cells were treated with either DMSO (control) or 116-9e for 24 hours in combination with serial dilutions of HU for 3 days. Data are the average and SD from three replicates (****P<0.0001 compared to HU only treated cells, t-test). (C) 116-9e synergizes with triapine treatment. HAP1 cells were treated with either DMSO (control) or 116-9e for 24 hours, then further treated with serial dilutions of triapine for 3 days. Data are the average and SD from three replicates (***P<0.0001 compared to triapine treated cells, t-test). (D) Combination assay for 116-9e and HU. HAP1 cells were treated with combinations of 116-9e and HU for 72 h and growth inhibition was determined using CellTiter-Glo assay. Combination Index (CI, measure of drug synergy) was determined using Chou-Talalay method via Compusyn software. CI values of <1 indicate drug synergy. (E) Combination assay for 116-9e and triapine. HAP1 cells were treated with combinations of 116-9e and triapine for 72 h and growth inhibition was determined using CellTiter-Glo assay. Combination Index (CI, measure of drug synergy) was determined using Chou-Talalay method via Compusyn software. CI values of <1 indicate drug synergy.

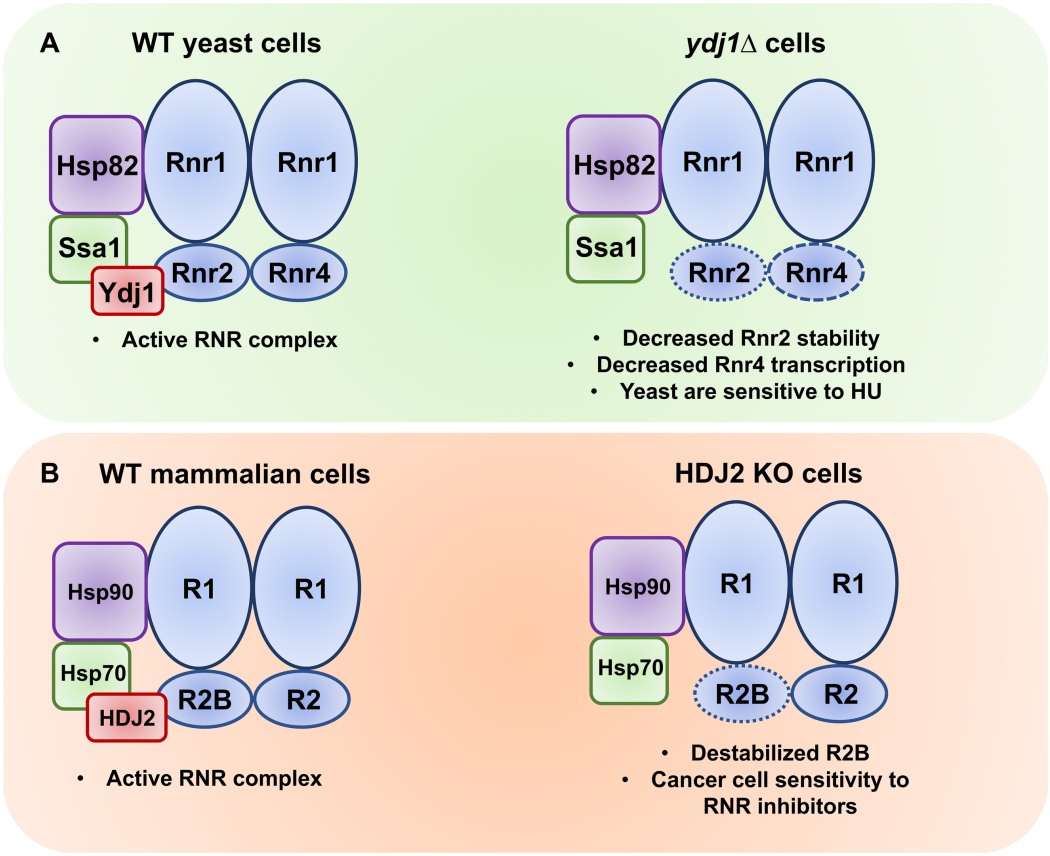

Figure 10. Ydj1/HDJ2 support RNR activity in yeast and mammalian cells.
(A) In yeast, Ssa1, Hsp82 and Ydj1 bind and stabilize the RNR complex allowing dNTP synthesis required cell cycle progression and DNA repair. Loss of Ydj1 in yeast results in lowered Rnr2 levels (increased Rnr2 degradation) and Rnr4 (decreased RNR4transcription). (B) In mammalian cells, HSP70, HSP90 and HDJ2 bind and stabilize the RNR complex allowing dNTP synthesis required cell cycle progression and DNA repair. Loss of HDJ2 activity (through either CRISPR-mediated deletion or 116-9e) promotes lowering of R2B levels, sensitizing cells to RNR-inhibiting agents such as HU and triapine.

CHAPTER 3: UNDERSTANDING CYTOSOLIC HSP70 ISOFORM-SPECIFIC REGULATION OF THE RIBONUCLEOTIDE REDUCTASE COMPLEX

3.1 Introduction

Heat Shock Protein 70 (Hsp70) is a highly conserved, essential molecular chaperone. Hsp70 is responsible for stabilization, folding and degradation of a large majority of the proteome (2, 47, 59). Overall, Hsp70 is required for the stability of several housekeeping proteins, and thus essential for cell viability (2). It is well known that Hsp70 is vital for cancer cell proliferation in order to maintain the function of unstable oncoproteins and its overexpression is associated with cancer including breast and prostate cancer (14, 85, 86).

Organisms possess numerous highly similar isoforms (115). The model organism, *S. cerevisiae* (budding yeast) contains 4 cytosolic Hsp70 isoforms from the Stress Seventy sub-family A (SSA) consisting of; Ssa1, 2, 3 and 4 (115-119). Previously, Hsp70 isoforms were thought to be functionally indistinguishable apart from spatio-temporal expression pattern, however recent findings suggest unique functions for Ssa isoforms (115, 116).

Ssa isoforms arose from genome duplication and are highly conserved, with Ssa1 sharing 99%, 84% and 85% amino acid identity with Ssa2, 3 and 4, respectively (115). Hsp70 isoforms contain 2 domains; a nucleotide-binding domain (NBD) and a substrate-binding domain (SBD) connected by a flexible linker region (115-119). The most prominent difference between the Ssa1-4 isoforms is their expression levels; Ssa1/2 are expressed constitutively at high levels whereas Ssa3/4 are only expressed during cell stress (61-64, 115, 120). Hsp70 chaperones do not work alone but are assisted by a suite of co-

chaperones (47, 59, 60). Co-chaperones are comprised of J-proteins and nucleotide exchange factors (NEFs) that facilitate the stimulation of Hsp70 activity promoting transfer and folding of client proteins (47, 60, 121).

In this study, in order to better understand functional differences between Ssa1-4, we utilized the model chaperone client Ribonucleotide Reductase (RNR). RNR is an enzyme that is important for the production of deoxyribonucleotides (dNTPs) which are used in DNA synthesis and repair (122). RNR is comprised of two diverse subunits, the large subunit R1 (R1 in vertebrates, Rnr1/Rnr3 in yeast) which contains the allosteric regulatory sites (123) and the small subunit R2 (R2/R2B in vertebrates, Rnr2/Rnr4 in yeast) which consists of a cell cycle regulated binuclear iron center and a tyrosyl free radical (30-34). Due to its crucial role in maintenance of genome integrity and subsequently cell survival, RNR is an attractive target in cancer treatments (30, 33, 36). Several RNR inhibitors have been developed and used in a clinical setting including hydroxyurea (HU), triapine and gemcitabine (30, 37, 38, 124).

Previous studies in both yeast and mammalian cells have identified Hsp70 as an important regulator of RNR and chaperone inhibitors such as 17-AAG trigger RNR subunit degradation (25, 125, 126). Consequently, Hsp70 inhibition sensitizes cancer cells to gemcitabine, which has the potential to be a novel anti-cancer therapeutic (25, 41-43, 125, 126). Recently, the co-chaperone Ydj1/HDJ2 (yeast/mammalian) was identified to assist Hsp70 in the regulation of RNR. Lack of Ydj1 in *S. cerevisiae* resulted in reduced RNR2 subunit expression and stability (125, 126). This interaction was found to be conserved in humans, where HDJ2 and R2B assist RNR complex stability and activity in mammalian cells (125, 126). Additionally, inhibition of HDJ2 with 116-9e, a small molecule inhibitor

that blocks Hsp40 binding to Hsp70 through the J-domain resulted in disruption of R2B-HDJ2 interaction and sensitized cells to HU and triapine (125, 126).

Interestingly, recent findings have shown that Hsp70 isoform binds and regulates specific set of client proteins (80, 127, 128). Hsp70 isoforms maintaining unique sets of clients could dictate their different roles propagating cellular homeostasis and function. Since Ssa1-4 are all able to sustain cellular function under "normal" conditions it is important to investigate the differences between these isoforms by examining their capacity under stress conditions such as DNA Damage. In this study, we identify constitutively expressed Ssa1 and Ssa2 as regulators of RNR activity in yeast whereas Ssa4 expressing cells were sensitized to DNA damaging agents. Moreover, we demonstrate that both diminished interaction with Ydj1 and possible differential binding between Ssa4 and RNR contribute to sensitization to HU in cells solely expressing the stress induced Hsp70 isoform.

3.2 Materials and Methods

Yeast Strains and growth conditions

Yeast cultures were grown in either YPD (1% yeast extract, 2% glucose, 2% peptone) or grown in SD (0.67% yeast nitrogen base without amino acids and carbohydrates, 2% glucose) supplemented with the appropriate nutrients to select for plasmids and tagged genes. Escherichia coli DH5α was used to propagate all plasmids. E. coli cells were cultured in Luria broth medium (1% Bacto tryptone, 0.5% Bacto yeast extract, 1% NaCl) and transformed to ampicillin resistance by standard methods. Hsp70 isoform plasmids pRS315P_{SSA2}-SSA1, pRS315P_{SSA2}-SSA2, pRS315P_{SSA2}-SSA3,

pRS315P$_{SSA2}$-SSA4 (129) were transformed into yeast strain ssa1–4Δ (69) using PEG/lithium acetate. After restreaking onto media lacking leucine, transformants were streaked again onto media lacking leucine and containing 5-fluoro-orotic acid (5-FOA), resulting in yeast that expressed Hsp70 isoforms as the sole cytoplasmic Hsp70 in the cell. For tagging the genomic copy of RNR1, RNR2 and RNR4 with a HA epitope at the carboxy-terminus, the pFA6a-HA-His3MX6 plasmid was used. A full table of yeast strains and plasmids that were used can be found in S1-2 Tables (Figure 17). For serial dilutions, cells were grown to mid-log phase, 10-fold serially diluted and then plated onto appropriate media using a 48-pin replica-plating tool. Images of plates were taken after 3 days at 30°C. 200mM HU was used for serial dilutions and to stress yeast cells, a concentration established in Tkach et al. (130).

For IC_{50} calculations, cells were grown to mid-log phase, diluted in a sterile 96 well plate in media containing HU 10-fold serially diluted. Cells were continuously shaken for 24 hours at 30^{o}C and the optical density of the reaction was measured at 600nm. The mean and standard deviation from three independent transformants were calculated.

β-Galactosidase assays

For RNR3-lacZ fusion expression experiments, *Ssa1-4*Δ yeast cells were grown overnight in SD-URA media at 30°C and then re-inoculated at OD600 of 0.2–0.4 and then grown for a further 4 hours. Cells were treated with 150 mM or 200 mM HU for 3 hours and then RNR3- lacZ fusion assays were carried out as described previously in Truman et al. (100). Briefly, protein was extracted through bead beating and protein was quantitated via Bradford assay. The b-Galactosidase reaction containing 50 μg of protein extract in 1

ml Z-Buffer (30) was initiated by addition of 200 µl ONPG (4 mg/ml) and incubated at 28°C until the appearance of a pale-yellow color was noted. The reaction was quenched via the addition of 500 µl Na2CO3 (1M) solution. The optical density of the reaction was measured at 420nm. β-Gal activity was calculated using ((OD420 x 1.7)/(0.0045 x protein x reaction time)), where protein is measured in mg, and time is in minutes. The mean and standard deviation from three independent transformants were calculated.

Gal promoter shut off experiments

*Ssa1-4*Δ yeast cells containing either Ssa1, 2, 3 or 4 as the sole Hsp70 isoform were transformed with either pGAL1-HA-Rnr1, 2 or 4 plasmids were grown to mid-log phase in YP Gal medium (1% yeast extract, 2% galactose, 2% peptone). Transcription of pGAL1-HA-Rnr1, 2 or 4 was shut off by addition of 2% glucose to cultures. Aliquots of cells were collected at 0 and 4 hours after addition of glucose. Cell lysates from these samples were analyzed by Western Blotting for stability of RNR subunit (HA antibody) and loading control (GAPDH).

Western blotting

Protein extracts were made as described (Kamada et al., 1995). 20 µg of protein was separated by 4%–12% NuPAGE SDS-PAGE (Thermo) (131). Proteins were detected using the following antibodies; anti-HA tag (Thermo #26183), Anti-FLAG tag (Sigma, #F1365), anti-GAPDH (Thermo #MA5-15738), anti-Ydj1 (StressMarq #SMC-166D).

Blots were imaged on a ChemiDoc MP imaging system (Bio-Rad). After treatment with SuperSignal West Pico Chemiluminescent Substrate (GE). Blots were stripped and re-probed with the relevant antibodies using Restore Western Blot Stripping Buffer (Thermo).

Purification of HA-tagged Rnr1, 2 and 4 from yeast

*Ssa1-4*Δ yeast cells containing integrated with HA epitope of RNR1, RNR2 and RNR4 transformed with Ssa1-4 pRS315 plasmids were grown overnight in SD-LEU media, and then reinoculated into a larger culture of selectable media and grown to an OD600 of 0.800. The cells were then either unstressed or stressed with 200 mM HU for four hours. Cells were harvested and FLAG-tagged proteins were isolated as follows: Protein was extracted via bead beating in 500 µl binding buffer (50 mM Na-phosphate pH 8.0, 300 mM NaCl, 0.01% Tween-20). 200 µg of protein extract was incubated with 30 µl anti-HA magnetic beads (Sigma) at 4°C overnight. Anti-HA beads were collected by magnet then washed 5 times with 500 µl binding buffer. After the final wash, the buffer was aspirated and beads were incubated with 65 µl Elution buffer (binding buffer supplemented with 10 µg/ml 3X HA peptide (Apex Bio)) for 1 hour at 4° C, then beads were collected via magnet. The supernatant containing purified HA-RNR1, 2, and 4 were transferred to a fresh tube, 25 µl of 5x SDS-PAGE sample buffer was added and the sample was denatured for 5 min at 95° C. 20 µl of sample was analyzed by SDS-PAGE.

Quantitation of yeast RNR subunit transcription

Quantitation of yeast RNR transcription was carried out as in Zhang et al. (132). Briefly, *Ssa1-4*Δ yeast cells were grown overnight in YPD media at 30°C, re-inoculated at

OD600 of 0.2–0.4 and then grown for a further 4 hours. Cells were treated with 200 mM for 2 hours and total RNA was extracted from cells using a GeneJet RNA extraction kit. Total RNA (1 μg) was treated with 10 units of RNase-free DNase I (Thermo) for 30 min at 37°C to remove contaminating DNA. DNAse I activity was stopped by adding 1 μL of 50 mM EDTA and incubating at 65°C for 10 minutes. cDNA synthesis was carried out by iScript reverse transcriptase (BioRad) on aliquots of 1 μg RNA. The single-stranded cDNA products were used in qPCR on an ABI Fast 2000 real-time PCR detection system based on SYBR Green fluorescence. Sequences of oligo pairs (same as used in (132)) are listed in S1 Table. Signals of RNR1, RNR2 and RNR4 were normalized against that of ACT1 in each strain and the resulting ratios in WT cells were defined as onefold.

Yeast Two Hybrid Analysis

*Ssa1-4*Δ cells were transformed with the appropriate Two-hybrid plasmids (see Figure 16). Interaction strength was measured via β-galactosidase assays (Millson et al., 2005).

3.3 Results

Stress inducible Ssa3 and Ssa4 isoforms are sensitive to DNA damaging agents

It is not well understood why cells contain multiple variants of Hsp70 and whether they maintain identical roles within maintenance of cellular processes. It is well known that Hsp70 mediates the DNA damage response by interacting with RNR and other important DDR players. In order to better understand the unique roles of the yeast Hsp70 isoforms

Ssa1-4 within the regulation of the DDR, we screened cells expressing either Ssa1, 2, 3 or 4 (using the Ssa2 promoter) as the sole cytosolic Hsp70 against various DNA damaging agents including hydroxyurea (HU), methyl methanesulfonate (MMS), 5-fluorouracil (5-FU), and ultraviolet light (UV) (Figure 11A). Cells containing only Ssa1 or Ssa2 were resistant to all of the DNA damaging agents as well as heat stress (37^{o}C). The Ssa3 isoform showed increased sensitivity to all of the stresses and Ssa4 appeared to only be sensitive to DNA damaging agents while remaining resistant to heat stress. Because Ssa3 appeared to be slow growing even at normal temperatures we wanted to next calculate the IC50s for each of the isoforms (Figure 11B). We decided to focus our efforts on understanding resistance to hydroxyurea since RNR is a well characterized model client of Hsp70. Interestingly, the IC50 of HU for both Ssa3 and Ssa4 isoforms appeared to be lowered as compared to Ssa1 and Ssa2, however only Ssa4 showed a statistically significant decreased.

Ssa1 isoforms differentially support DDR-mediated transcription.

HU is a potent activator of the DNA damage response pathway, triggering transcription of DNA repair enzymes. In an effort to determine whether Ssa1-4 all control transcriptional output of the DNA damage response, we compared expression of β-galactosidase driven by a DNA-damage responsive promoter (RNR3 promoter-lacZ) in HU-treated cells expressing (Ssa2 promoter) only Ssa1, 2, 3 or 4. In cells containing Ssa1, 2 and 4 all showed significant induction ($p < 0.0001$) of RNR3 transcription suggesting activation of the DNA damage response upon treatment of HU (Figure 11C). Cells containing only Ssa3 showed significant decreased ($p < 0.05$) induction of RNR3-LacZ.

Surprisingly, cells containing Ssa4 as the sole isoform showed increased levels of RNR-LacZ for both untreated and HU treatments as compared to Ssa1 and Ssa2 cells ($p < 0.0001$).

RNR subunit transcription and stability is compromised in cells only expressing Ssa3 or Ssa4

Since it was previously shown that Hsp70 was necessary for RNR stability in both yeast and humans we wanted to test if all the Ssa1-4 isoforms shared equal roles in this. We integrated HA-epitope tags onto RNR subunits queried the total levels of Rnr1, Rnr2 and Rnr4 protein in cells expressing either Ssa1, 2, 3 or 4 (using the Ssa2 promoter) as the sole isoform. While Rnr1 levels were unchanged, Rnr2 and Rnr4 levels were compromised in cells containing only Ssa3 and Ssa4 under both unstressed and hydroxyurea treated cells (Figure 12A). Protein levels in cells are balanced by both rate of transcription and protein degradation. To determine whether the decreased RNR subunit expression observed in Ssa3 and Ssa4 cells was a result of altered transcription, we quantified RNR1, RNR2 and RNR4 mRNA expression in using RT-qPCR. RNR4 transcription were partially decreased in cells in cells expressing only Ssa3 and Ssa4 (Figure 12B). To determine whether the protein stability of Rnr1, Rnr2 and Rn4 had also been compromised Ssa3 and Ssa4 cells, we examined the half-life of these proteins by transcriptional shut-off experiments. While Rnr1 and Rnr4 stability were unchanged inSsa3 and Ssa4 cells significantly, Rnr2 stability was substantially lowered (Figure 12C).

RNR displays a binding preference for Ssa1 and Ssa2

Hsp70 has been shown to play an essential role in the regulation and stability of the RNR complex. In order to determine if RNR instability was a consequence of lack of interaction between the RNR subunits and the individual Hsp70 isoforms. We assessed physical interaction between Rnr1, Rnr2 and Rnr4 proteins and Ssa1, 2, 3, and 4 by yeast two-hybrid analysis. Rnr1-AD showed similar interaction patterns with Ssa1, 2, 3 and 4 (Figure 13). Rnr2-AD associated most strongly with Ssa1-BD and Ssa2-BD and showed significantly lower association with Ssa3-BD and Ssa4-BD (Figure 13). This pattern between Ssa1-4 was consistent for Rnr4-AD as well (Figure 13).

RNR-Ydj1 interaction is weaker in cells solely expressing Ssa3 and 4

Previous studies have demonstrated that Ydj1 regulates Hsp70-RNR interaction. Given that Ydj1 binds to Hsp70 and plays a role in RNR activity, we sought to determine whether this interaction was conserved between Ssa1-4. We immunoprecipitated HA tagged Rnr1, Rnr2, Rnr4 from cells and probed for the presence of Ydj1. Ydj1 interacted with Rnr1 equally in Ssa1-4 cells in both unstressed and HU-treated cells (Figure 14). Interestingly, Ydj1 interaction was significantly decreased with both Rnr2 and Rnr4 in cells solely expressing Ssa3 and Ssa4 in both unstressed and HU-treated cells (Figure 14).

The C-terminus of Ssa2 is required for HU resistance

Hsp70 is comprised of 2 domains connected by a flexible linker. The N-terminus is comprised of the Nucleotide binding domain (NBD) while the C-terminus is the Substrate binding domain (SBD). We previously saw that cells solely expressing the Ssa2 isoform were resistant to DNA damaging drugs while cells solely expressing the Ssa4 isoform were sensitive. Ssa2 and Ssa4 share 84% sequence similarity with the SBD being the highest variable region (Figure 15A). To query the structural requirement for Ssa2-mediated HU resistance, we analyzed an array of Ssa2-Ssa4 chimeras (116) and their resistance to HU containing media. Ssa24 is constructed of the N-terminus of Ssa2 and the C-terminus of Ssa4 and vice-versa for the Ssa42 construct. From the serial dilution, Ssa24 displays similar sensitivity to HU as Ssa4 while Ssa42 appeared to be HU resistant (Figure 15B). In an effort to determine whether the C-terminus of Ssa2 controlled transcriptional output of the DNA damage response, we again compared expression of β-galactosidase driven by a DNA-damage responsive promoter (RNR3 promoter-lacZ) in HU-treated cells expressing Ssa2, Ssa4, Ssa24 and Ssa42. Interestingly, Ssa24 displayed similar increase in RNR3 promoter activation that is seen in Ssa4 (Figure 15C).

3.4 Discussion

Yeast Hsp70 constitutive isoforms regulate the cellular response to hydroxyurea

Hsp70 has been shown to be an important regulator of the DNA damage response and RNR activity (125, 126). Recently, the cytosolic co-chaperone Ydj1 was shown to play an important role in the regulation of RNR (125, 126). There are four cytosolic Hsp70

isoforms in yeast (Ssa1-4) which were previously only thought to differ in expression levels in the cell. However, several recent studies have suggested unique roles for the isoforms in various mechanisms (115, 116, 133-135). In this study, we identified constitutively expressed Ssa1 and Ssa2 to be resistant to several DNA damaging agents including HU, MMS, 5-FU and UV radiation when expressed as the sole Hsp70 isoforms in the cell. Conversely, stress induced isoforms Ssa3 and Ssa4 were sensitive to all four DNA damaging treatments. In order to determine if Ssa3 and Ssa4 were sensitive to another stress we heat shocked the cells at 37ºC. Interestingly, only Ssa3 showed susceptibility to heat which suggest that it may just be defective in general cellular function compared to the other isoforms. In order to further examine this, we decided to calculate IC50s for the isoforms and focused our efforts on the RNR inhibitor drug hydroxyurea. Surprisingly, while the IC50 for Ssa3 was lower than both the constitutive isoforms, the IC50 for Ssa4 was significantly subjacent to all other isoforms.

Ssa isoforms contribute differentially to the DNA damage response

Previously it has been shown that Hsp70 regulates several steps in the DNA damage response signaling pathways (125, 126). In order to determine if the DDR is activated equally by the Ssa isoforms we measured the DNA-damage induced transcription (RNR3 promoter-lacZ) in untreated and HU treated cells expressing either Ssa1, 2, 3, or 4 as the sole isoform. Interestingly, in cells only expressing Ssa4 the DDR pathway appeared to be overactivated when compared to that in Ssa1 and 2 cells. This may suggest that the defect in Ssa4 cells exists near the terminus of the DDR pathway, possibly with activation or regulation of the RNR complex. In cells expressing solely Ssa3 the induction of RNR3

promoter-lacZ was significantly lower than the other isoforms. These findings may suggest that Ssa3 is deficient in regulation and activation of several steps of the DDR pathway.

Ssa1 and Ssa2 are required for both RNR subunit expression and stability

Hsp70 and its corresponding co-chaperone Ydj1 have been shown to play a role in stabilization of the RNR subunits in both yeast and human cells (125, 126). We show here that in cells solely expressing Ssa3 and Ssa4 results in lowered RNR expression via both transcription and protein stability. RNR4 mRNA expression is significantly decreased in Ssa3 and Ssa4 cells. RNR1 expression remains unchanged between Ssa1-4 isoforms which suggest the role in transcription is specific. Interestingly mRNA expression is slightly increased in Ssa3 and Ssa4 cells. Additionally, in cells solely expressing Ssa3 and Ssa4, levels of Rnr2 are significantly decreased as compared to Ssa1 and Ssa2. Rnr4 levels were affected in a less significant manner; Ssa3 and Ssa4 cells show a decrease in Rnr4 only in HU-treated cells. In order to further examine why protein levels of Rnr4 are lower in Ssa3 and Ssa4 cells while their mRNA expression levels are increased, we investigated the stability of the RNR subunits. Interestingly, both Rnr2 and Rnr4 half-lives were decreased in Ssa3 and Ssa4 cells as compared to the constitutive isoforms. This may explain the decreased Rnr4 protein levels seen in Ssa3 and 4 cells under HU treatment and the dramatically lower Rnr2 protein levels.

Ssa-RNR binding differences may be explained by Ydj1

Loss of the co-chaperone Ydj1 was shown to destabilize the RNR complex (125, 126). It is not well understood if the co-chaperones interact equally with the Ssa1-4 isoforms. Here

we show that in cells solely expressing Ssa3 and Ssa4, Ydj1 interacts with both Rnr2 and Rnr4 at significantly lower levels in both untreated and HU treated cells as compared to Ssa1 and 2. Interaction with Rnr1 was similar for all of the isoforms. The decreased affinity for Ydj1 to bind to Rnr2 and Rnr4 may suggest destabilization of the RNR complex and subsequently sensitivity to DNA damaging agents. Using Yeast 2 Hybrid analysis, we determined that Ssa3 and Ssa4 interacted with Rnr2 and Rnr4 much less than their constitutive counterparts. This may be due to differential co-chaperone binding which is essential for client activation and stabilization. Previously it has been shown that Ydj1 has a significantly higher binding affinity to Ssa2 as compared to Ssa4. This suggests that lack of proper Ydj1 binding may contribute to the deficit of RNR stabilization seen in Ssa4 cells.

Structural elements of Ssa2 required for HU resistance

Hsp70 is comprised of a nucleotide binding domain (NBD) which is important for co-chaperone binding and ATPase activity, a substrate binding domain (SBD) which is important for client interaction and a C-terminal 10-kDa α-helical subdomain (CTD) that acts as a lid over the binding pocket in the SBD. It has previously been shown that the co-chaperone Ydj1 interacts with Hsp70 on both the NBD and CTD domains (116, 136). Interaction between Ydj1 and Hsp70's CTD is vital for substrate transfer. Out of the four isoforms, Ssa2 isoform appears to be the most resistant to DNA damaging agents including HU, while Ssa4 is highly sensitive. In order to further explore the structural requirements of the Ssa isoforms for HU resistance we used Ssa2-Ssa4 chimeras (116). Here we show the chimera constructed of the NBD/SBD of Ssa2 and the CTD of Ssa4 was sensitive to

HU, suggesting the CTD domain of Ssa2 contributes it its HU resistance. Interestingly, the highest sequence variation between Ssa2 and Ssa4 occurs within the SBD, specifically the outer-facing region of the "lid". This data suggests that there is variation within the C-terminus of Ssa4, as compared to Ssa2, may render it unable to properly bind to one or more of the RNR subunits and consequently it is unable to stabilize the complex. This could potentially be contributing to the destabilization of Rnr2 and Rnr4 and the sensitivity to DNA damaging agents seen in cells solely expressing Ssa4.

Conclusions

It is becoming evident that although Hsp70 isoforms have overlapping functions, there are particular roles dictated by co-chaperone and client interactions. The interaction between Hsp70 and its corresponding co-chaperones and clients is complex and highly dynamic. Previous data suggests that either Ydj1 transports and transfers RNR components to Hsp70 or more likely exists in a complex with RNR and Hsp70 to maintain RNR activity. From previous studies and the data presented here, it can be suggested that the co-chaperone Ydj1 possesses differential binding affinity between Ssa1-4 isoforms. Consequently, since co-chaperones assist in client binding and stabilization, this may contribute to disparate interaction between Hsp70 isoforms and essential clients such as RNR. Considering the high variation between the client binding domain of Ssa2 and Ssa4, we can also conclude this may be instrumental to the isoform's ability to bind to certain clients. Understanding the differences between Hsp70 isoforms will expand our overall view of their roles in essential signaling pathways such as DNA damage.

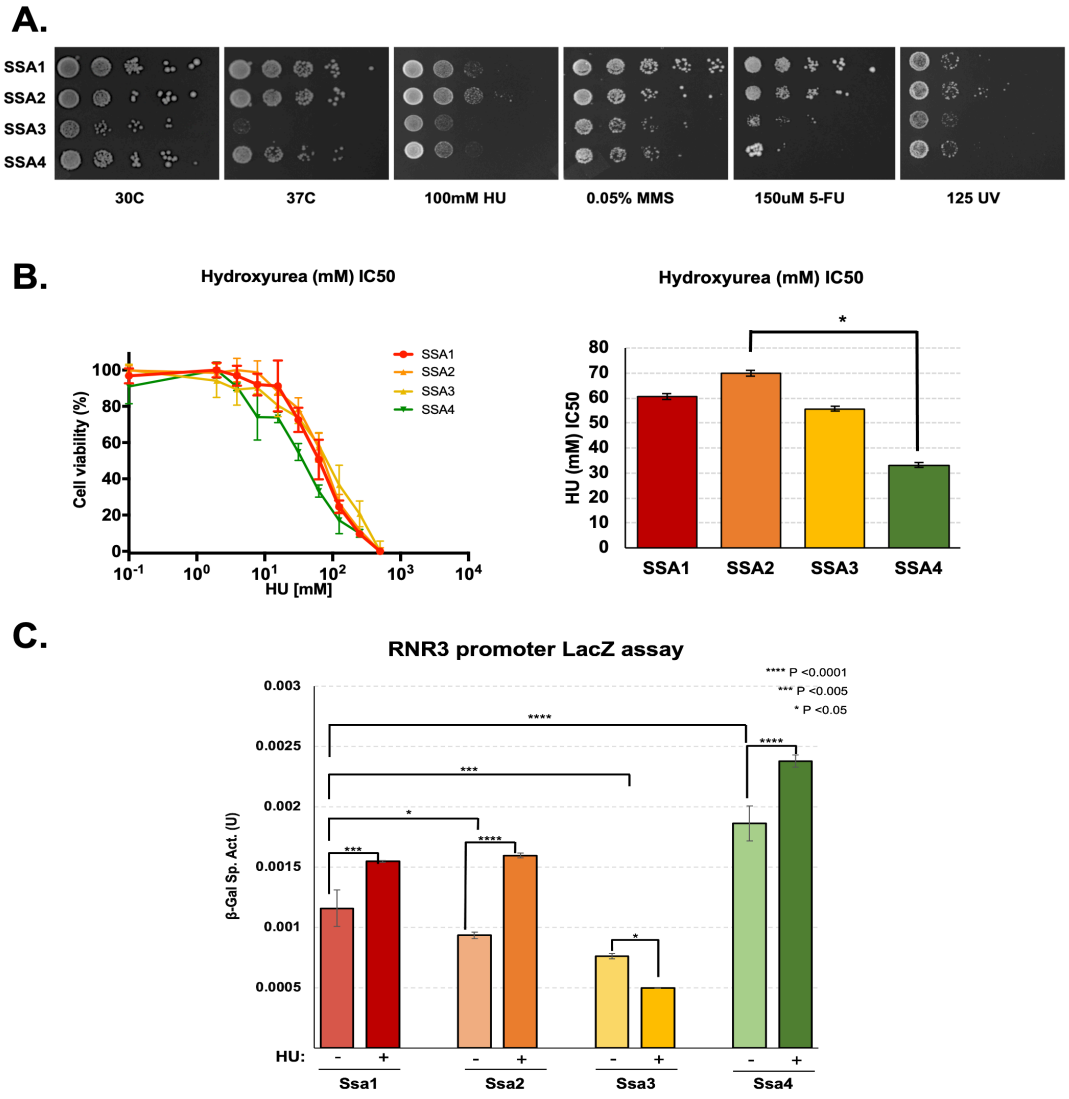

Figure 11. Stress inducible Ssa3 and Ssa4 isoforms are sensitive to DNA damaging agents
(A) Yeast containing only Ssa3 or Ssa4 are sensitive to several DNA damaging agents, Ssa3 is also seen to be temperature sensitive. Cells expressing either Ssa1, 2, 3 or 4 as the sole Hsp70 were grown overnight to saturation and serial 10-fold dilutions were plated by pin plating from 96-well plates onto YPD alone or YPD containing DNA damaging agents. Heat stress was conducted at 37ºC on YPD plates. Plates were imaged after 3 days. (B) For IC_{50} calculations, cells were grown to mid-log phase, diluted in a sterile 96 well plate in media containing HU 10-fold serially diluted. The IC_{50} for cells solely expressing Ssa4 was significantly lower than that of Ssa2. (C) Cells expressing Ssa3 were compromised for DNA damage response pathway transcription. An RNR3-LacZ reporter plasmid was transformed into the indicated yeast strains. Cells expressing Ssa4 are overactive in DNA damage response pathway activation. Transformants were grown and subjected to 0, 200mM HU for 3 hours. β-Galactosidase activity was measured in crude extracts. β-Galactosidase specific activity (in units) [-Gal Sp. Act. (U)] is shown on the y axis. Each value represents the mean and standard deviation (error bar) from three independent transformants; *, P≤0.05**, P≤0.01; ***, P≤0.001 as compared to Ssa1 cell controls.

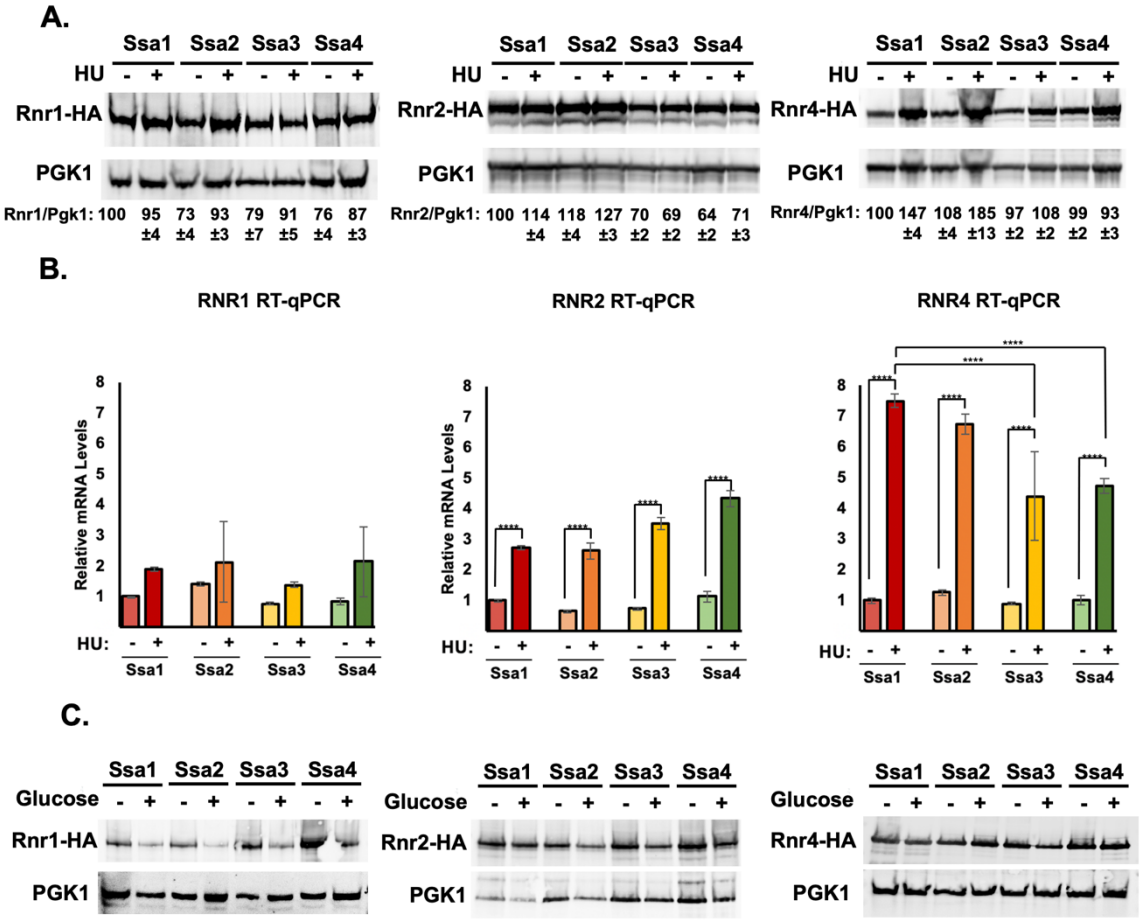

Figure 12. Rnr2 is destabilized in ydj1Δ cells. (A) Ssa1, 2,3 or 4 cells expressing endogenously tagged Rnr1-HA, Rnr2-HA or Rnr4-HA were grown to exponential phase and were either left untreated or were treated with 200mM HU for 3 hours. Cell extracts were obtained, resolved on SDS-PAGE gels and analyzed by immunoblotting with anti-HA and PGK1 antibodies. (B) Quantitation of RNR1, RNR2 and RNR4 transcription in Ssa1, 2,3 or 4 cells. Levels of RNR1, RNR2 and RNR4 mRNAs in Ssa1, 2,3 or 4 cells were determined by reverse transcription and RT-qPCR. Signals of RNR1, RNR2 and RNR4 were normalized against that of ACT1 in each strain, and the resulting ratios in Ssa1 cells were arbitrarily defined as onefold. Data are the average and SD from three replicates. (C) RNR subunit stability is compromised in cells lacking expressing a single isoform. Ssa1, 2,3 or 4 cells transformed with either pGAL1-HA-Rnr1, 2 or 4 plasmids were grown to mid-log phase in YP Galactose medium. Transcription of pGAL1-HA-Rnr1, 2 or 4 was shut off by addition of 2% glucose to cultures. Cell lysates from these samples were analyzed by Western Blotting for stability of HA-RNR subunit (HA antibody) and loading control (PGK1).

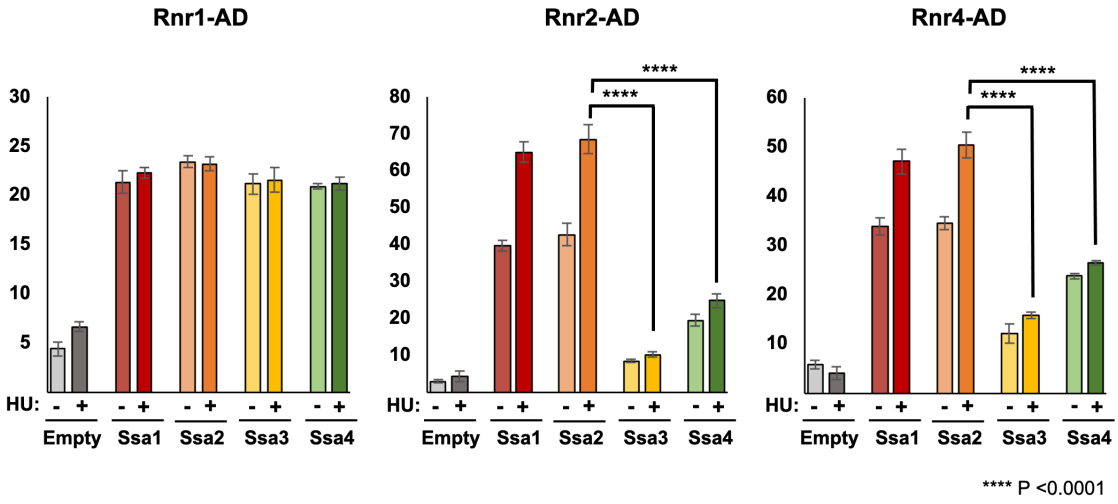

Figure 13. Ssa Proteins 1, 2, 3 and 4 interact differently with RNR subunits. Ssa1-4 interact with RNR subunits in yeast two-hybrid assays. β-galactosidase activity was measured in protein extracts obtained from *Ssa1-4*Δ cells transformed with the appropriate AD-Rnr and BD-Ssa fusions. Rnr1-AD showed similar interaction patterns with Ssa1, 2, 3 and 4. Rnr2-AD associated most strongly with Ssa1-BD and Ssa2-BD and showed significantly lower association with Ssa3-BD and Ssa4-BD. This pattern between Ssa1-4 was consistent for Rnr4-AD. Data in grey bars represent AD-control fusion versus BD-Ssa. Each value represents the mean ± SD (n = 3). Statistical significance between samples was calculated using Graph pad Anova Multiple comparisons. (**** $p < 0.01$).

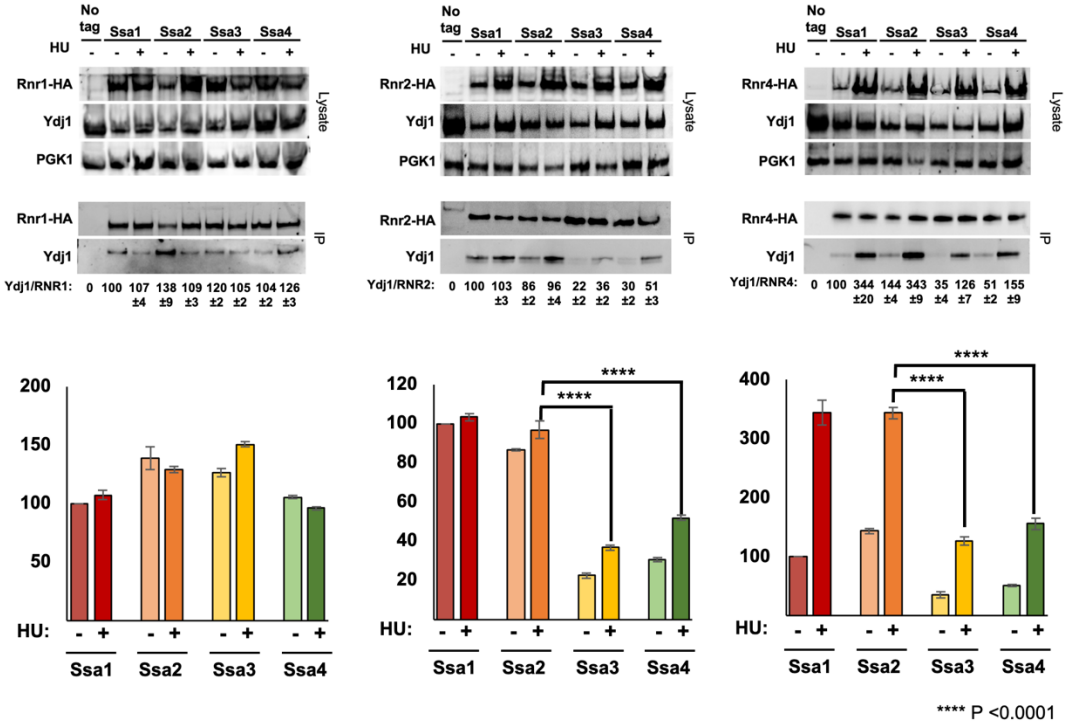

Figure 14. RNR subunits have decreased binding with Ydj1 in Ssa3 and Ssa4 cells. (A) Rnr2 and Ydj1interaction varies in yeast cells expressing either Ssa1, 2 ,3 or 4. HA-tagged Rnr1, Rnr2, and Rnr4 cells containing either Ssa1, 2 ,3 or 4 were grown to exponential phase and were either left untreated or were treated with HU. Cell extracts (lysate) and immunoprecipitated (IP) with anti-HA magnetic beads were subjected to SDS-PAGE and analyzed by immunoblotting with anti-HA antibodies to detect the Rnr subunits or anti-Ydj1 antibodies to detect Ydj1. In cells only expressing Ssa3 or 4, Ydj1 showed decreased interaction with both Rnr2 and Rnr4 in unstressed and HU treated samples.) Each value represents the mean ± SD (n = 3). Statistical significance between samples was calculated using Graph pad Anova Multiple comparisons. (**** $p < 0.01$).

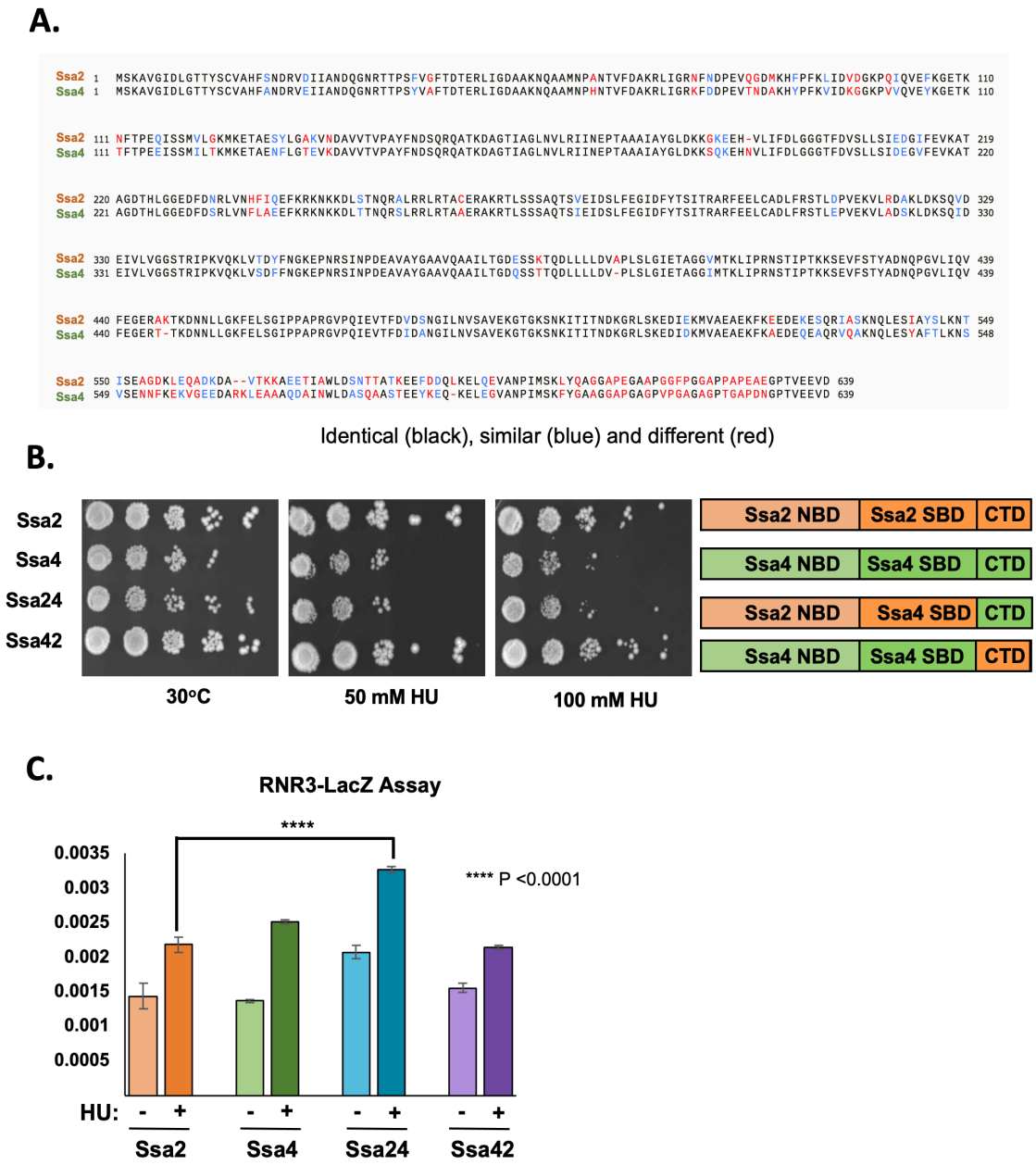

Figure 15. The C-terminus of Ssa2 is required for HU resistance. (A) Sequence alignment between Ssa2 and Ssa4 created using Clustal Omega (https://www.ebi.ac.uk/Tools/msa/clustalo/) . Amino acids are labeled either Black (identical), Blue (similar) or Red (different). (B) Cells expressing either Ssa2, 4, 24 or 42 as the sole Hsp70 were grown overnight to saturation and serial 10-fold dilutions were plated by pin plating from 96-well plates onto YPD alone or YPD containing Hydroxyurea. Plates were imaged after 3 days. (C) An RNR3-LacZ reporter plasmid was transformed into the indicated yeast strains. Cells expressing Ssa4 are overactive in DNA damage response pathway activation. Transformants were grown and subjected to 0, 200mM HU for 3 hours. β-Galactosidase activity was measured in crude extracts. β-Galactosidase specific activity (in units) [-Gal Sp. Act. (U)] is shown on the y axis. Each value represents the mean and standard deviation (error bar) from three independent transformants; *, P≤0.05**, P≤0.01; ***, P≤0.001 as compared to Ssa2 cell controls.

Table S1. Yeast Strains Used in This Study

Strain	Genotype	Reference/Source
yAT414	MATa (MH272) ssa1Δ::trp1 ssa2::HisG ssa3::HisG ssa4::HisG (ssa1-4) [YCPlac33 SSA1]	Jaiswal et al., 2011
yAT423	MATa (MH272) ssa1Δ::trp1 ssa2::HisG ssa3::HisG ssa4::HisG (ssa1-4) [YCPlac33 SSA1]):: RNR1-HA-HIS3MX6	This study
yAT424	MATa (MH272) ssa1Δ::trp1 ssa2::HisG ssa3::HisG ssa4::HisG (ssa1-4) [YCPlac33 SSA1]):: RNR2-HA-HIS3MX6	This study
yAT425	MATa (MH272) ssa1Δ::trp1 ssa2::HisG ssa3::HisG ssa4::HisG (ssa1-4) [YCPlac33 SSA1]):: RNR4-HA-HIS3MX6	This study
yAT307	MATa (PJ69-4a) pOAD RNR1	Uetz et al., 2000
yAT305	MATa (PJ69-4a) pOAD RNR2	Uetz et al., 2000
yAT301	MATa (PJ69-4a)	Uetz et al., 2000

Table S2. Plasmids Used in This Study

Plasmid	Description	Reference/Source
pAT625	pRS315P_{SSA2}-SSA1(LEU2)	Sharma and Masison 2008
pAT626	pRS315P_{SSA2}-SSA2(LEU2)	Sharma and Masison 2008
pAT627	pRS315P_{SSA2}-SSA3(LEU2)	Sharma and Masison 2008
pAT628	pRS315P_{SSA2}-SSA4(LEU2)	Sharma and Masison 2008
pAT659	pRS315P_{SSA2}-SSA24(LEU2)	Sharma 2020
pAT660	pRS315P_{SSA2}-SSA42(LEU2)	Sharma 2020
pAT592	RNR3 promoter-lacZ	W. Xiao 1996
pAT289	pBD-SSA1	Wegele et al., 2003
pAT293	pBD-SSA2	Wegele et al., 2003
pAT283	pBD-SSA3	Wegele et al., 2003
pAT294	pBD-SSA4	Wegele et al., 2003
pAT295	pBD-SSA4	Wegele et al., 2003
pAT739	pOAD-RNR4	This Study
pAT716	pBG1085-GAL1 promoter-ZZ-HA-RNR1	Dharmacon
pAT717	pBG1085-GAL1 promoter-ZZ-HA-RNR2	Dharmacon
pAT718	pBG1085-GAL1 promoter-ZZ-HA-RNR4	Dharmacon
pAT705	pFA6a-HA-HIS3MX6	J. Pringle

Table S3. RT PCR Primers Used in This Study

Gene	Primers
RNR1 forward	5′-GTGTTCAAGGTCTCGCTGAC-3′
RNR1 forward	5′-CGTATGGACCGTCCTTCTGA-3′
RNR2 forward	5′-CCTAAAGAGACCCCTTCCAAAG-3′
RNR2 reverse	5′-GCCTTGTGATTTTCAGCGTC-3′
RNR3 forward	5′-GCCTCCGCTGCTATTCAA-3′
RNR3 reverse	5′- CAGATGCCGCCTTTTGTT-3′
RNR4 forward	5′-CATAAGGCTGCTTTCATCGAG-3′
RNR4 reverse	5′-CTGTTGGCCATTGCTAAACC-3′
ACT1 forward	5′-GTATGTGTAAAGCCGGTTTTG-3′
ACT1 reverse	5′-CATGATACCTTGGTGTCTTGG-3′

Figure 16. Table of Yeast strains, plasmids and primers used in study.

CHAPTER 4: CHEMOGENOMIC SCREENING OF ENDOPLASMIC RETICULUM CO-CHAPERONE ISOFORM AS A HUB FOR ANTI-CANCER DRUG RESISTANCE

4.1 Introduction

Hsp70 is a well-conserved 70kDa molecular chaperone responsible for the folding of newly synthesized and misfolded proteins "clients" (137). Like cytoplasmic Hsp70, the ER-resident Hsp70 orthologue, BiP, is also critical both for folding of new proteins and for targeted degradation of proteins that can no longer be refolded (83, 138). This activity is essential since one-third of the proteome matures in the ER. BiP also plays an important role in oncogenesis, with BiP overexpression conferring resistance to a variety of anticancer agents (139-141). This role has made BiP an interesting target for anti-cancer treatments. Currently, three compounds have been characterized that inhibit BiP function, HA15, NKP-1339 (IT-139) and HKH40 (142). Discovery of other agents that target this pathway or enhance existing anticancer therapies would be of great value for both therapeutic applications and in basic research.

While it is well-established that the activity of the Hsp70 chaperone family is fine-tuned by co-chaperone "helper" proteins, the specific roles of the yeast and human ER co-chaperone proteins have yet to be full characterized (47, 48, 81). The effect of co-chaperones on specific Hsp70 or BiP-dependent client proteins and pathways are difficult to study because total inhibition of general chaperone function is lethal for the cell. One such co-chaperone family is the ERdj proteins, which are Hsp40 homologs in the ER (81, 83). There are 8 ERdj co-chaperone isoforms in humans (83). The unique functions of these

individual co-chaperone isoforms are not thoroughly studies. Like other chaperone isoforms, ERdj1-8 have high similarity but unique characteristics and functions.

ERdj1 is transmembrane with a cytosolic domain that affiliates with ribosomes to inhibit translation when BiP disassociates with its ER domain. ERdj1's main function appears to be a translation safeguard, ensuring BiP is present to fold nascent polypeptides. ERdj1, along with ERdj2 and ERdj8 are not induced by the unfolded protein response (UPR) indicating their lack of a role in the response to this stress (83, 143).

ERdj2 also contains both an ER and cytosolic domain. ERdj2 has a well characterized yeast homologue Sec63. Sec63 is known to play an important role in posttranslational protein translocation. However, in mammalian cells this not conserved and proteins are translocated co-translationally so ERdj2's role is not obvious (83, 144).

ERdj3 is the most well-studied ERdj protein and has been seen to maintain a complex with BiP (145). ERdj3 is upregulated during the UPR and is thought to assist the recruitment of BiP to the substrates to be folded. Through yeast homologue studies, ERdj3 is also thought to play a part in the Endoplasmic-reticulum-associated protein degradation (ERAD) (83, 145). Interestingly, there have been a few studies done on ERdj3 and cancer progression. Overexpression of ERdj3 was seen to enhance hepatocellular carcinoma (HCC) oncogene progression by inhibiting Z AAT degradation (146). Z AAT is a mutant form of the alpha-1-antitrypsin protein that becomes accumulation within hepatocytes and results in increased cirrhosis (146).

ERdj4 is the most UPR inducible ERdj protein, although during unstressed conditions is the least abundant (83). It has been shown to be important in the ERAD pathway, recruiting clients to important ERAD sites. ERdj4 is unique as it is anchored to

the membrane by a cleavable signal sequence and once cleaved it becomes soluble (147). Interestingly, overexpression ERdj4 was seen to suppress cell death as a consequence of ER stress (148).

ERdj5 has a unique structure compared to the other ERdj proteins. Along with a J-domain that is typical for all co-chaperone proteins, it also contains four thioredoxin-like domains. This specialized domain adds to ERdj5's reductase activity. This function was found to be useful in the ERAD pathway to break disulfide bonds in certain substrate proteins (149).

ERdj6 contains both a J-domain as well as a tetratricopeptide repeat domain. ERdj6 is believed to work as a complex with BiP and promote protein folding. It is also an important player in the UPR and acts as a negative regulator of kinase EIF2AK4, which activates elF2 alpha that in turns controls protein production (81).

ERdj7 and ERdj8 were just recently discovered and thus very little is known about their specific function (83). ERdj7 was originally discovered in canines via mass spectrometry studies. Although its unique role has yet to be determined, it is not regulated by the UPR, so it is unlikely to assist in the ERAD pathway or protein folding. Like ERdj5, ERdj8 is thought to contain both a J domain and a thioredoxin domain. It has been shown to localize at the ER-mitochondria contact size and has been seen to be upregulated during proteotoxic stress. (150, 151)

As previously mentioned, there are three compounds which have been characterized that inhibit Hsp70 isoform BiP, HA15, NKP-1339 (IT-139) and HKH40. HA15 is a thiazole benzenesulfonamide that binds to BiP directly and displays potent anticancer effects on melanoma cells and tumors (152). HHK40, the 8-methoxy analog of

WMC79, is a synthetic agent with promising *in vitro* and *in vivo* antitumor activity, especially against solid tumors. It decreases BiP levels and corresponding ER protein folding pathway activity. The only drug in clinical trials to specifically inhibit BiP NKP-1339 (IT-139) but has resulted in patient toxicity (142). Because of their broad functionality, inhibiting Hsp70 isoforms is detrimental to normal cells as well. An alternative strategy is to target co-chaperones which has been shown to reduce toxic effects (58). In order to accomplish this, we must first better understand ERdj co-chaperones specific functions, which will provide a variety of benefits; if chaperone function can be selectively altered through ERdj manipulation, novel tools can be developed to investigate chaperone clients without abolishing essential chaperone housekeeping activities. In addition, inhibition of specific ERdj proteins may offer novel specific ways to target chaperone function in disease such as cancer (81).

To address these questions, we performed a chemogenomic screen using the NIH Approved oncology drug set comprised of 133 anti-cancer drugs in combination with CHO cell lines that have been depleted of one the ERdj1-8 co-chaperones. From this screen we identified several compounds that showed increased potency with at least one of the ERdj KO cells as well as some molecules that had an antagonist effect. We performed drug target ontology analysis on these hits, which revealed a unique pattern between the ERdjs, suggesting specificity of function. Consistent with ERdjs displaying overlapping core functions while mediating distinct cellular processes, all ERdj KO cells displayed increased sensitivity to drugs that targeted DNA synthesis and cytoskeleton, while varying dramatically in response to molecules that targeted signal transduction. This study

demonstrates the idea that ERdj inhibition may offer a novel way to sensitize cancers cells to a range of therapeutics agents while possibly reducing toxicity.

4.2 Materials and Methods

Cell culture

The CHO-k1 S21 cell line and ERDJ1-8 knockout CHO-K1 S21 cell line was kindly gifted by David Ron PhD (45) were cultured in Ham's F-12 Medium (Invitrogen) with 10% fetal bovine serum (Gibco), 100 units/ml penicillin, and 100 μg/ml streptomycin at 5% CO_2 and 37° C.

Drug Screening

As done in *Nitika et al. 202 (153).* Approved Oncology Drug plates consisting of the most current FDA approved anticancer drugs were obtained from National Cancer Institute (NCI). For experiments delineating the synergy between the loss of the ERdj1-8 protein isoforms and approved anticancer drug, CHO-K1 cells and CHO-K1 (ERDJ1-8 KO) cells were plated in growth media at 20% confluency 1 day prior to drug treatment. On Day 1 of treatment, cells were treated with DMSO (control), Approved oncology anticancer drugs at 50 μM for 72 hours. Following drug treatments, Cell Titer-Glo reagent was added directly to the wells according to manufacturer's instructions. The luminescence was measured on Bio-Tek Plate reader. Luminescence reading was normalized to and expressed as a relative percentage of the plate averaged DMSO control. The data shown are the mean and SEM of three independent biological replicates.

Bioinformatics

Cancer genome data and Cancer Cell Line Encyclopedia data were accessed from the cBioPortal (www.cbioportal.org) for Cancer Genomics (154). Copy number and gene expression data was calculated using Xena Functional Genomics Explorer (https://xenabrowser.net) created by the University of California at Santa Cruz. The TCGA Pan-Can Atlas (10,967 samples in 32 studies) was used in analysis. Total patient numbers and detailed information regarding published datasets and associated publications are indicated in Fig1-2.

Heatmap analysis of ERdj1-8 KO cells drug resistance to NCI Approved Oncology Drug plates

To create the heatmap using Excel, a table was created displaying the 133 cancer drugs from the NCI Approved Oncology Drug plates listed along the Y-axis, along with the coinciding normalized Log_2 ratio viability (CHO^{ERDJKO}/ CHO^{WT}) values for each ERdj isoforms listed along the X-axis. The drugs were clustered based on biological pathway they target. Conditional formatting was used to label the Log_2 ratio values in a gradient format, with Log_2 ratio values of +/- 1 were considered significant. The labeling is as follows; deepest pink with a value of -17.0, grey with a value between -1 and +1, deepest blue with a value of +7.

Phylogenetic tree analysis of ERdj1-8

Human ERdj1-8 sequences were obtained from Universal Protein Resource (UniProt; http://www.uniprot.org/), respectively. Sequences were aligned using Clustal

Omega Multiple Sequence Alignment (http://www.ebi.ac.uk/Tools/msa/clustalo/). Using these aligned sequences and the software program Mega7, a phylogenetic tree was constructed using the neighbor-joining method with 1000 bootstrap replications. To create the dendrogram comparing the similarities between the ERdj1-8 isoforms based off drug resistance to the approved Oncology drug plates from NCI, a table was created displaying the 133 cancer drugs from the NCI Approved Oncology Drug plates listed along the Y-axis, along with the coinciding normalized luminescence readings for each ERdj isoforms listed along the X-axis (Log2 viability . A distance matrix was created using R using the function distance matrix to compute the pair wise distances between all rows of the matrix. Using the distance matrix table, a cluster dendrogram was created in R using hclust(as.dist(table),method="average") function. This clustogram was then plotted using plot(clus).

Statistical analysis

Data was analyzed using GraphPad Prism built-in statistical tests indicated in relevant figure legends. The following asterisk system for P value was used: $P < 0.05$; $P < 0.01$; 0.001; and $P < 0.0001$. Correlation coefficient was analyzed using Xena statistical tool and a strong correlation value is considered >0.7.

4.3 Results

ERdj1-8 are mutated and overexpressed in a variety of cancers

Although BiP has been shown to be highly overexpressed in a variety of cancers, the role that co-chaperones such as ERdj1-8 play in tumorigenesis is not well studied. Using the cBioportal (cbioportal.org) cancer genomic database, we first observed the incidence of BiP alterations in cancer (154, 155). Analysis of the TCGA Pan-Can Atlas (10,967 samples in 32 studies) showed that BiP was altered at a frequency of at least 1% in multiple cancer types. We repeated this analysis for BiP's co-chaperones ERdj1-8. Between these 9 proteins, alterations varied in abundance as well as cancer type (Figure 17A). BiP was seen to be mutated in endometrial carcinoma and melanoma at a frequency of 4.27% and 2.03% respectively. The BiP gene was seen to be amplified at a rate of 2.11% in esophageal squamous cell carcinoma. Interestingly ERdj1, ERdj5, ERdj6 and ERdj8 were also mutated in melanoma cases at frequencies of 3.38%, 2.25%, 3.6% respectively. Like BiP, most of the ERdj genes show some type of alteration in endometrial carcinoma. In endometrial carcinoma, ERdj1, 2, 3, 5, 6, 7, and 8 were all seen to be amplified. Out of the 8 co-chaperones, ERdj1 had the highest frequency of deep deletion alteration in cancer studies with the highest frequency occurring in mature B-cell neoplasm (10.42% amplified). By far, ERdj3 was the most frequently altered co-chaperone in the TCGA Pan-Can database. ERdj3 was seen to be amplified in esophageal squamous cell carcinoma (25.26%), non-small cell lung cancer (15.76%), ovarian epithelia tumor (16.27%), cervical squamous cell carcinoma (14.74%), and in head and neck squamous cell carcinoma (13.96%).

To determine whether mutations in BiP and the ERdjs were independent of each other, we analyzed the co-occurrence of alterations in the TCGA Pan-Can samples that BiP and ERdj1-8 were seen to be modified (Figure 17B). Interestingly, we saw that co-occurrence happened at very low frequencies (average of 4%), with the highest between BiP and ERdj6 (6.9%). This may suggest that alteration of more than one of these ER chaperones is detrimental to the cell.

Like the majority of chaperones, BiP plays an important role in oncogenesis with BiP overexpression conferring resistance to a variety of anticancer agents (154, 156). This role can be attributed to chaperone's essential role in protein homeostasis. To determine if the ERdj genes were also overexpressed in cancer, we analyzed the expression data using TCGA Pan-Can dataset. (Figure 18A). Overall, the ERDJ1-8 were expressed at significantly higher levels in cancer samples, with a median mRNA expression in cancer with log2 ratio values as high as 16.47 as compared to BiP with a maximum value of 17.05 (Figure 18A).

The steady state level of a protein is a result of the fine balance between protein transcription, translation and protein degradation. We queried whether the large ERdj expression observed in cancer could be attributed to gene amplification (Figure 18B). Using the Xena functional genomics explorer, we analyzed the correlation between copy number changes and mRNA expression for BiP and ERdj1-8 in the TCGA Pan-Can dataset. Statistical analysis showed there was no strong correlation coefficient ($r > 0.7$) for any of the 9 chaperones.

Chemogenomic profiling of ERdj KO cells.

In order to characterize the roles ERdj1-8 play in anti-cancer drug resistance, we obtained a collection of verified individual ERdj1-8 KO mammalian cell lines to screen against the NIH Approved Oncology collection (131 compounds) for their relative potency (Figure 19). For this screen, each plate contained control wells treated with vehicle (1% DMSO). The final concentration of the screening compounds was 50 μmol/L. Positive hits (synergistic) or negative hits (antagonistic) were determined by normalizing the Log2 ratio of viability of the 8 ERdJ knockout cells over WT cells. The Log_2 ratio values of +/- 2 were considered significant. According to pharmacologic action, the compounds in the library have been divided into seven categories: Protein synthesis inhibitors, Proteasome inhibitors, Epigenetic modifiers, Metabolic inhibitors, Cytoskeletal inhibitors, Signal transduction inhibitors and DNA synthesis and repair inhibitors. The drugs list was arranged according to these seven categories and the fold-change ratios are showed in a heat map (Figure 20A). Overall, analysis shows the majority of the ERdj KO cells were synergistic with at least 40% of the drugs from the screen. While ERdj1 KO had the highest percent synergy with the drug set (52.6%) and ERdj3 KO had the lowest percent synergy (24.1%). (Figure 21). There were very few drugs that had an antagonistic effect with the ERdj KO cells. The highest percent antagonistic effect was seen in ERdj3 KO cells (3.0%). Interestingly, all of the ERdj KO cells were highly antagonistic with the drug Vismodegib (Hedgehog pathway inhibitor) (157).

Drug resistance and sequence analysis of ERdj1-8 isoforms from Humans

In order to determine if similarity in sequence correlated with functional resemblance, we investigated the phylogenetic relationship between the ERdjs based off of sequence analysis and relative drug resistance. CLUSTAL analysis revealed a high-sequence similarity between the ERdj1-8 isoforms (Figure 20B). From the phylogenetic tree, ERdj7 appears to be the most dissimilar to all of the 8 ERdj isoforms. ERdj2 and ERdj6 are highly similar even though they do not appear to have similar topologies. Based off sequence analysis, ERdj3 and 4 appear to be closely related and are thought to maintain similar functions within the ER. Interestingly, the phylogenetic tree based off of drug resistance of the NCI Approved Oncology Drug plates is very different compared to the phylogenetic tree based off of sequences (Figure 20C). From the drug screen, it appears that ERdj6, 7 and 8 are highly similar. As in the sequence phylogenetic tree, ERdj3, 4, and 5 are in the same cluster, however ERdj3 and ERdj5 are most similar.

Drug Ontology analysis of ERdj1-8

We performed drug target ontology analysis on the significant hits from the screen, looking for enriched clusters of drugs that target specific biological pathways (Figure 22A-B). This analysis was done for drugs whose potency increased or decreased with ERdj1-8 KO. Drug target analysis was carried out by calculating fold enrichment of positive hits (synergistic) or negative hits (antagonistic) over the total number of drugs in that category. Fold enrichment greater than 1 was considered significant. While the ERdjs share similarities in their top categories for both synergistic and antagonistic drugs, there are

differences indicating unique function between the isoforms (Figure 22A-B). The top categories in the gene ontology analysis for the ERdj KOs for drugs that were synergistic are epigenetic modifiers, cytoskeleton and protein synthesis. Interestingly, ERdj5 is unique with protein synthesis as its top drug ontology category. For drugs that are antagonistic, the most common category was signal transduction. ERdj2 KO and ERdj3 KO were unique with top categories being cytoskeleton and proteasome inhibitor respectively.

4.4 Discussion

ERdj co-chaperones as possible anti-cancer therapeutic targets

While several BiP inhibitors have been created in a research setting, the administration of these compounds on patients has been impeded due to toxicity issues. Our study set out to investigate whether inhibition of individual ERdj proteins may offer novel ways to fine-tune BiP activity as a more effective anticancer strategy. Our bioinformatic analysis of ERdj1-8 expression and mutations clearly identifies them as being altered in various cancers. Remarkably, ERdj3 was seen to be altered in much higher frequency as compared to BiP and the other ERdj co-chaperones. Surprisingly, even though BiP and ERdj1-8 have been seen to be substantially overexpressed in a variety of cancers, there isn't a strong correlation between ERdj copy number and level of expression. This suggests that some other factor is regulating the overexpression that is seen in cancer samples. While beyond the scope of this study, it is possible that the high levels of BiP and its corresponding co-chaperone proteins in cancer are due to increase in transcription as a result of hyperactive signaling pathways seen in cancer. It should also be noted that,

deletion of one of the ERdjs may result in overexpression of the other ER 7 co-chaperones. This would need to be investigated further in order to determine the effect it may have on the ER and additionally whether it would be advantageous to target more than one ERdj simultaneously.

Combination of anti-cancer drugs and depletion of the ERdjs showed both synergistic and antagonistic effects

Chemogenomic screening of ERdj1-8 knockout cell lines present advantageous mechanistic and translational understanding of isoform protein function. Finding current anti-cancer drugs that are synergistic with the ERdj KO cells will provide a novel way to increase the potency of therapeutics that are already approved and is key to better understanding ERdj co-chaperones cellular roles. It is also important to note the drugs that showed an antagonistic effect when combined with ERdj1-8 KO cells. If a drug becomes less effective in killing cancer cells when ERdj is knocked out, then overexpressing an ERdj should have the reverse effect. We previously saw in our analysis that ERdj1-8 are overexpressed various cancers. From this, it may suggest drugs that will work better in cancers over expressing ERdjs. One of the most interesting finds of the screen was the high antagonistic effect that was shared between all of the ERdj KO cell lines and the drug vismodegib, hedgehog signaling (Hh) pathway inhibitor. This is fascinating since a connection between the Hh pathway and the ER has never been shown. This may suggest that vismodegib has other targets in the cell.

Understanding functional relationships of ERdjs through chemical-genetic interactions

Surprisingly, there was a dramatic difference between the phylogenetic sequence analysis of the ERdjs and the functional drug resistance cladogram. For example, while ERdj3 and ERdj4 are highly similar in sequence and structure, ERdj3 was seen to be more closely related to ERdj5 in regard to resistance in the NCI approved Oncology drug screen. This suggests that sequence affinity does not always translate to functional correlation. The phylogenetic relationship based off drug resistance between the ERdj's may change based off the categories of drugs the screen is comprised of.

Drug ontology analysis revealed uniqueness between the ERdjs in regards to response to anti-cancer drugs which were separated into 7 categories; Protein synthesis inhibitors (3 drugs), Epigenetic modifiers (6 drugs), Metabolic inhibitors (6 drugs), Proteasome inhibitors (6 drugs), Cytoskeletal inhibitors (9 drugs), Signal transduction inhibitors (50 drugs) and DNA synthesis and repair inhibitors (53 drugs). Surprisingly, none of the ERdj's shared the same order of categories in the drug ontology analysis. ERdj5 was synergistic with all 3 protein synthesis inhibitors and thus was the only ERdj with it as the top category, this may suggest an exclusive role for ERdj5. Interestingly, only 4 drugs out of 133 were antagonistic with at least one of the ERdj KO, because there were so few negative hits (antagonistic), this impacted the drug ontology analysis. Additionally, for ERdj4- 8, vismodegib was the only drug that showed an antagonistic effect.

ERdj co-chaperones regulate the DDR

The majority of the drugs from the screen belong to a class of DNA synthesis and repair inhibitors. Interestingly, there have been a few observed connections between the DNA damage response (DDR) and the ER. Several studies have shown that alleviation of the ER stress response increases DNA damage repair mechanisms (158, 159). Stress to the ER by using thapsigargin which blocks the calcium flux over the ER membrane, causes induction of BiP and consequently triggering the UPR. This stress induces translation of the p53 isoform p53/47 and prevents p53-induced p21 translation which eventually leads to G2 arrest. This mechanism was shown to lower the apoptotic threshold to Doxorubicin, a DNA damaging drug (160). Doxorubicin works by blocking topoisomerase II enzyme and is regularly used in combination with other therapies (161). Interestingly, ERdj1, 5, 6, 7, 8 KOs also showed synergy with Doxorubicin from the chemogenomic screen with Log_2 ratio viability values of -13.62, -3.25, -1.36, -1.62, and 2.08 respectively (values less than -1 considered significant). Doxorubicin had the most synergistic effect with ERdj1 KO cells out of the DNA damaging inhibitors and ERdj KO cell lines. There were few drugs from DDR group that were antagonistic with the ERdj KO cells. Mitoxantrone, another topoisomerase II inhibitor that functions by intercalation between DNA bases. Mitoxantrone is used as an anti-cancer drugs as well as treating Multiple Sclerosis (162). Mitoxantrone was antagonistic with ERdj1 KO with a Log_2 ratio of viability ($CHO^{ERDJ1KO}$/ CHO^{WT}) of 1.64 (values above 1 considered significant), while the remainder of the ERdj KO's remained unchanged. Interestingly, Idarubicin hydrochloride was synergist with ERdj1 and ERdj1 while antagonistic with ERdj2 and ERdj3. Idarubicin hydrochloride has been shown to inhibit topoisomerase II by a similar mechanism to Mitoxantrone. It is

interesting that two drugs with similar mechanisms and targets produce different results within the same cell line, this suggests that one of these topoisomerase II inhibitors may have additional cellular targets and effects. These results also demonstrate the differences in function between the ERdj isoforms.

Differential effects of ERdj co-chaperones on signal transduction

The second largest class of drugs from the screen is signal transduction inhibitors. Chaperones have been seen to play a vital role in various signal transduction pathways. BiP and its associated co-chaperones have been shown to be master regulators of the ER and the signaling pathway of the UPR. Because of the location and importance of the ER in the cell, it has been shown to be an important component of various signaling pathways (163). Strikingly, the drug Vismodegib is highly antagonistic with all of the ERdj co-chaperone KO cells with Log_2 viability (CHO^{ERDJKO}/ CHO^{WT}) values greater than 4.0. Vismodegib is a small-molecule inhibitor of the Hedgehog signaling pathway that is used to treat advanced basal-cell carcinoma (164). The Hedgehog signaling pathway is essential for various cellular processes such as cell proliferation and differentiation. Interestingly, a connection between ER stress and Hedgehog regulation of chondrocyte (cartilage secreting cells) proliferation has been seen (165). Furthermore, the Hedgehog inhibitor GANT61 has been shown to induce ER stress mediated autophagy (166). Enzalutamide, which inhibits multiple steps of the androgen receptor pathway and used to treat prostate cancer showed the highest synergy within the screen, specifically with ERdj1 KO (167, 168). One implication from our study is that ERdj1 inhibition might significantly enhance the effect of Enzalutamide therapy for prostate cancer.

The majority of cytoskeleton inhibitors are synergistic with ERdj KO cells

Interestingly, many of the drugs from the cytoskeleton class (89%) were significantly synergistic with one of the ERdj KO cell lines. The effect of the chemotherapy drug Vinorelbine tartrate in combination with ERdj1-8 KO cells was varied. Vinorelbine tartrate was highly synergistic with ERdj1 KO while antagonistic with ERdj2 and 3 KO cell lines. This again shows the uniqueness of the ERdj co-chaperones. Vinorelbine tartrate binding to microtubular proteins in the mitotic spindle, consequently inhibiting cell division during metaphase. Drug ontology analysis of drugs whose potency increases with ERdj KOs showed cytoskeleton inhibitors as the top category for ERdj2, 3, 4, 7 and the second top category for ERdj1, 5, 8. There has been some connection seen between the ER structure and function to the cytoskeleton (169). Specifically, the ER and microtubules have been shown to have an interdependent relationship, which is a possible reason for synergy between ERdj KO and cytoskeleton inhibitors (170).

The effect of ERdj KO cells in combination with metabolic inhibitors

Conversely, only 33.3% of metabolic inhibitors were synergistic with the ERdj KO cell lines. One of the metabolic inhibitors, Abiraterone was synergistic with all ERdj1-8 KO. Abiraterone is a hormone therapy drug that blocks testosterone and is used to treat prostate cancer (171). Interestingly, two different drugs, Abiraterone and Enzalutamide inhibit testosterone in distinct ways are both synergistic with the ERdj KO cells lines. This

suggests the ERdj co-chaperones may play a role in the androgen receptor pathway, specifically ERdj1 that was highly synergistic with both drugs.

Conclusions

While it is not well understood why cells contain express highly similar co-chaperones, this study exposes clear differences between ERdjs. A spectacular example of this is the highly varied response of ERdj KO cells to Vinorelbine tartrate, a microtubule inhibitor. Since chaperones are highly mutated and overexpressed in cancers, researchers have targeted them for therapies. The continuing issue with this method has been that inhibiting chaperones such as Hsp70 or its various cellular isoforms is too toxic. Inhibiting co-chaperones as an alternative strategy to sensitive cancer cells has the potential to be an effective therapy and will have far less toxicity.

4.5 Figures

A.

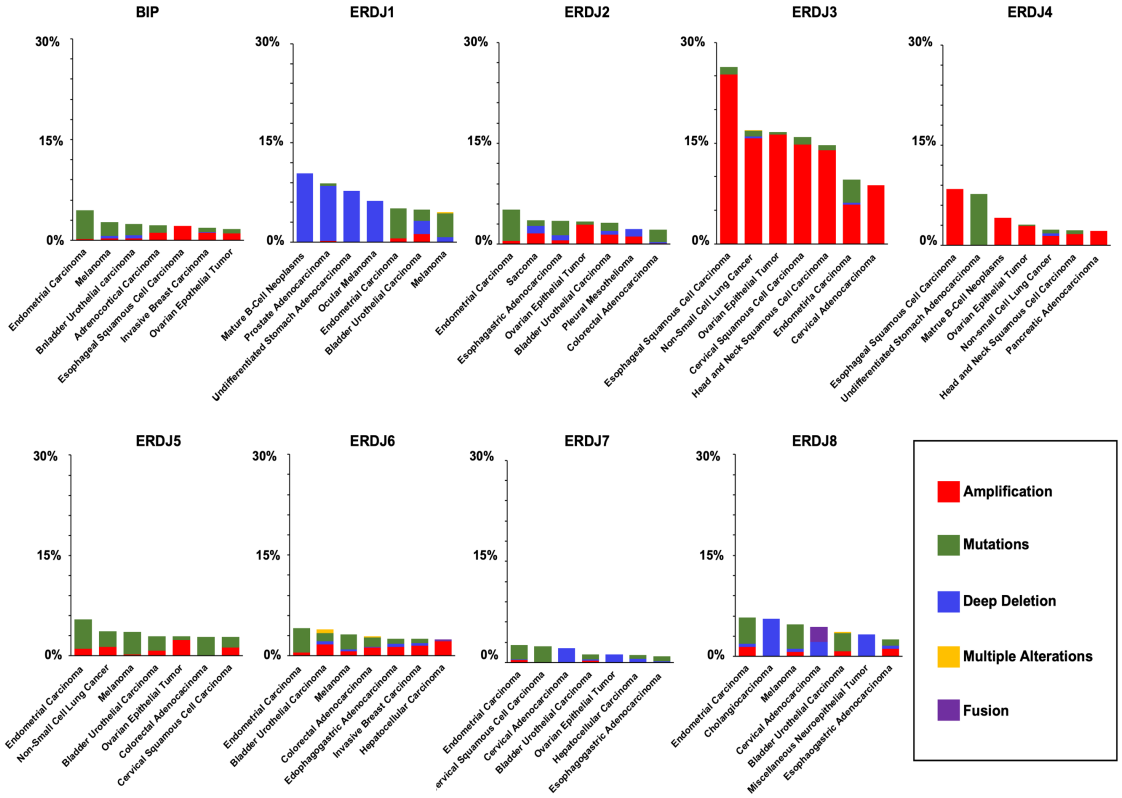

B.

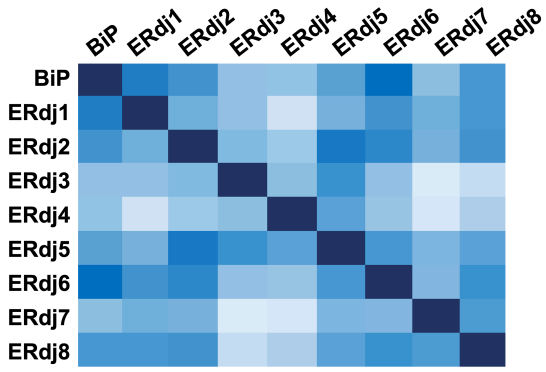

Figure 17. ERdj1-8 are altered in cancers from TCGA Pan-Can studies. (A) Prevalence of ERdj alterations in various cancer genomes analyzed via the cBioPortal. Red bar, amplification. Blue bar, homozygous deletion. Green square, missense mutation. Yellow square, multiple alterations. (B) Oncoprint data was analyzed via the cBioPortal, showing coinciding alterations between ERdj1-8 from various cancer studies. Distance matrix created using number of cases were two chaperones were altered at the same time / total number of cases one of the two co-chaperones were altered. Boxes were then formatted depending on frequency co-occurrence was seen, with blue being the highest frequencies were labeled blue and then decreasing with the gradient to white.

A.

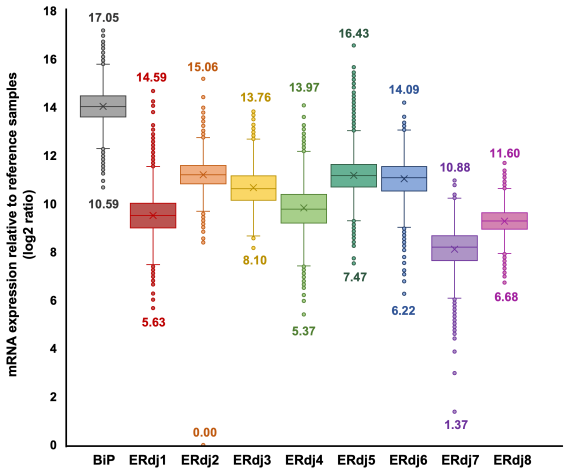

B.

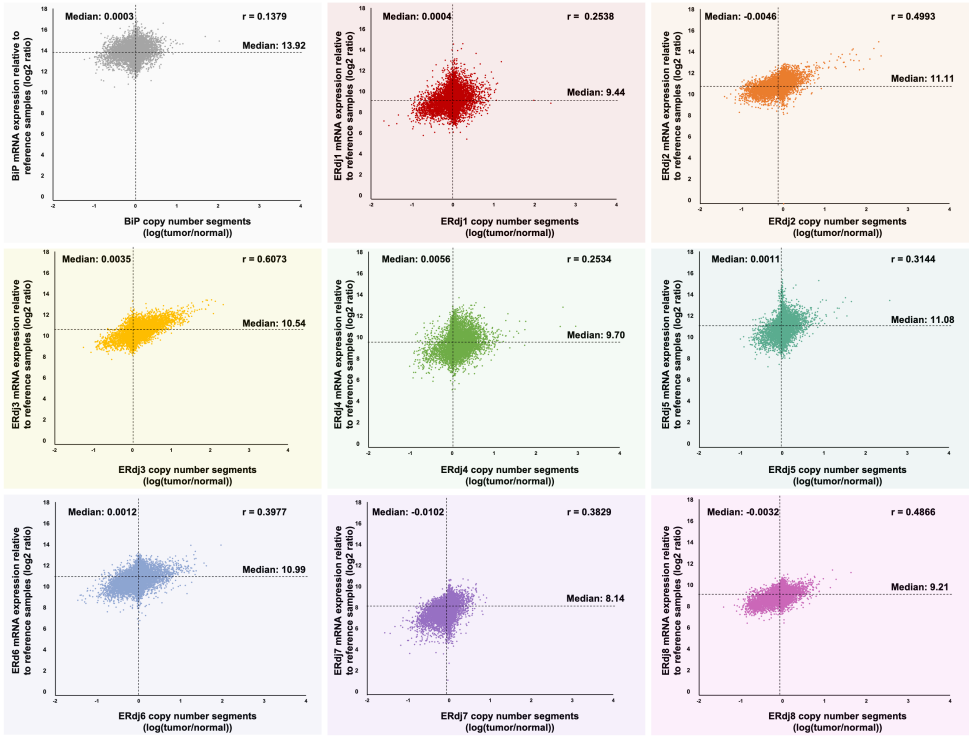

Figure 18. ERdj1-8 are overexpressed in cancers.
(A) Relative mRNA expression levels of BiP and ERdj1-8 co-chaperones in TCGA Pan-Can database**.** BIP and ERDJ1-8 mRNA expression relative to reference samples was plotted using a box plot with mean, maximum and minimum values. **(B)** Correlation between gene amplification and mRNA expression in ERdj1-8 in TCGA Pan-Can database. Increased BIP and ERDJ1-8 expression is not driven by copy number increase. ERDJ1-8 copy number vs ERDJ1-8 was plotted and Pearson's correlation coefficient (R-value) was calculated. ERDJ3 showed the highest correlation at r= 0.603. Median of both variables is marked by dotted line on the graph. Strong correlation considered to be r > 0.7

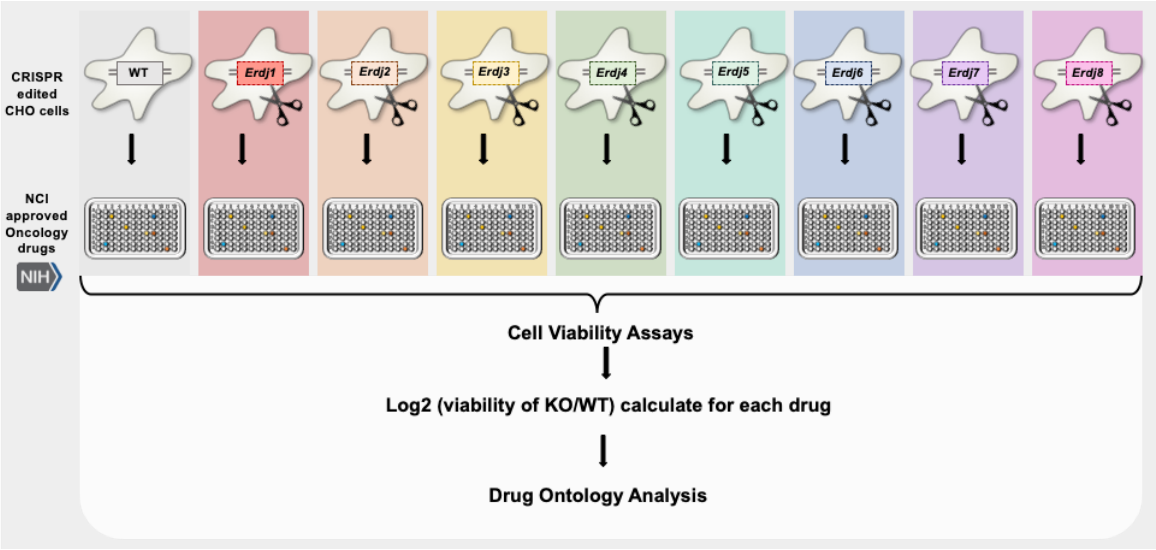

Figure 19. Cells lacking ERdj1-8 were analyzed for their response to the NCI approved oncology drug collection. Workflow of high-throughput cell-based screen. A collection of 133 drugs were screened at 50µmol/L with Wild-type and Erdj1-8 KO cells. ERDJ1-8 KO cells were plated in growth media at 20% confluency 1 day prior to drug treatment. On Day 1 of treatment, cells were treated with DMSO (control), Approved oncology anticancer drugs at 50 µM for 72 hours. Following drug treatments, Cell Titer-Glo reagent was added directly to the wells according to the manufacturer's instructions. The luminescence was measured on Bio-Tek Plate reader. Luminescence reading was normalized to and expressed as a relative percentage of the plate averaged DMSO control. The data shown are the mean and SEM of three independent biological replicates.

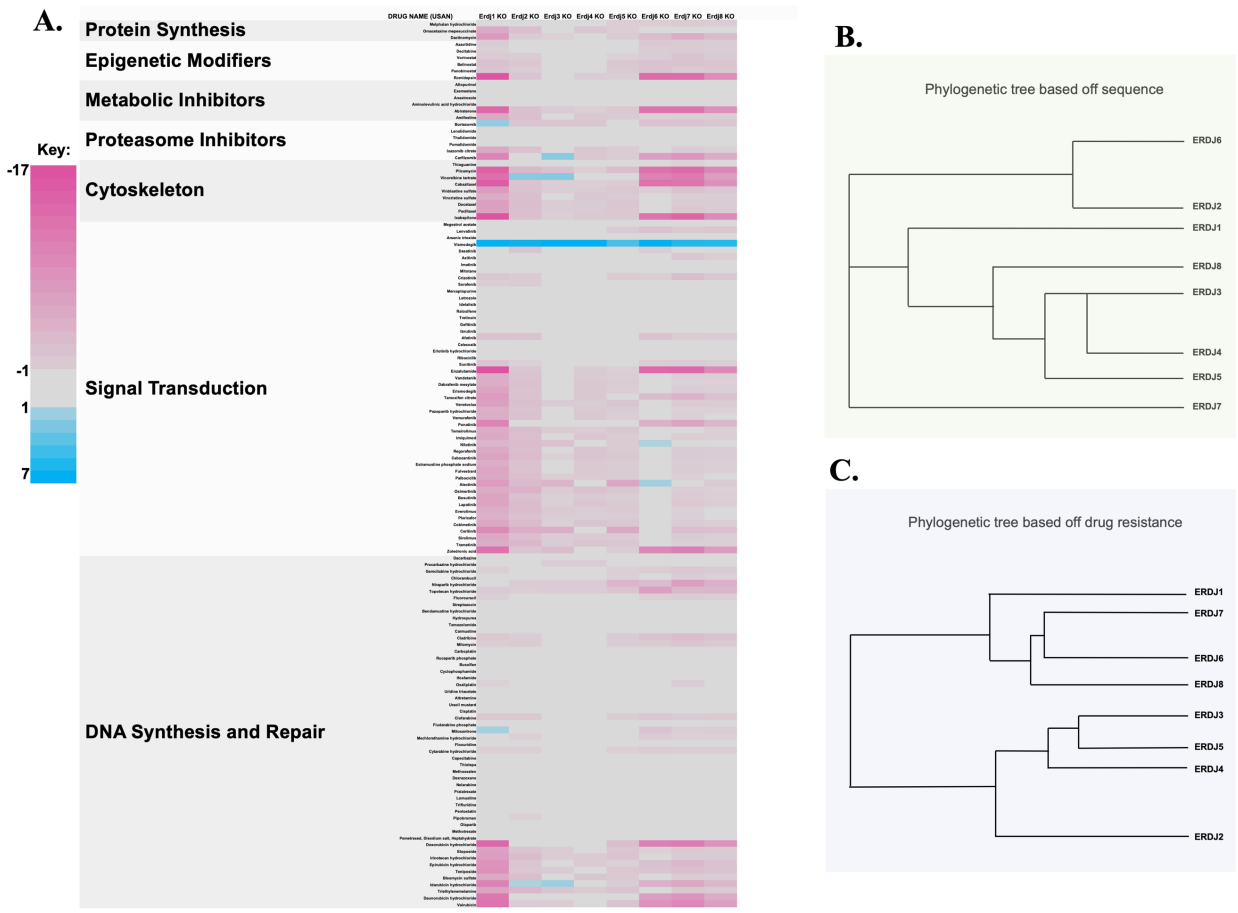

Figure 20. Sensitivity of WT and ERdj1-8 knockout cells to the NIH Approved Oncology Collection. A. Relative response of ERdj knockout cells to NCI approved oncology collection compared to WT cells. Drugs were screened at 50µmol/L with Wild-type and ERDJ KO cells. Results are the average of at least triplicates and error is SEM. Molecules with increased potency are colored pink, those with decreased potency are colored blue. **B.** Phylogenetic comparison of human ERdj1-8 isoforms. Sequences were aligned using Clustal Omega and used to produce a NJ tree with bootstrap using MEGA7. **C.** Phylogenetic tree based off of drug resistance of the NCI Approved Oncology Drug plates. A distance matrix table comparing similarity between ERdj1-8 KO cell lines resistance. A cluster dendrogram was created in R using hclust(as.dist(table),method="average") function.

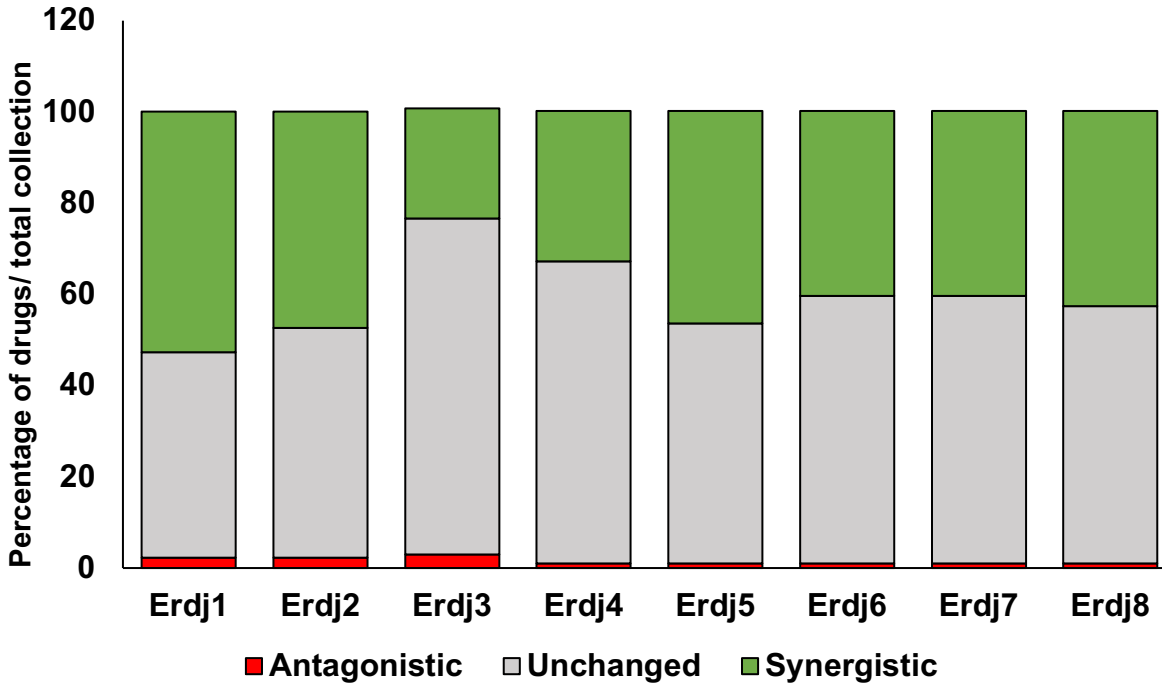

Figure 21. Chemogenomic analysis of ERdj1-8 knockout cells. Percent of drugs from the NCI approved oncology collection that were synergistic (green), antagonistic (red) or unchanged (grey) when combined with ERdj1-8 KO CHO cells over total number of drugs in screen (133).

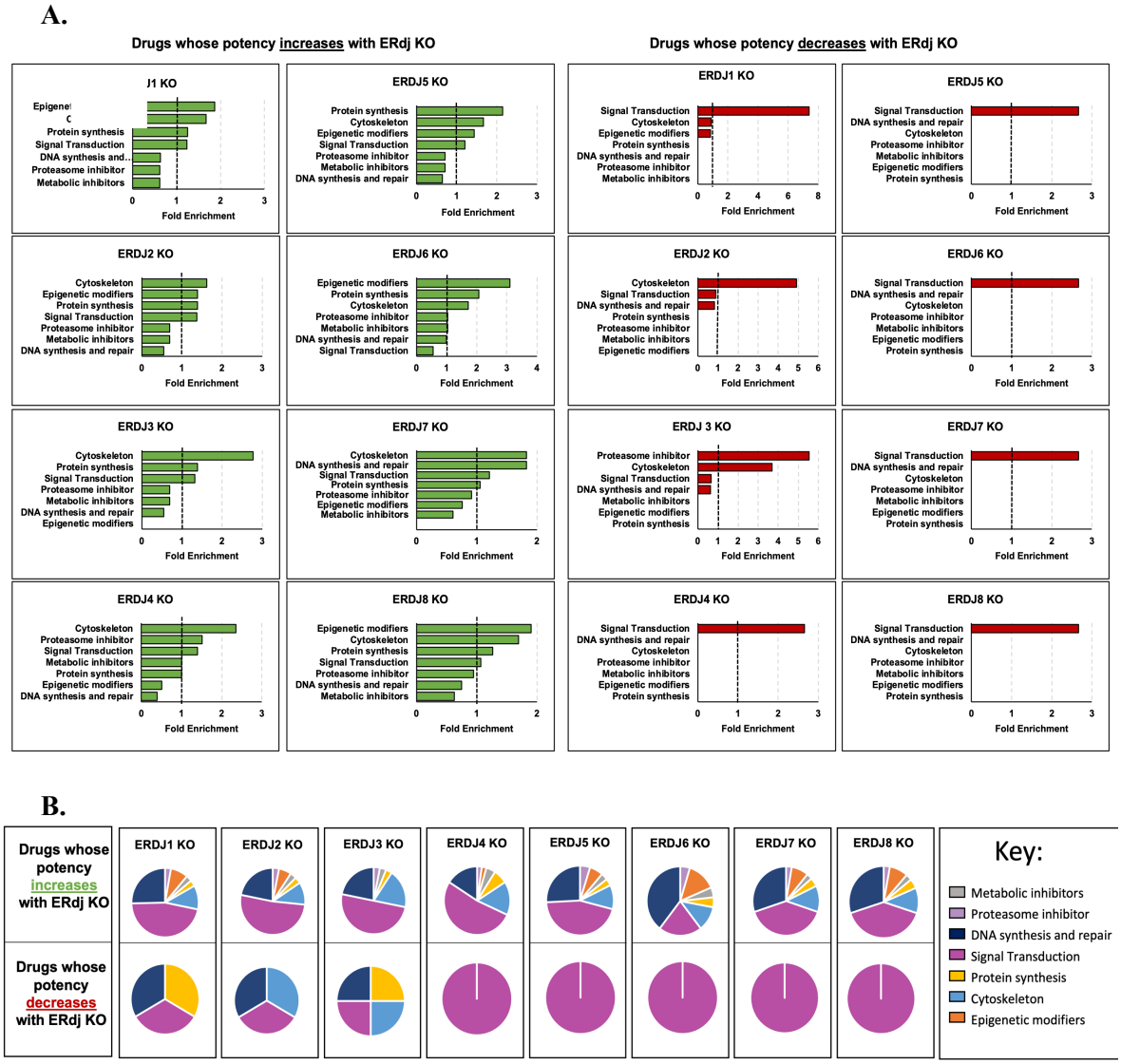

Figure 22. Drug target ontology of ERdj KO cells. (A) Drug ontology of synergistic and antagonistic hits based on the pathways affected by the approved oncology drugs in the screen. Small molecules inhibitors altered for potency by Log2 values of +/- 2 compared to WT cells were analyzed for drug target categories **(B)** Drug ontology of synergistic and antagonistic hits based on the pathways affected by the approved oncology drugs in the screen analyzed using pie charts. ERdj3-8 KO cells were only antagonistic with 1 drug out of 133 (Vismodegib, signal transduction inhibitor)

CHAPTER 5: CONCLUSIONS

Molecular chaperones have been studied for over 50 years, but the question remains why does a cell need to express so many Hsp70 and co-chaperone variants? While research suggests they have greatly overlapping function, it is clear that they have unique roles that go beyond differences in transcriptional patterns. Ssa3 and Ssa4 are clearly functionally different to Ssa1 and Ssa2, even when expressed at equal levels. Ssa3 and Ssa4 expressing yeast are unable to fully support RNR function, or V-Src, and FBP1(71, 115, 116). Given their high homology, where then does the specificity arise? Differences in ATPase activities are not substantial enough to explain these differences. Our study and other suggest the C-terminal lid may be important in these differences. While beyond the scope of this thesis, future studies may use site-directed mutagenesis to pin down important amino acids required for functional specificity. Previous studies and the work presented here on the Ydj1 activation of RNR suggest that Hsp70 co-chaperones dictate specificity, each binding a slightly overlapping, but mostly unique pool of clients. It is then highly likely that many of the functional differences seen in Ssa isoforms arises from altered co-chaperone binding. Ssa4 has weaker binding to Ydj1 than Ssa2 (116) and in this thesis we show that in Ssa4-expressing cells, RNR subunits display diminished interaction with both Ydj1 and Ssa4. Large-scale analysis of Hsp70 isoform interactomes by high-resolution mass spectrometry of the type seen in (20, 29, 134) would confirm that even the small amino acid differences present in Hsp70 isoforms can greatly impact co-chaperone and client- binding specificity.

RNR has been a longstanding anticancer drug target because of its prominent role in DNA synthesis and repair (30, 33, 36). Likewise, because of Hsp70 and Hsp90's cytoprotective qualities, researchers have developed several chaperone inhibitors that show success in cancer cell studies (6, 51, 52, 93, 109, 172). However, both RNR and chaperone inhibitors are highly toxic to patients which makes dosing and treatment difficult.

Cells solely expressing Ssa3 and Ssa4 show decrease in RNR subunit transcription and stability. While their constitutively expressed counterparts, Ssa1 and Ssa2 are able to fully support RNR function as the sole isoforms and are resistance to RNR inhibitors such as hydroxyurea. Understanding the differences between isoform client specificity may contribute to future efforts in inhibiting a singular isoforms and consequently targeting specific signaling pathways rather than overall chaperone function (115). This novel approach has the potential to reduce toxic effects seen in mammalian cells with current anti-chaperone drugs. Alternatively, targeting co-chaperones may be an easier way to fine-tune chaperone function in human pathologies. We clearly demonstrate that RNR requires HDJ2 for function and that 116-9e can sensitize cancer cells to a range of RNR inhibitors.

Although combination therapies that simultaneously target both chaperones and RNR appear to be highly synergistic, whether this is fully translatable to patients remains to be seen. Future translational studies on mice will determine toxicity and selectivity of 116-9e/RNR inhibitor therapeutic strategies.

Aside from targeting cytoplasmic co-chaperones, we show the effectiveness of inhibiting ER-localized co-chaperones in cancer. There are 8 co-chaperones that assist the ER-specific Hsp70 BiP. Similar to other Hsp70's, BiP plays a major role in maintaining cellular homeostasis by folding the majority of the proteome that develops within ER (81,

163). As with other anti-chaperone strategies, inhibiting BiP as an anti-cancer treatment has been shown to be detrimental to non-tumorgenic cells. Here we show synergy between KO of specific ER co-chaperone proteins and current anti-cancer drugs. While validations of this study are necessary, targeting co-chaperones in combination with current anti-cancer drugs has the potential to be an novel and rather potent therapy that reduces harmful effects on patients.

REFERENCES

1. Freilich R, Arhar T, Abrams JL, Gestwicki JE. Protein-Protein Interactions in the Molecular Chaperone Network. Acc Chem Res. 2018;51(4):940-9.
2. Kim YE, Hipp MS, Bracher A, Hayer-Hartl M, Hartl FU. Molecular chaperone functions in protein folding and proteostasis. Annu Rev Biochem. 2013;82:323-55.
3. Rodina A, Wang T, Yan P, Gomes ED, Dunphy MP, Pillarsetty N, et al. The epichaperome is an integrated chaperome network that facilitates tumour survival. Nature. 2016;538(7625):397-401.
4. Tai W, Guzman ML, Chiosis G. The epichaperome: the power of many as the power of one. Oncoscience. 2016;3(9-10):266-7.
5. Li QQ, Hao JJ, Zhang Z, Krane LS, Hammerich KH, Sanford T, et al. Proteomic analysis of proteome and histone post-translational modifications in heat shock protein 90 inhibition-mediated bladder cancer therapeutics. Sci Rep. 2017;7(1):201.
6. McClellan AJ, Xia Y, Deutschbauer AM, Davis RW, Gerstein M, Frydman J. Diverse cellular functions of the Hsp90 molecular chaperone uncovered using systems approaches. Cell. 2007;131(1):121-35.
7. Pennisi R, Ascenzi P, di Masi A. Hsp90: A New Player in DNA Repair? Biomolecules. 2015;5(4):2589-618.
8. Sato N, Torigoe T. The molecular chaperones in cell cycle control. Ann N Y Acad Sci. 1998;851:61-6.
9. Trepel J, Mollapour M, Giaccone G, Neckers L. Targeting the dynamic HSP90 complex in cancer. Nat Rev Cancer. 2010;10(8):537-49.
10. Wegele H, Muller L, Buchner J. Hsp70 and Hsp90--a relay team for protein folding. Rev Physiol Biochem Pharmacol. 2004;151:1-44.
11. Calderwood SK, Gong J. Heat Shock Proteins Promote Cancer: It's a Protection Racket. Trends Biochem Sci. 2016;41(4):311-23.
12. Calderwood SK, Neckers L. Hsp90 in Cancer: Transcriptional Roles in the Nucleus. Adv Cancer Res. 2016;129:89-106.
13. Cesa LC, Shao H, Srinivasan SR, Tse E, Jain C, Zuiderweg ERP, et al. X-linked inhibitor of apoptosis protein (XIAP) is a client of heat shock protein 70 (Hsp70) and a biomarker of its inhibition. J Biol Chem. 2018;293(7):2370-80.
14. Lianos GD, Alexiou GA, Mangano A, Mangano A, Rausei S, Boni L, et al. The role of heat shock proteins in cancer. Cancer Lett. 2015;360(2):114-8.
15. Sherman MY, Gabai VL. Hsp70 in cancer: back to the future. Oncogene. 2015;34(32):4153-61.
16. Bachman AB, Keramisanou D, Xu W, Beebe K, Moses MA, Vasantha Kumar MV, et al. Phosphorylation induced cochaperone unfolding promotes kinase recruitment and client class-specific Hsp90 phosphorylation. Nat Commun. 2018;9(1):265.
17. Dong J, Wu Z, Wang D, Pascal LE, Nelson JB, Wipf P, et al. Hsp70 binds to the androgen receptor N-terminal domain and modulates the receptor function in prostate cancer cells. Mol Cancer Ther. 2018.
18. Hallett ST, Pastok MW, Morgan RML, Wittner A, Blundell K, Felletar I, et al. Differential Regulation of G1 CDK Complexes by the Hsp90-Cdc37 Chaperone System. Cell Rep. 2017;21(5):1386-98.

19. Joshi S, Wang T, Araujo TLS, Sharma S, Brodsky JL, Chiosis G. Adapting to stress - chaperome networks in cancer. Nat Rev Cancer. 2018;18(9):562-75.
20. Truman AW, Kristjansdottir K, Wolfgeher D, Hasin N, Polier S, Zhang H, et al. CDK-dependent Hsp70 Phosphorylation controls G1 cyclin abundance and cell-cycle progression. Cell. 2012;151(6):1308-18.
21. Truman AW, Millson SH, Nuttall JM, King V, Mollapour M, Prodromou C, et al. Expressed in the yeast Saccharomyces cerevisiae, human ERK5 is a client of the Hsp90 chaperone that complements loss of the Slt2p (Mpk1p) cell integrity stress-activated protein kinase. Eukaryot Cell. 2006;5(11):1914-24.
22. Mollapour M, Neckers L. Detecting HSP90 phosphorylation. Methods Mol Biol. 2011;787:67-74.
23. Taipale M, Krykbaeva I, Koeva M, Kayatekin C, Westover KD, Karras GI, et al. Quantitative analysis of HSP90-client interactions reveals principles of substrate recognition. Cell. 2012;150(5):987-1001.
24. Taldone T, Ochiana SO, Patel PD, Chiosis G. Selective targeting of the stress chaperome as a therapeutic strategy. Trends Pharmacol Sci. 2014;35(11):592-603.
25. Truman AW, Kristjansdottir K, Wolfgeher D, Ricco N, Mayampurath A, Volchenboum SL, et al. Quantitative proteomics of the yeast Hsp70/Hsp90 interactomes during DNA damage reveal chaperone-dependent regulation of ribonucleotide reductase. J Proteomics. 2015;112:285-300.
26. Dunn DM, Woodford MR, Truman AW, Jensen SM, Schulman J, Caza T, et al. c-Abl Mediated Tyrosine Phosphorylation of Aha1 Activates Its Co-chaperone Function in Cancer Cells. Cell Rep. 2015;12(6):1006-18.
27. Mollapour M, Tsutsumi S, Truman AW, Xu W, Vaughan CK, Beebe K, et al. Threonine 22 phosphorylation attenuates Hsp90 interaction with cochaperones and affects its chaperone activity. Mol Cell. 2011;41(6):672-81.
28. Woodford MR, Truman AW, Dunn DM, Jensen SM, Cotran R, Bullard R, et al. Mps1 Mediated Phosphorylation of Hsp90 Confers Renal Cell Carcinoma Sensitivity and Selectivity to Hsp90 Inhibitors. Cell Rep. 2016;14(4):872-84.
29. Truman AW, Kristjansdottir K, Wolfgeher D, Ricco N, Mayampurath A, Volchenboum SL, et al. The quantitative changes in the yeast Hsp70 and Hsp90 interactomes upon DNA damage. Data Brief. 2015;2:12-5.
30. Cerqueira NM, Fernandes PA, Ramos MJ. Ribonucleotide reductase: a critical enzyme for cancer chemotherapy and antiviral agents. Recent Pat Anticancer Drug Discov. 2007;2(1):11-29.
31. Cerqueira NM, Pereira S, Fernandes PA, Ramos MJ. Overview of ribonucleotide reductase inhibitors: an appealing target in anti-tumour therapy. Curr Med Chem. 2005;12(11):1283-94.
32. Chabes A, Domkin V, Larsson G, Liu A, Graslund A, Wijmenga S, et al. Yeast ribonucleotide reductase has a heterodimeric iron-radical-containing subunit. Proc Natl Acad Sci U S A. 2000;97(6):2474-9.
33. Nordlund P, Reichard P. Ribonucleotide reductases. Annu Rev Biochem. 2006;75:681-706.
34. Wang PJ, Chabes A, Casagrande R, Tian XC, Thelander L, Huffaker TC. Rnr4p, a novel ribonucleotide reductase small-subunit protein. Mol Cell Biol. 1997;17(10):6114-21.

35. Perlstein DL, Ge J, Ortigosa AD, Robblee JH, Zhang Z, Huang M, et al. The active form of the Saccharomyces cerevisiae ribonucleotide reductase small subunit is a heterodimer in vitro and in vivo. Biochemistry. 2005;44(46):15366-77.
36. Mulder KW, Winkler GS, Timmers HT. DNA damage and replication stress induced transcription of RNR genes is dependent on the Ccr4-Not complex. Nucleic Acids Res. 2005;33(19):6384-92.
37. Singh A, Xu YJ. The Cell Killing Mechanisms of Hydroxyurea. Genes (Basel). 2016;7(11).
38. Yarbro JW. Mechanism of action of hydroxyurea. Semin Oncol. 1992;19(3 Suppl 9):1-10.
39. Cerqueira NM, Fernandes PA, Ramos MJ. Understanding ribonucleotide reductase inactivation by gemcitabine. Chemistry. 2007;13(30):8507-15.
40. Plunkett W, Huang P, Xu YZ, Heinemann V, Grunewald R, Gandhi V. Gemcitabine: metabolism, mechanisms of action, and self-potentiation. Seminars in oncology. 1995;22(4 Suppl 11):3-10.
41. Arlander SJ, Eapen AK, Vroman BT, McDonald RJ, Toft DO, Karnitz LM. Hsp90 inhibition depletes Chk1 and sensitizes tumor cells to replication stress. J Biol Chem. 2003;278(52):52572-7.
42. Ghadban T, Dibbern JL, Reeh M, Miro JT, Tsui TY, Wellner U, et al. HSP90 is a promising target in gemcitabine and 5-fluorouracil resistant pancreatic cancer. Apoptosis. 2017;22(3):369-80.
43. Pedersen KS, Kim GP, Foster NR, Wang-Gillam A, Erlichman C, McWilliams RR. Phase II trial of gemcitabine and tanespimycin (17AAG) in metastatic pancreatic cancer: a Mayo Clinic Phase II Consortium study. Invest New Drugs. 2015;33(4):963-8.
44. Caplan AJ. What is a co-chaperone? Cell Stress Chaperones. 2003;8(2):105-7.
45. Amin-Wetzel N, Saunders RA, Kamphuis MJ, Rato C, Preissler S, Harding HP, et al. A J-Protein Co-chaperone Recruits BiP to Monomerize IRE1 and Repress the Unfolded Protein Response. Cell. 2017;171(7):1625-37 e13.
46. Connell P, Ballinger CA, Jiang J, Wu Y, Thompson LJ, Hohfeld J, et al. The co-chaperone CHIP regulates protein triage decisions mediated by heat-shock proteins. Nat Cell Biol. 2001;3(1):93-6.
47. Craig EA, Marszalek J. How Do J-Proteins Get Hsp70 to Do So Many Different Things? Trends Biochem Sci. 2017;42(5):355-68.
48. Kampinga HH, Craig EA. The HSP70 chaperone machinery: J proteins as drivers of functional specificity. Nat Rev Mol Cell Biol. 2011;11(8):579-92.
49. Aron R, Higurashi T, Sahi C, Craig EA. J-protein co-chaperone Sis1 required for generation of [RNQ+] seeds necessary for prion propagation. EMBO J. 2007;26(16):3794-803.
50. Lu Z, Cyr DM. Protein folding activity of Hsp70 is modified differentially by the hsp40 co-chaperones Sis1 and Ydj1. J Biol Chem. 1998;273(43):27824-30.
51. Calderwood SK. Molecular cochaperones: tumor growth and cancer treatment. Scientifica (Cairo). 2013;2013:217513.
52. Weeks SA, Miller DJ. The heat shock protein 70 cochaperone YDJ1 is required for efficient membrane-specific flock house virus RNA replication complex assembly and function in Saccharomyces cerevisiae. J Virol. 2008;82(4):2004-12.

53. He HL, Lee YE, Chen HP, Hsing CH, Chang IW, Shiue YL, et al. Overexpression of DNAJC12 predicts poor response to neoadjuvant concurrent chemoradiotherapy in patients with rectal cancer. Exp Mol Pathol. 2015;98(3):338-45.
54. Parrales A, Ranjan A, Iyer SV, Padhye S, Weir SJ, Roy A, et al. DNAJA1 controls the fate of misfolded mutant p53 through the mevalonate pathway. Nat Cell Biol. 2016;18(11):1233-43.
55. Sopha P, Ren HY, Grove DE, Cyr DM. Endoplasmic reticulum stress-induced degradation of DNAJB12 stimulates BOK accumulation and primes cancer cells for apoptosis. J Biol Chem. 2017;292(28):11792-803.
56. Tracz-Gaszewska Z, Klimczak M, Biecek P, Herok M, Kosinski M, Olszewski MB, et al. Molecular chaperones in the acquisition of cancer cell chemoresistance with mutated TP53 and MDM2 up-regulation. Oncotarget. 2017;8(47):82123-43.
57. Erlichman C. Tanespimycin: the opportunities and challenges of targeting heat shock protein 90. Expert Opin Investig Drugs. 2009;18(6):861-8.
58. Moses MA, Kim YS, Rivera-Marquez GM, Oshima N, Watson MJ, Beebe KE, et al. Targeting the Hsp40/Hsp70 Chaperone Axis as a Novel Strategy to Treat Castration-Resistant Prostate Cancer. Cancer Res. 2018;78(14):4022-35.
59. Nillegoda NB, Wentink AS, Bukau B. Protein Disaggregation in Multicellular Organisms. Trends Biochem Sci. 2018;43(4):285-300.
60. Walsh P, Bursac D, Law YC, Cyr D, Lithgow T. The J-protein family: modulating protein assembly, disassembly and translocation. EMBO Rep. 2004;5(6):567-71.
61. Werner-Washburne M, Stone DE, Craig EA. Complex interactions among members of an essential subfamily of hsp70 genes in Saccharomyces cerevisiae. Mol Cell Biol. 1987;7(7):2568-77.
62. Werner-Washburne M, Becker J, Kosic-Smithers J, Craig EA. Yeast Hsp70 RNA levels vary in response to the physiological status of the cell. J Bacteriol. 1989;171(5):2680-8.
63. Boorstein WR, Craig EA. Structure and regulation of the SSA4 HSP70 gene of Saccharomyces cerevisiae. J Biol Chem. 1990;265(31):18912-21.
64. Werner-Washburne M, Craig EA. Expression of members of the Saccharomyces cerevisiae hsp70 multigene family. Genome. 1989;31(2):684-9.
65. Christiano R, Nagaraj N, Frohlich F, Walther TC. Global proteome turnover analyses of the Yeasts S. cerevisiae and S. pombe. Cell Rep. 2014;9(5):1959-65.
66. Gardner JM, Jaspersen SL. Manipulating the yeast genome: deletion, mutation, and tagging by PCR. Methods Mol Biol. 2014;1205:45-78.
67. Becker J, Walter W, Yan W, Craig EA. Functional interaction of cytosolic hsp70 and a DnaJ-related protein, Ydj1p, in protein translocation in vivo. Mol Cell Biol. 1996;16(8):4378-86.
68. Jung G, Jones G, Wegrzyn RD, Masison DC. A role for cytosolic hsp70 in yeast [PSI(+)] prion propagation and [PSI(+)] as a cellular stress. Genetics. 2000;156(2):559-70.
69. Jaiswal H, Conz C, Otto H, Wolfle T, Fitzke E, Mayer MP, et al. The chaperone network connected to human ribosome-associated complex. Mol Cell Biol. 2011;31(6):1160-73.
70. Gao BC, Biosca J, Craig EA, Greene LE, Eisenberg E. Uncoating of coated vesicles by yeast hsp70 proteins. J Biol Chem. 1991;266(29):19565-71.

71. Brown CR, McCann JA, Chiang HL. The heat shock protein Ssa2p is required for import of fructose-1, 6-bisphosphatase into Vid vesicles. J Cell Biol. 2000;150(1):65-76.
72. Sharma D, Masison DC. Single methyl group determines prion propagation and protein degradation activities of yeast heat shock protein (Hsp)-70 chaperones Ssa1p and Ssa2p. Proc Natl Acad Sci U S A. 2011;108(33):13665-70.
73. Huang D, Moffat J, Andrews B. Dissection of a complex phenotype by functional genomics reveals roles for the yeast cyclin-dependent protein kinase Pho85 in stress adaptation and cell integrity. Mol Cell Biol. 2002;22(14):5076-88.
74. Kuzmin E, VanderSluis B, Wang W, Tan G, Deshpande R, Chen Y, et al. Systematic analysis of complex genetic interactions. Science. 2018;360(6386).
75. van Leeuwen J, Pons C, Mellor JC, Yamaguchi TN, Friesen H, Koschwanez J, et al. Exploring genetic suppression interactions on a global scale. Science. 2016;354(6312).
76. van Leeuwen J, Boone C, Andrews BJ. Mapping a diversity of genetic interactions in yeast. Curr Opin Syst Biol. 2017;6:14-21.
77. Dushukyan N, Dunn DM, Sager RA, Woodford MR, Loiselle DR, Daneshvar M, et al. Phosphorylation and Ubiquitination Regulate Protein Phosphatase 5 Activity and Its Prosurvival Role in Kidney Cancer. Cell Rep. 2017;21(7):1883-95.
78. Woodford MR, Dunn D, Miller JB, Jamal S, Neckers L, Mollapour M. Impact of Posttranslational Modifications on the Anticancer Activity of Hsp90 Inhibitors. Adv Cancer Res. 2016;129:31-50.
79. Wolfgeher D, Dunn DM, Woodford MR, Bourboulia D, Bratslavsky G, Mollapour M, et al. The dynamic interactome of human Aha1 upon Y223 phosphorylation. Data Brief. 2015;5:752-5.
80. Hasin N, Cusack SA, Ali SS, Fitzpatrick DA, Jones GW. Global transcript and phenotypic analysis of yeast cells expressing Ssa1, Ssa2, Ssa3 or Ssa4 as sole source of cytosolic Hsp70-Ssa chaperone activity. BMC Genomics. 2014;15:194.
81. Pobre KFR, Poet GJ, Hendershot LM. The endoplasmic reticulum (ER) chaperone BiP is a master regulator of ER functions: Getting by with a little help from ERdj friends. J Biol Chem. 2019;294(6):2098-108.
82. Zacchi LF, Wu HC, Bell SL, Millen L, Paton AW, Paton JC, et al. The BiP molecular chaperone plays multiple roles during the biogenesis of torsinA, an AAA+ ATPase associated with the neurological disease early-onset torsion dystonia. J Biol Chem. 2014;289(18):12727-47.
83. Otero JH, Lizak B, Hendershot LM. Life and death of a BiP substrate. Semin Cell Dev Biol. 2010;21(5):472-8.
84. Behnke J, Mann MJ, Scruggs FL, Feige MJ, Hendershot LM. Members of the Hsp70 Family Recognize Distinct Types of Sequences to Execute ER Quality Control. Mol Cell. 2016;63(5):739-52.
85. Shevtsov M, Huile G, Multhoff G. Membrane heat shock protein 70: a theranostic target for cancer therapy. Philos Trans R Soc Lond B Biol Sci. 2018;373(1738).
86. Rohde M, Daugaard M, Jensen MH, Helin K, Nylandsted J, Jaattela M. Members of the heat-shock protein 70 family promote cancer cell growth by distinct mechanisms. Genes Dev. 2005;19(5):570-82.
87. Luke MM, Sutton A, Arndt KT. Characterization of SIS1, a Saccharomyces cerevisiae homologue of bacterial dnaJ proteins. J Cell Biol. 1991;114(4):623-38.

88. Caplan AJ, Douglas MG. Characterization of YDJ1: a yeast homologue of the bacterial dnaJ protein. J Cell Biol. 1991;114(4):609-21.
89. Kirkland PA, Reidy M, Masison DC. Functions of yeast Hsp40 chaperone Sis1p dispensable for prion propagation but important for prion curing and protection from prion toxicity. Genetics. 2011;188(3):565-77.
90. Escusa-Toret S, Vonk WI, Frydman J. Spatial sequestration of misfolded proteins by a dynamic chaperone pathway enhances cellular fitness during stress. Nat Cell Biol. 2013;15(10):1231-43.
91. Flom GA, Lemieszek M, Fortunato EA, Johnson JL. Farnesylation of Ydj1 is required for in vivo interaction with Hsp90 client proteins. Mol Biol Cell. 2008;19(12):5249-58.
92. Stark JL, Mehla K, Chaika N, Acton TB, Xiao R, Singh PK, et al. Structure and function of human DnaJ homologue subfamily a member 1 (DNAJA1) and its relationship to pancreatic cancer. Biochemistry. 2014;53(8):1360-72.
93. Assimon VA, Gillies AT, Rauch JN, Gestwicki JE. Hsp70 protein complexes as drug targets. Curr Pharm Des. 2013;19(3):404-17.
94. Sanvisens N, de Llanos R, Puig S. Function and regulation of yeast ribonucleotide reductase: cell cycle, genotoxic stress, and iron bioavailability. Biomed J. 2013;36(2):51-8.
95. Cotruvo JA, Stubbe J. Escherichia coli class Ib ribonucleotide reductase contains a dimanganese(III)-tyrosyl radical cofactor in vivo. Biochemistry. 2011;50(10):1672-81.
96. Kolberg M, Strand KR, Graff P, Andersson KK. Structure, function, and mechanism of ribonucleotide reductases. Biochim Biophys Acta. 2004;1699(1-2):1-34.
97. Hsu HW, Wall NR, Hsueh CT, Kim S, Ferris RL, Chen CS, et al. Combination antiangiogenic therapy and radiation in head and neck cancers. Oral Oncol. 2014;50(1):19-26.
98. Loehrer PJ, Sr., Feng Y, Cardenes H, Wagner L, Brell JM, Cella D, et al. Gemcitabine alone versus gemcitabine plus radiotherapy in patients with locally advanced pancreatic cancer: an Eastern Cooperative Oncology Group trial. J Clin Oncol. 2011;29(31):4105-12.
99. Mornex F, Girard N. Gemcitabine and radiation therapy in non-small cell lung cancer: state of the art. Ann Oncol. 2006;17(12):1743-7.
100. Truman AW, Millson SH, Nuttall JM, Mollapour M, Prodromou C, Piper PW. In the yeast heat shock response, Hsf1-directed induction of Hsp90 facilitates the activation of the Slt2 (Mpk1) mitogen-activated protein kinase required for cell integrity. Eukaryot Cell. 2007;6(4):744-52.
101. Li J, Qian X, Sha B. Heat shock protein 40: structural studies and their functional implications. Protein Pept Lett. 2009;16(6):606-12.
102. Johnson JL, Craig EA. A role for the Hsp40 Ydj1 in repression of basal steroid receptor activity in yeast. Mol Cell Biol. 2000;20(9):3027-36.
103. Johnson JL, Craig EA. An essential role for the substrate-binding region of Hsp40s in Saccharomyces cerevisiae. J Cell Biol. 2001;152(4):851-6.
104. Yan W, Craig EA. The glycine-phenylalanine-rich region determines the specificity of the yeast Hsp40 Sis1. Mol Cell Biol. 1999;19(11):7751-8.

105. Reidy M, Sharma R, Shastry S, Roberts BL, Albino-Flores I, Wickner S, et al. Hsp40s specify functions of Hsp104 and Hsp90 protein chaperone machines. PLoS Genet. 2014;10(10):e1004720.
106. Borges JC, Seraphim TV, Mokry DZ, Almeida FC, Cyr DM, Ramos CH. Identification of regions involved in substrate binding and dimer stabilization within the central domains of yeast Hsp40 Sis1. PLoS One. 2012;7(12):e50927.
107. Caplan AJ, Tsai J, Casey PJ, Douglas MG. Farnesylation of YDJ1p is required for function at elevated growth temperatures in Saccharomyces cerevisiae. J Biol Chem. 1992;267(26):18890-5.
108. Saarikangas J, Caudron F, Prasad R, Moreno DF, Bolognesi A, Aldea M, et al. Compartmentalization of ER-Bound Chaperone Confines Protein Deposit Formation to the Aging Yeast Cell. Curr Biol. 2017;27(6):773-83.
109. Fan CY, Lee S, Cyr DM. Mechanisms for regulation of Hsp70 function by Hsp40. Cell Stress Chaperones. 2003;8(4):309-16.
110. Tsai J, Douglas MG. A conserved HPD sequence of the J-domain is necessary for YDJ1 stimulation of Hsp70 ATPase activity at a site distinct from substrate binding. J Biol Chem. 1996;271(16):9347-54.
111. Wisen S, Bertelsen EB, Thompson AD, Patury S, Ung P, Chang L, et al. Binding of a small molecule at a protein-protein interface regulates the chaperone activity of hsp70-hsp40. ACS Chem Biol. 2010;5(6):611-22.
112. Quanz M, Herbette A, Sayarath M, de Koning L, Dubois T, Sun JS, et al. Heat shock protein 90alpha (Hsp90alpha) is phosphorylated in response to DNA damage and accumulates in repair foci. J Biol Chem. 2012;287(12):8803-15.
113. Solier S, Kohn KW, Scroggins B, Xu W, Trepel J, Neckers L, et al. Heat shock protein 90alpha (HSP90alpha), a substrate and chaperone of DNA-PK necessary for the apoptotic response. Proc Natl Acad Sci U S A. 2012;109(32):12866-72.
114. Echtenkamp FJ, Zelin E, Oxelmark E, Woo JI, Andrews BJ, Garabedian M, et al. Global functional map of the p23 molecular chaperone reveals an extensive cellular network. Mol Cell. 2011;43(2):229-41.
115. Lotz SK, Knighton LE, Nitika, Jones GW, Truman AW. Not quite the SSAme: unique roles for the yeast cytosolic Hsp70s. Curr Genet. 2019;65(5):1127-34.
116. Gaur D, Singh P, Guleria J, Gupta A, Kaur S, Sharma D. The Yeast Hsp70 Co-chaperone Ydj1 Regulates Functional Distinction of Ssa Hsp70s in the Hsp90 Chaperoning Pathway. Genetics. 2020.
117. Hageman J, van Waarde MA, Zylicz A, Walerych D, Kampinga HH. The diverse members of the mammalian HSP70 machine show distinct chaperone-like activities. Biochem J. 2011;435(1):127-42.
118. Mayer MP. Intra-molecular pathways of allosteric control in Hsp70s. Philos Trans R Soc Lond B Biol Sci. 2018;373(1749).
119. Mayer MP, Bukau B. Hsp70 chaperones: cellular functions and molecular mechanism. Cell Mol Life Sci. 2005;62(6):670-84.
120. Boorstein WR, Craig EA. Transcriptional regulation of SSA3, an HSP70 gene from Saccharomyces cerevisiae. Mol Cell Biol. 1990;10(6):3262-7.
121. Kampinga HH, Craig EA. The HSP70 chaperone machinery: J proteins as drivers of functional specificity. Nat Rev Mol Cell Biol. 2010;11(8):579-92.

122. Mikolaskova B, Jurcik M, Cipakova I, Kretova M, Chovanec M, Cipak L. Maintenance of genome stability: the unifying role of interconnections between the DNA damage response and RNA-processing pathways. Curr Genet. 2018;64(5):971-83.
123. Maicher A, Kupiec M. Rnr1's role in telomere elongation cannot be replaced by Rnr3: a role beyond dNTPs? Curr Genet. 2018;64(3):547-50.
124. Gandhi V, Plunkett W, Cortes JE. Omacetaxine: a protein translation inhibitor for treatment of chronic myelogenous leukemia. Clin Cancer Res. 2014;20(7):1735-40.
125. Sluder IT, Nitika, Knighton LE, Truman AW. The Hsp70 co-chaperone Ydj1/HDJ2 regulates ribonucleotide reductase activity. PLoS Genet. 2018;14(11):e1007462.
126. Knighton LE, Delgado LE, Truman AW. Novel insights into molecular chaperone regulation of ribonucleotide reductase. Curr Genet. 2019;65(2):477-82.
127. Sharma D, Martineau CN, Le Dall MT, Reidy M, Masison DC, Kabani M. Function of SSA subfamily of Hsp70 within and across species varies widely in complementing Saccharomyces cerevisiae cell growth and prion propagation. PLoS One. 2009;4(8):e6644.
128. Schwimmer C, Masison DC. Antagonistic interactions between yeast [PSI(+)] and [URE3] prions and curing of [URE3] by Hsp70 protein chaperone Ssa1p but not by Ssa2p. Mol Cell Biol. 2002;22(11):3590-8.
129. Sharma D, Masison DC. Functionally redundant isoforms of a yeast Hsp70 chaperone subfamily have different antiprion effects. Genetics. 2008;179(3):1301-11.
130. Tkach JM, Yimit A, Lee AY, Riffle M, Costanzo M, Jaschob D, et al. Dissecting DNA damage response pathways by analysing protein localization and abundance changes during DNA replication stress. Nat Cell Biol. 2012;14(9):966-76.
131. Kamada Y, Jung US, Piotrowski J, Levin DE. The protein kinase C-activated MAP kinase pathway of Saccharomyces cerevisiae mediates a novel aspect of the heat shock response. Genes Dev. 1995;9(13):1559-71.
132. Zhang Y, Li H, Zhang C, An X, Liu L, Stubbe J, et al. Conserved electron donor complex Dre2-Tah18 is required for ribonucleotide reductase metallocofactor assembly and DNA synthesis. Proc Natl Acad Sci U S A. 2014;111(17):E1695-704.
133. Knighton LE, Nitika, Wolfgeher D, Reitzel AM, Truman AW. Dataset of Nematostella vectensis Hsp70 isoform interactomes upon heat shock. Data Brief. 2019;27:104580.
134. Knighton LE, Nitika, Waller SJ, Strom O, Wolfgeher D, Reitzel AM, et al. Dynamic remodeling of the interactomes of Nematostella vectensis Hsp70 isoforms under heat shock. J Proteomics. 2019;206:103416.
135. Waller SJ, Knighton LE, Crabtree LM, Perkins AL, Reitzel AM, Truman AW. Characterizing functional differences in sea anemone Hsp70 isoforms using budding yeast. Cell Stress Chaperones. 2018;23(5):933-41.
136. Gong W, Hu W, Xu L, Wu H, Wu S, Zhang H, et al. The C-terminal GGAP motif of Hsp70 mediates substrate recognition and stress response in yeast. J Biol Chem. 2018;293(46):17663-75.
137. Rosenzweig R, Nillegoda NB, Mayer MP, Bukau B. The Hsp70 chaperone network. Nat Rev Mol Cell Biol. 2019;20(11):665-80.
138. Stolz A, Wolf DH. Endoplasmic reticulum associated protein degradation: a chaperone assisted journey to hell. Biochim Biophys Acta. 2010;1803(6):694-705.

139. Al-Rawashdeh FY, Scriven P, Cameron IC, Vergani PV, Wyld L. Unfolded protein response activation contributes to chemoresistance in hepatocellular carcinoma. Eur J Gastroenterol Hepatol. 2010;22(9):1099-105.
140. Kern J, Untergasser G, Zenzmaier C, Sarg B, Gastl G, Gunsilius E, et al. GRP-78 secreted by tumor cells blocks the antiangiogenic activity of bortezomib. Blood. 2009;114(18):3960-7.
141. Pyrko P, Schonthal AH, Hofman FM, Chen TC, Lee AS. The unfolded protein response regulator GRP78/BiP as a novel target for increasing chemosensitivity in malignant gliomas. Cancer Res. 2007;67(20):9809-16.
142. Burris HA, Bakewell S, Bendell JC, Infante J, Jones SF, Spigel DR, et al. Safety and activity of IT-139, a ruthenium-based compound, in patients with advanced solid tumours: a first-in-human, open-label, dose-escalation phase I study with expansion cohort. ESMO Open. 2016;1(6):e000154.
143. Kroczynska B, King-Simmons L, Alloza L, Alava MA, Elguindi EC, Blond SY. BIP co-chaperone MTJ1/ERDJ1 interacts with inter-alpha-trypsin inhibitor heavy chain 4. Biochem Biophys Res Commun. 2005;338(3):1467-77.
144. Shen Y, Meunier L, Hendershot LM. Identification and characterization of a novel endoplasmic reticulum (ER) DnaJ homologue, which stimulates ATPase activity of BiP in vitro and is induced by ER stress. J Biol Chem. 2002;277(18):15947-56.
145. Shen Y, Hendershot LM. ERdj3, a stress-inducible endoplasmic reticulum DnaJ homologue, serves as a cofactor for BiP's interactions with unfolded substrates. Mol Biol Cell. 2005;16(1):40-50.
146. Pan J, Cao D, Gong J. The endoplasmic reticulum co-chaperone ERdj3/DNAJB11 promotes hepatocellular carcinoma progression through suppressing AATZ degradation. Future Oncol. 2018;14(29):3001-13.
147. Lai CW, Otero JH, Hendershot LM, Snapp E. ERdj4 protein is a soluble endoplasmic reticulum (ER) DnaJ family protein that interacts with ER-associated degradation machinery. J Biol Chem. 2012;287(11):7969-78.
148. Kurisu J, Honma A, Miyajima H, Kondo S, Okumura M, Imaizumi K. MDG1/ERdj4, an ER-resident DnaJ family member, suppresses cell death induced by ER stress. Genes Cells. 2003;8(2):189-202.
149. Oka M, Nakai M, Endo T, Lim CR, Kimata Y, Kohno K. Loss of Hsp70-Hsp40 chaperone activity causes abnormal nuclear distribution and aberrant microtubule formation in M-phase of Saccharomyces cerevisiae. J Biol Chem. 1998;273(45):29727-37.
150. Kampinga HH, Andreasson C, Barducci A, Cheetham ME, Cyr D, Emanuelsson C, et al. Function, evolution, and structure of J-domain proteins. Cell Stress Chaperones. 2019;24(1):7-15.
151. Ohta M, Takaiwa F. Emerging features of ER resident J-proteins in plants. Plant Signal Behav. 2014;9(3):e28194.
152. Cerezo M, Lehraiki A, Millet A, Rouaud F, Plaisant M, Jaune E, et al. Compounds Triggering ER Stress Exert Anti-Melanoma Effects and Overcome BRAF Inhibitor Resistance. Cancer Cell. 2016;29(6):805-19.
153. Nitika, Blackman JS, Knighton LE, Takakuwa JE, Calderwood SK, Truman AW. Chemogenomic screening Identifies the Hsp70 Co-chaperone HDJ2 as a Hub for Anticancer Drug Resistance. bioRxiv. 2019:818427.

154. Gao J, Aksoy BA, Dogrusoz U, Dresdner G, Gross B, Sumer SO, et al. Integrative analysis of complex cancer genomics and clinical profiles using the cBioPortal. Sci Signal. 2013;6(269):pl1.
155. Cerami E, Gao J, Dogrusoz U, Gross BE, Sumer SO, Aksoy BA, et al. The cBio cancer genomics portal: an open platform for exploring multidimensional cancer genomics data. Cancer Discov. 2012;2(5):401-4.
156. Murphy ME. The HSP70 family and cancer. Carcinogenesis. 2013;34(6):1181-8.
157. Meiss F, Andrlova H, Zeiser R. Vismodegib. Recent Results Cancer Res. 2018;211:125-39.
158. Dicks N, Gutierrez K, Michalak M, Bordignon V, Agellon LB. Endoplasmic reticulum stress, genome damage, and cancer. Front Oncol. 2015;5:11.
159. Dicks N, Bohrer RC, Gutierrez K, Michalak M, Agellon LB, Bordignon V. Relief of endoplasmic reticulum stress enhances DNA damage repair and improves development of pre-implantation embryos. PLoS One. 2017;12(11):e0187717.
160. Mlynarczyk C, Fahraeus R. Endoplasmic reticulum stress sensitizes cells to DNA damage-induced apoptosis through p53-dependent suppression of p21(CDKN1A). Nat Commun. 2014;5:5067.
161. Mizutani H, Tada-Oikawa S, Hiraku Y, Kojima M, Kawanishi S. Mechanism of apoptosis induced by doxorubicin through the generation of hydrogen peroxide. Life Sci. 2005;76(13):1439-53.
162. Enache M, Toader AM, Enache MI. Mitoxantrone-Surfactant Interactions: A Physicochemical Overview. Molecules. 2016;21(10).
163. Hendershot LM. The ER function BiP is a master regulator of ER function. Mt Sinai J Med. 2004;71(5):289-97.
164. Dlugosz A, Agrawal S, Kirkpatrick P. Vismodegib. Nat Rev Drug Discov. 2012;11(6):437-8.
165. Saito A, Kanemoto S, Zhang Y, Asada R, Hino K, Imaizumi K. Chondrocyte proliferation regulated by secreted luminal domain of ER stress transducer BBF2H7/CREB3L2. Mol Cell. 2014;53(1):127-39.
166. Li J, Zhang L, Xia Q, Fu J, Zhou Z, Lin F. Hedgehog signaling inhibitor GANT61 induces endoplasmic reticulum stress-mediated protective autophagy in hepatic stellate cells. Biochem Biophys Res Commun. 2017;493(1):487-93.
167. Scott LJ. Enzalutamide: A Review in Castration-Resistant Prostate Cancer. Drugs. 2018;78(18):1913-24.
168. Saad F. Evidence for the efficacy of enzalutamide in postchemotherapy metastatic castrate-resistant prostate cancer. Ther Adv Urol. 2013;5(4):201-10.
169. Gurel PS, Hatch AL, Higgs HN. Connecting the cytoskeleton to the endoplasmic reticulum and Golgi. Curr Biol. 2014;24(14):R660-R72.
170. Terasaki M, Chen LB, Fujiwara K. Microtubules and the endoplasmic reticulum are highly interdependent structures. J Cell Biol. 1986;103(4):1557-68.
171. Simigdala N, Pancholi S, Ribas R, Folkerd E, Liccardi G, Nikitorowicz-Buniak J, et al. Abiraterone shows alternate activity in models of endocrine resistant and sensitive disease. Br J Cancer. 2018;119(3):313-22.
172. Galluzzi L, Giordanetto F, Kroemer G. Targeting HSP70 for cancer therapy. Mol Cell. 2009;36(2):176-7.